

What Drives the Growth of Black Holes?

D. M. Alexander^a, R. C. Hickox^{a,b}

^a*Department of Physics, Durham University, South Road, Durham DH1 3LE, UK*

^b*Department of Physics and Astronomy, Dartmouth College, 6127 Wilder Laboratory, Hanover, NH 03755, USA*

Abstract

Massive black holes (BHs) are at once exotic and yet ubiquitous, residing in the centers of massive galaxies in the local Universe. Recent years have seen remarkable advances in our understanding of how these BHs form and grow over cosmic time, during which they are revealed as active galactic nuclei (AGN). However, despite decades of research, we still lack a coherent picture of the physical drivers of BH growth, the connection between the growth of BHs and their host galaxies, the role of large-scale environment on the fueling of BHs, and the impact of BH-driven outflows on the growth of galaxies. In this paper we review our progress in addressing these key issues, motivated by the science presented at the “What Drives the Growth of Black Holes?” workshop held at Durham on 26th–29th July 2010, and discuss how these questions may be tackled with current and future facilities.

Keywords:

black holes, galaxies, active galactic nuclei, quasars, accretion

1. Introduction

One of the most astounding astronomical discoveries of the last ≈ 10 –20 yrs is the finding that massive galaxies in the local Universe host a central massive black hole (BH; $M_{\text{BH}} \approx 10^5$ – $10^{10} M_{\odot}$) with a mass proportional to that of the galaxy spheroid (e.g., Kormendy & Richstone, 1995; Magorrian et al., 1998; Ferrarese & Merritt, 2000; Gebhardt et al., 2000; Tremaine et al., 2002; Marconi & Hunt, 2003; Gültekin et al., 2009).¹ The tightness of this BH–spheroid mass relationship suggests a symbiotic connection between the formation and growth of BHs and galaxy spheroids. Identifying the physical drivers behind the BH–spheroid mass relationship is one of the major challenges in extragalactic astrophysics and cosmology.

BHs primarily grow through mass accretion during which the central source is revealed as an active galactic nucleus (AGN; e.g., Salpeter 1964; Lynden-Bell 1969; Shakura & Sunyaev 1973; Soltan 1982; Rees 1984). A

huge amount of energy is liberated during these mass-accretion events ($\epsilon \approx 0.05$ – 0.42 of the rest mass is converted into energy, depending on the spin of the BH; e.g., Kerr 1963; Shapiro & Teukolsky 1983), yielding large luminosities from comparatively modest mass-accretion rates:

$$\dot{m}_{\text{BH}} = 0.15 \left(\frac{0.1}{\epsilon} \right) \left(\frac{L_{\text{bol}}}{10^{45} \text{ergs}^{-1}} \right) M_{\odot} \text{yr}^{-1}, \quad (1)$$

where ϵ is the mass–energy efficiency conversion (typically estimated to be $\epsilon \approx 0.1$; e.g., Marconi et al. 2004; Merloni 2004) and L_{bol} is the bolometric luminosity of the AGN. For example, the accretion of just $\approx 1 M_{\odot} \text{yr}^{-1}$ (equivalent to the mass of the Moon each second) is sufficient for an AGN to outshine the entire host galaxy. A broad range of AGN activity is found even in the local Universe, with mass accretion rates ranging from $\approx 10^{-5}$ – $1 M_{\odot} \text{yr}^{-1}$. In Fig. 1 we illustrate some of the diversity in the AGN population within just ≈ 300 Mpc; we note here that Sgr A* is not strictly an AGN but has been included to demonstrate that even BHs in relatively quiescent galaxies are growing to some extent.

A direct connection between the growth of the BH and galaxy spheroid might be expected since both processes are predominantly driven by a cold-gas supply, which is provided by the host galaxy or the larger-scale extragalactic environment. However, the nine orders of

Email addresses: d.m.alexander@durham.ac.uk
(D. M. Alexander), ryan.c.hickox@dartmouth.edu
(R. C. Hickox)

¹The evidence for this BH–spheroid mass relationship comes from tight connection between M_{BH} and the velocity dispersion, luminosity, and mass of the galaxy spheroid for ≈ 50 –100 galaxies in the local Universe. These constraints imply $M_{\text{BH}} \approx (0.001$ – $0.002) M_{\text{sph}}$.

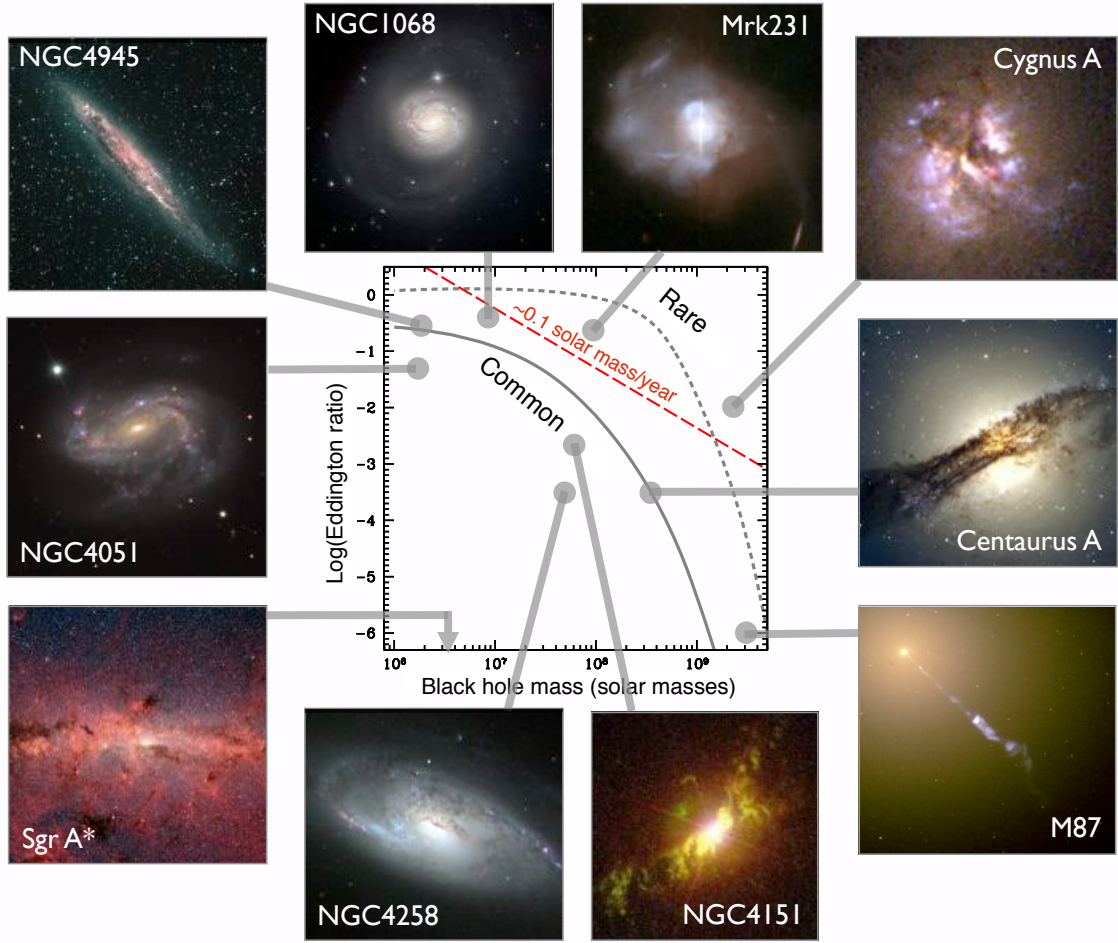


Figure 1: The Eddington-ratio versus black-hole mass plane illustrating part of the range of mass-accretion phenomena seen in the local Universe ($d < 300$ Mpc). The plotted systems include radio-loud AGNs (Centaurus A, Cygnus A, and M 87), an ultra-luminous IR galaxy (Mrk 231), as well as typical low-to-moderate luminous AGNs (NGC 1068, NGC 4051, NGC 4151, NGC4258, and NGC 4945). All of the systems plotted here have reliable black-hole masses that are measured independently of the host-galaxy properties. The Eddington ratio of Sgr A, the accreting black-hole at the centre of the Galaxy, is $\approx 10^{-8}$ – 10^{-9} and cannot be directly plotted on this figure. The curves indicate the space density of BHs growing at a given Eddington ratio, based on the synthetic AGN model of Merloni & Heinz (2008): $\Phi = 10^{-5} \text{ Mpc}^{-3}$ (solid curve) and $\Phi = 10^{-7} \text{ Mpc}^{-3}$ (dotted curve). The dashed line indicates a mass-accretion rate of $1 M_{\odot} \text{ yr}^{-1}$, which corresponds to a bolometric luminosity of $L_{\text{bol}} \approx 7 \times 10^{44} \text{ erg s}^{-1}$, which is equivalent to $L_{2-10\text{keV}} \approx 3 \times 10^{43} \text{ erg s}^{-1}$. Systems lying below the solid curve are common mass-accretion events in the local Universe while systems lying above the dashed curve are rare events in the local Universe. Black hole mass and luminosity data are taken from the literature (Gültekin et al., 2009; Kawakatu et al., 2007; Goulding et al., 2010; Baganoff et al., 2003; Yamada et al., 2009; Braito et al., 2004; Young et al., 2002; Di Matteo et al., 2003). Image credits: *NGC 4945*–2P2 Team, WFI, MPG/ESO 2.2-m Telescope, La Silla, ESO; *NGC 1068*–Francois and Shelley Pelletier/Adam Block/NOAO/AURA/NSF; *Mrk 231*–NASA, ESA, the Hubble Heritage (STScI/AURA)-ESA/Hubble Collaboration, and A. Evans (University of Virginia, Charlottesville/NRAO/Stony Brook University); *Cygnus A*–NASA, ESA, Neal Jackson (Jodrell Bank), Robert Fosbury (ESO); *Centaurus A*–ESO; *M87*–NASA and The Hubble Heritage Team (STScI/AURA); *NGC 4151*–John Hutchings (Dominion Astrophysical Observatory), Bruce Woodgate (GSFC/NASA), Mary Beth Kaiser (Johns Hopkins University), Steven Kraemer (Catholic University of America), the STIS Team., and NASA; *Sgr A**–Susan Stolovy (SSC/Caltech) et al., JPL-Caltech, NASA; *NGC 4051*–George Seitz/Adam Block/NOAO/AURA/NSF.

difference in physical size scale between the BH and the galaxy spheroid would appear to preclude a direct causal connection. Many processes have been proposed which could forge a direct connection between the growth of the BH and galaxy spheroid, including

galaxy major mergers, star-formation winds, and AGN-driven outflows. There is clear observational evidence for many of these processes occurring in individual systems. However, it is often far from clear how universal they are and what impact they have on the over-

all BH–spheroid growth. There are also many different observational and theoretical studies providing apparently contradictory results on the physical drivers of BH growth, with theorists often disagreeing with observers (and observers/theorists disagreeing with other observers/theorists). A cause of these discrepancies may be that (apparently) contradicting studies are exploring systems with different ranges in BH mass, Eddington ratio, redshift, or environment.

To address these potential conflicts we organised the “What Drives the Growth of Black Holes?” workshop at Durham on 26th–29th July 2010. This workshop explored the processes that drive accretion onto BHs, from the most luminous distant quasars to more quiescent local systems. A key aim of the workshop was to clarify the ranges of parameter space that are probed by different studies to better help understand how various key physical processes vary with these parameters. The workshop was organised into four main sessions that addressed the following key issues:

- How does the gas accrete onto black holes, from kilo-parsec to sub-parsec scales?
- What are the links between black-hole growth and their host galaxies and large-scale environments?
- What fuels the rapid growth of the most massive (and also the first) black holes?
- What is the detailed nature of AGN feedback and its effects on black-hole fuelling and star formation?

One hundred and twenty participants attended across the 3.5 days duration of the workshop, the vast majority of which presented scientific results: 53 gave oral presentations [18 invited; 35 contributed] and 49 gave poster presentations.² In this paper we review our progress in addressing these key issues, motivated by the science presented at the workshop. We also provide background material on the challenges faced in addressing these issues to motivate discussion. However, given the large breadth of science covered by this review, we cannot provide a complete assessment of each paper in the literature for every component of every issue (see Brandt & Hasinger 2005; Veilleux et al. 2005; Remillard & McClintock 2006; Done et al. 2007; McNamara & Nulsen 2007; Ho 2008; Shankar 2009; Volonteri 2010; Brandt & Alexander 2010 for some recent indepth

²The presentations can be found at the workshop web page: <http://astro.dur.ac.uk/growthofblackholes/index.php>

reviews on individual components within individual issues). Our aim is therefore to provide a solid grounding in the current scientific picture and hence a starting point for more detailed future investigations.

2. How does the gas accrete onto black holes, from kilo-parsec to sub-parsec scales?

The growth of the BH relies on the accretion of cool gas originally on scales orders of magnitude larger than the BH accretion disc, either from the host galaxy or the extragalactic environment (e.g., a companion galaxy; the dark-matter halo; cluster gas). The goal is to determine what physical processes deliver the gas from ≈ 10 kpc host-galaxy scales down to the BH accretion disc at $r < 0.1$ pc – an epic journey by any stretch of the imagination! Substantial barriers against the gas reaching the central regions are angular momentum and the gas collapsing and forming stars rather than accreting onto the BH. In this section we explore the mechanisms that can deliver gas into the nuclear region, including the competition for gas between star formation and AGN activity, the connection between accreting gas/dust and obscuration, and the process of mass accretion onto the BH.

2.1. Driving the gas into the vicinity of the black hole

The vast difference in size scale between the host galaxy and the BH means that the gas has to be driven down to ≈ 10 pc before it will come under the gravitational influence of the BH. The formidable force that needs to be overcome to deliver the gas from the host galaxy into the vicinity of the BH is angular momentum: the gas has to lose $\approx 99.9\%$ of its angular momentum to go from a stable orbit at $r = 10$ kpc down to $r = 10$ pc (e.g., Jogee, 2006). The challenges are to map the gas inflow from the host galaxy into the vicinity of the BH and to identify the triggering mechanisms of AGN activity.

Large-scale gravitational torques, such as those produced by galaxy bars, galaxy interactions, and galaxy major mergers have the potential to remove significant amounts of angular momentum and drive the gas into the central regions of galaxies (e.g., Shlosman et al., 1989, 1990; Barnes & Hernquist, 1992, 1996; Mihos & Hernquist, 1996; Bournaud & Combes, 2002; García-Burillo et al., 2005); see Fig. 2. However, the gravitational torques exerted on the gas by these large-scale processes will have a limited effect on sub-kpc scales, and smaller-scale processes (e.g., nested bars and nuclear spirals; Englmaier & Shlosman 2004; Maciejew-

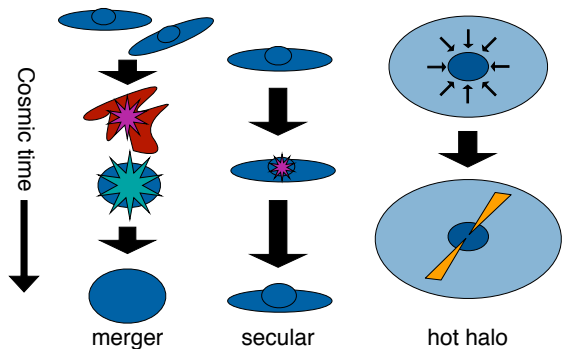


Figure 2: Schematic diagrams to illustrate the large-scale processes that are thought to be responsible for triggering AGN activity: major mergers of gas-rich galaxies, secular evolution (which includes both internal secular evolution and external secular evolution, the latter of which is driven by galaxy interactions), and hot halo accretion, which is presumed to be the dominate BH growth mode for low-excitation radio-loud AGNs.

ski 2004) are predicted to drive the gas down to ≈ 10 – 100 pc.

The physics of gas inflow can be explored in some detail using multi-scale smoothed-particle hydrodynamical simulations. For example, adopting this approach Hopkins & Quataert (2010) traced the dynamics of gas inflow over a broad range of scales (from ≈ 10 kpc down to < 1 pc), taking into account the effects of stars, star formation, stellar feedback, and the gravitational influence of the BH. Their simulations revealed a much broader range of gas morphologies than typically expected, including spirals, rings, clumps, bars within bars, and nuclear spirals. All of these processes were effective at driving the gas down to ≈ 10 – 100 pc but the gas inflow was found to be neither smooth nor continuous. Any individual process was also found to be comparatively short lived, complicating attempts of relating morphological features to the presence of AGN activity, particularly on > 100 pc scales.

Indeed, there is at best a marginal relationship between the presence of AGN activity and galaxy bars in the local Universe, with AGNs and galaxies not hosting AGN activity equally likely to host kpc-scale bars (e.g., Mulchaey & Regan, 1997; Knapen et al., 2000; Martini et al., 2003; Simões Lopes et al., 2007); however, we note that a relationship is found for narrow-line Seyfert 1 galaxies (see §3.2.3). On smaller ≈ 100 pc scales, high-resolution imaging of nearby systems has also failed to reveal any strong differences between the circumnuclear morphologies of AGNs and late-type galaxies not hosting AGN activity, with nuclear bars, spirals, discs, and circumnuclear dust equally likely to

be found in all late-type systems (e.g., Laine et al., 2002; Pogge & Martini, 2002; Martini et al., 2003; Hunt & Malkan, 2004). By contrast, a difference in the circumnuclear regions between AGNs hosted in early type galaxies and inactive early type galaxies is found, with the AGNs only found in dusty environments (Simões Lopes et al., 2007), suggesting that dusty structures are a necessary but not sufficient condition for BH growth. Although imaging studies have not revealed a morphological signature on 100-pc scales that *uniquely* reveals the trigger of AGN activity, triggers of AGN activity and the identification of significant gas inflow may be more discernable using spectroscopic data.

Integral Field Unit (IFU) observations provide spatially resolved spectroscopy and are a key tool to determine the dynamics of gas and stars in nearby systems. IFU observations of nearby AGNs have revealed clear differences between the gas and stellar kinematics on < 1 kpc scales, with the gas velocity fields showing significant departures from the regular circular orbits traced by the stars (e.g., Dumas et al., 2007; Stoklasová et al., 2009; Rodríguez-Zaurín et al., 2011). The gas kinematics uncover a broad range of features not revealed by the photometric data, including warps, counter-rotating discs, and motions out of the galactic plane, likely due to gas inflow and outflow. However, these features are also seen in galaxies *not* hosting AGN activity, indicating that the gas inflow that feeds the BH must occur on yet smaller scales.

IFU observations on ≈ 10 pc scales of several nearby AGNs are starting to reveal nuclear gas inflows, when contributions from the stellar potential are carefully modelled and removed from the ionised gas kinematics (e.g., Fathi et al., 2006; Dumas et al., 2007; Storchi-Bergmann et al., 2007; Riffel et al., 2008; Davies et al., 2009; Schnorr Müller et al., 2011). The strongest evidence for a nuclear gas inflow to date is from NGC 1097, where the gas is seen streaming along spiral structures towards the nucleus on ≈ 3.5 pc scales, with inflow velocities of up to ≈ 60 km s $^{-1}$ (e.g., Fathi et al. 2006; Davies et al. 2009; see also Prieto et al. 2005). However, a significant restriction in the identification of nuclear-scale gas inflows is that the gas kinematics of luminous AGNs are often dominated by gas-outflow signatures (e.g., Storchi-Bergmann et al. 2010; Hicks et al. in prep), and therefore the best constraints to date are limited to low-luminosity AGNs where the gas-inflow rates are comparatively low. This observational challenge can be overcome, in at least some cases, using spectropolarimetry, which can help distinguish between structures with different geometries (such as gas inflow from gas outflow) even in spatially unresolved

regions (e.g., Young, 2000; Smith et al., 2004). For example, using spectropolarimetry Young et al. (in prep) identified small-scale gas inflows in the Seyfert 1 galaxies NGC 4151 and Mrk 509, with inward radial velocities of $\approx 900 \text{ km s}^{-1}$ and mass inflow rates of $\approx 0.2\text{--}0.7 M_{\odot} \text{ yr}^{-1}$.

IFU observations have revealed the signatures of gas inflow down to $\approx 10 \text{ pc}$ scales in several nearby AGNs. However, paradoxically, the gas inflow rates estimated from the ionised gas are often significantly lower than the BH accretion rate (e.g., Fathi et al., 2006; Storchi-Bergmann et al., 2007; Riffel et al., 2008; Davies et al., 2009; Schnorr Müller et al., 2011). These discrepancies may indicate that the ionised gas provides a poor tracer of the inflowing gas rate, which is expected to be dominated by cold molecular gas (e.g. Davies et al., 2009; Hicks et al., 2009; Müller Sánchez et al., 2009); the ionised gas may be the outer skin of the molecular gas inflow (e.g., Riffel et al., 2008). Indeed, the mass inflow rates estimated using molecular gas tracers in several nearby AGNs are large enough to power the observed AGN activity (e.g., Davies et al., 2009; Müller Sánchez et al., 2009). The molecular gas luminosities of AGNs on $< 100 \text{ pc}$ scales are also potentially larger than those found in galaxies not hosting AGN activity, suggesting a greater reservoir of cold circumnuclear gas in at least some AGNs (e.g., Müller Sánchez et al. 2009; Hicks et al., in prep).

The current consensus view is therefore one where gas inflow from kpc scales down to the central $\approx 10\text{--}100 \text{ pc}$ region occurs in all gas-rich galaxies. The gas is driven into the central region through a series of gravitational instabilities, which helps to overcome the angular momentum of the gas. The clearest triggers of AGN activity in the local Universe are on the smallest scales, which is perhaps not surprising given that the gas inflow time from the host galaxy down to the pc-scale of the BH accretion disc is likely to be $\gtrsim 10^8$ years, comparable to or longer than the duration of the AGN phase (e.g., Martini et al., 2003; Hopkins & Quataert, 2010).

2.2. The competition between star formation and black-hole accretion

On scales of order $\approx 1\text{--}10 \text{ pc}$ the inflowing gas is expected to hit a bottleneck. The axisymmetric structures that have driven the gas from $\approx 10 \text{ kpc}$ down to $\approx 10 \text{ pc}$ are likely to have a negligible effect on the gas in these inner regions (e.g., Hopkins & Quataert, 2010). It is also on these scales that the gravitational influence from the BH will overcome that of the host galaxy; this radius is determined from the BH mass (M_{BH}) and the spheroid

velocity dispersion (σ_{sph}) as

$$r < \frac{GM_{\text{BH}}}{\sigma_{\text{sph}}^2}. \quad (2)$$

The density of the gas on these scales can be high and if it becomes unstable then it will collapse and form stars (e.g., Toomre, 1964; Kennicutt, 1989; Thompson et al., 2005), potentially robbing the BH of the fuel that it needs to grow. For example, an isothermal gas disc is expected to become unstable when

$$\Sigma_{\text{g}} > \frac{c_{\text{s}}\kappa}{\pi G}, \quad (3)$$

which is equivalent to $Q < 1$ in terms of the Toomre parameter (e.g., Toomre, 1964; Thompson et al., 2005; McKee & Ostriker, 2007). In this equation c_{s} is the effective sound speed in the gas, κ is the epicyclic frequency, and Σ_{g} is the gas surface density.

These size scales correspond to that expected for (and in some cases observed; e.g., Tristram et al. 2007, 2009; Raban et al. 2009; Kishimoto et al. 2011), the dusty molecular torus that is thought to obscure the central regions of the AGN in inclined systems (e.g., as postulated in the unified AGN model; Antonucci 1993). That these structures should be on similar scales is unlikely to be a coincidence – the dense gaseous and dusty structure is potentially both the outer regions of the BH fuel supply and a stellar nursery. Indeed, the change from the galaxy potential to the BH potential can produce warps in the gas that could obscure the accretion disc (e.g., Hopkins & Quataert, 2010; Lawrence & Elvis, 2010); see also Bregman & Alexander (2009) for warping of the accretion disc due to dense cusps around the BH. However, even at these small scales, the gas still has to lose $\approx 99\%$ of its angular momentum before it reaches the sub-pc scale of the accretion disc.

Numerous studies have shown that young stars are often found in the central regions of nearby AGNs (e.g., Storchi-Bergmann et al., 2001, 2005; Cid Fernandes et al., 2004), suggesting a connection (causal or non causal) between AGN activity and star formation. Using spatially resolved spectroscopy of the central regions ($\approx 10\text{--}100 \text{ pc}$) of nine nearby Seyfert galaxies, Davies et al. (2007) provided compelling evidence for a *causal* connection between AGN and star-formation activity in at least some systems (see also González Delgado et al. 2001). Davies et al. (2007) showed that the peak AGN activity occurs $\approx 50\text{--}200 \text{ Myrs}$ after the onset of star formation (see also Schawinski et al. 2009; Wild et al. 2010, and §3.2.3). The time delay between the star formation and AGN activity suggests that the star-forming

region may provide the fuel for the BH, via winds from massive stars and supernovae (e.g., Vollmer et al. 2008; however, see Hopkins 2011).

These studies imply a complex interplay between AGN activity, star formation, and stellar winds in the vicinity of the BH. A wide range of analytical models, numerical simulations, and hydrodynamical simulations indeed predict that stellar winds and supernovae will enhance the BH mass accretion by injecting turbulence into the gas disc (e.g., Wada & Norman, 2002; Schartmann et al., 2009; Hobbs et al., 2011). However, the magnitude of the effect depends on the assumed prescriptions of the stellar-related outflows and the gas accretion timescales. For example, if the gas accretion timescale is long then the majority of the gas will collapse and form stars rather than be directly accreted onto the BH (e.g., King & Pringle, 2007; Nayakshin et al., 2009). In this scenario the gas accreted onto the BH will be predominantly from stellar-related outflows (e.g., SNe; AGB stars) and is therefore triggered after the initial starburst activity. Assuming that the stellar-mass loss is dominated by AGB stars, the BH accretion–star formation ratio would be $\approx 10^{-2}$ – 10^{-3} (e.g., Jungwiert et al., 2001). By contrast, on the basis of their multi-scale hydrodynamical simulation, Hopkins & Quataert (2010) argue that a precessing eccentric disc will form within ≈ 10 pc of the BH in gas-rich systems, which can efficiently deliver gas to the accretion disc. The rate of BH accretion and star formation within the central 10 pc in the Hopkins & Quataert (2010) model is approximately equal, and therefore ≈ 2 – 3 orders of magnitude larger than that predicted from stellar-mass loss.

While there is disagreement over how the gas is delivered to the accretion disc from ≈ 10 pc, it is clear that the gas inflow is complex and cannot be easily prescribed as a simple equation (e.g., Hopkins & Quataert, 2010; Power et al., 2011). A popular approach in the treatment of BH accretion in galaxy formation simulations is the Bondi-Hoyle method (Bondi & Hoyle, 1944; Bondi, 1952), which assumes spherical accretion onto the BH and therefore doesn’t consider angular-momentum limitations (e.g., Di Matteo et al., 2005; Springel et al., 2005a; Booth & Schaye, 2009). To address this simplification, Power et al. (2011) have produced a physically self-consistent BH accretion model suitable for galaxy formation simulations that accounts for the angular momentum of the gas. The difference between their model and Bondi-Hoyle accretion is quite striking – with the Bondi-Hoyle method, the BH is accreting almost continuously in gas-rich systems at high mass accretion rates while, by contrast, a sizeable fraction of

the gas in the Power et al. (2011) model collapses to form stars and the mass accretion rate onto the BH is comparatively negligible.

The effect of stellar-mass loss on the BH accretion can be explored in even greater detail using small-scale hydrodynamical simulations of a nuclear starburst in the vicinity of the BH. The current suite of simulations (e.g., Wada et al., 2009; Schartmann et al., 2009, 2010) generically predict that stellar and supernova ejecta inject turbulence into the accretion disc, “puffing” it up and forming an optically and geometrically thick molecular torus – a single supernova can effect the whole torus and enhance the mass-accretion rate (Wada et al., 2009). Radiative heating and pressure can slow down or stop the accretion process while radiative drag can enhance accretion. Kawakatu & Wada (2008) show that the fractional amount accreted decreases with an increase in the fuel supply since star formation in the disc itself can dominate over the growth of the BH; indeed, the presence of nuclear stellar rings close to the BH in nearby quiescent galaxies provide indirect evidence in support of this hypothesis (e.g., Nayakshin & Sunyaev, 2005; Bender et al., 2005; Paumard et al., 2006; Schödel et al., 2007; Hopkins & Quataert, 2010).

The hydrodynamical simulations also predict that the gas can cause significant time-variable obscuration in the vicinity of the BH (e.g., Wada & Norman 2002; Wada et al. 2009; see Hicks et al. 2009 for observational constraints). The predicted column densities and time-variable obscuration are in good agreement with those measured in nearby obscured AGNs ($N_{\text{H}} > 10^{22}$ – 10^{25} cm $^{-2}$ with absorbing column changes on < 1 year timescales; e.g., Risaliti et al. 1999, 2002; Guainazzi et al. 2005; Cappi et al. 2006). Taking the properties derived for the Seyfert 2 galaxy NGC 1068 from Davies et al. (2007), Schartmann et al. (2010) used a hydrodynamical simulation to make detailed predictions of the properties of the obscuring torus (see Table 1 of Schartmann et al. 2010 for the initial parameters). They found that the torus can be built up through the ejection of energy from stellar winds. Their model reproduced the dense obscuring structure observed from interferometric mid-IR observations on ≈ 0.5 – 1 pc and compares well with the extent and mass of the rotating disc inferred from H $_2$ O maser observations (e.g., Greenhill & Gwinn, 1997; Raban et al., 2009).

Connections between the accretion onto the BH and obscuration in AGNs can be explored using X-ray data and mid-IR observations, which will probe the central source and the obscuring region, respectively. Using high-spatial mid-IR imaging (typically probing < 100 pc scales), Horst et al. (2008, 2009) and Gandhi

et al. (2009) found a tight correlation between the unresolved mid-IR core and the absorption-corrected X-ray luminosities of nearby AGNs, even in the presence of extreme Compton-thick ($N_{\text{H}} > 10^{24} \text{ cm}^{-2}$) absorption (see Lutz et al. 2004 for similar constraints from mid-IR spectroscopy). These results indicate that the obscuring structure is directly heated by the AGN and furthermore they suggest that the covering factor of the obscuring material is broadly constant (at a given AGN luminosity; see Lawrence e.g., 1991; Simpson e.g., 2005 for evidence of a luminosity-dependent covering factor). These results are inconsistent with the simplest dusty torus models, which assume a smooth distribution of obscuring dust (e.g., Pier & Krolik, 1992; Granato & Danese, 1994; Efstathiou & Rowan-Robinson, 1995) and therefore predict that the mid-IR emission will be strongly absorbed in systems when the torus is inclined to the line of sight. However, these results are consistent with clumpy torus models (e.g., Nenkova et al., 2002; Elitzur & Shlosman, 2006; Nenkova et al., 2008; Schartmann et al., 2008; Hönig et al., 2006; Hönig & Kishimoto, 2010), which predict no inclination-angle dependence on the strength of the mid-IR emission (see Mullaney et al. 2011a for full IR SED constraints that also support this view); dust in the narrow-line region can also lead to isotropic dust emission (e.g., Efstathiou et al., 1995; Schweitzer et al., 2008).

The results presented in this section show that it is challenging to accurately predict the fate of the gas on $\approx 1\text{--}10$ pc scales. Generically, the current models predict that the gas inflow on these scales will lead to a complex interplay between AGN activity, star formation, and stellar winds. However, different models predict different rates of mass accretion and star formation. The current view of the AGN dusty torus is that of a structure more dynamic than that originally postulated in the unified AGN model (e.g., Antonucci, 1993). The AGN “torus” is potentially both the outer gas reservoir for the BH accretion disc and a nuclear stellar nursery, built from the gas inflow and stellar-related winds and outflows.

2.3. Mass accretion onto the black hole

The power house behind AGN activity is mass accretion onto the BH on $\ll 1$ pc scales. The basic theory of the accretion disc (the so-called α disc) has been around for almost 40 years (e.g., Shakura & Sunyaev, 1973). In the case of optically thick accretion, viscosity (the α parameter, which is a major cause of uncertainty) causes the gas to lose angular momentum and fall towards the BH, transporting the angular momentum outwards. The optically thick accretion disc is geometrically thin and

the energy spectrum is comprised of multi-temperature components, which reach their peak temperature at the centre (e.g., Pringle, 1981; Rees, 1984). The local effective temperature approximates to (e.g., Goodman 2003)

$$T_{\text{eff}} \approx 6.2 \times 10^5 \left(\frac{\lambda}{\epsilon_{0.1} M_8} \right)^{1/4} \left(\frac{r}{R_s} \right)^{-3/4} \text{ K}, \quad (4)$$

where λ is the Eddington ratio ($L_{\text{bol}}/L_{\text{Edd}}$; defined below), $\epsilon_{0.1}$ is the radiative efficiency in units of 0.1, M_8 is M_{BH} in units of $10^8 M_{\odot}$, r is the radius, and R_s is the Schwarzschild radius (i.e., the event horizon), defined for a spherical non-rotating BH as

$$R_s = \frac{2GM_{\text{BH}}}{c^2}. \quad (5)$$

The Eddington ratio ($\lambda = L_{\text{bol}}/L_{\text{Edd}}$) indicates the relative growth rate of the BH based on the AGN bolometric luminosity (L_{bol}) and the Eddington luminosity (L_{Edd}), defined as

$$L_{\text{Edd}} = \frac{4\pi GM_{\text{BH}} m_p c}{\sigma_T}, \quad (6)$$

where m_p is the mass of the proton and σ_T is the cross section of the electron. The Eddington luminosity is achieved when the outward radiation pressure equals the inwards gravitational force – if the Eddington luminosity is exceeded then (in the absence of an additional inward pressure) the gas is expelled; see Fig. 1 for the Eddington ratios of some nearby AGNs.

An alternative solution to the accretion-disc equations is the optically thin accretion disc, a state achieved at low mass accretion rates and generically referred to as Radiatively Inefficient Accretion Flows (RIAFs; e.g., Narayan & Yi 1994; Blandford & Begelman 1999). The optically thin accretion disc is unable to cool efficiently (the cooling time exceeds the accretion time) and the energy is lost through non-radiative processes such as convective transport of energy and angular momentum to large radii or an outflowing wind. Magnetic fields are likely to dominate viscosity and the transport of angular momentum in accretion discs, as suggested by numerical simulations of Magneto-Rotational Instability (MRI; e.g., Balbus & Hawley 1991, 1998; Balbus 2003).

Depending on the accretion disc viscosity and the mass accretion rate, the accretion disc is predicted to change between an optically thick and an optically thin state – the transition from optically thin to optically thick is likely to correspond to an Eddington ratio of $\lambda \approx 10^{-3}\text{--}10^{-2}$ (e.g., Esin et al., 1997; Gallo et al., 2003; Maccarone, 2003). However, despite the accretion disc being the ultimate source of power in AGNs, we lack the

observational data to robustly test these models. There are hints that the emission from AGNs deviates from the simplest accretion-disc models. For example, microlensing of the central parsec region of the accretion disc in a number of quasars (e.g., Pooley et al., 2007; Floyd et al., 2009) have shown that the continuum emission profile drops more quickly than expected from the basic α accretion-disc model but is broadly consistent with that predicted from MRI accretion-disc models (e.g., Agol & Krolik, 2000).

Fortunately, significantly better tests of the accretion-disc models are available for accreting stellar-mass BHs, so called X-ray binaries (XRBs), for several key reasons: (1) the data is typically of a significantly higher signal-to-noise ratio than that found for AGNs since many XRBs lie in the Galaxy, (2) the accretion-disc state of XRBs can change on timescales of less than a day in response to changes in the mass accretion rate, allowing for different accretion-disc components to be identified and analysed; by comparison the accretion-disc state of AGNs will vary on timescales of centuries (the timescale is a function of the BH mass; Mirabel & Rodríguez 1998),³ and (3) the accretion disc of XRBs peaks in the X-ray band (≈ 1 keV; $\approx 10^7$ K; see Eqn. 4), where it can be studied in great detail using the current generation of X-ray telescopes. By comparison the accretion disc of AGNs peaks at far-UV wavelengths (≈ 10 eV; $\approx 10^5$ K; see Eqn. 4), where the emission is absorbed by the interstellar medium in the Galaxy. Despite these observational challenges in comparing AGNs and XRBs, there is good evidence that the accretion process is essentially the same for both small and large BHs and we can therefore use studies of XRBs to better understand mass accretion in AGNs (e.g., Merloni et al., 2003; Falcke et al., 2004; McHardy et al., 2006).

2.3.1. Accretion onto stellar-mass black holes

The X-ray spectra of XRBs are typically classified into “X-ray states”, which qualitatively describe their behaviour and broadly relate to the properties of the accretion disc (e.g., see Table 2 of Remillard & McClintock 2006) – a low-hard state, where the majority of the X-ray emission is produced at > 10 keV and a high-soft state, where the emission is strong at < 10 keV but weak at > 10 keV. An individual XRB can be seen to traverse from one X-ray state to another on timescales of less than a day in response to changes to the BH

³The X-ray variability of AGN seen on intra-day timescales is related to the mass accretion but is unrelated to the accretion-disc state (e.g., Ulrich et al., 1997; Vaughan et al., 2003; Uttley et al., 2005).

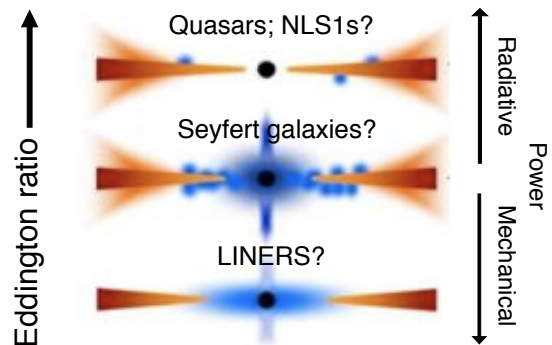


Figure 3: Schematic diagrams to illustrate the expected range of BH accretion modes as a function of Eddington ratio. The orange-red regions refer to the optically thick accretion disc and the blue regions refers to the X-ray “corona”. Adapted from the figure produced for X-ray binaries by Done, Gierlinski, & Kubota (2007) and revised to show how the various optical spectroscopic classes of AGNs might correspond to the different BH accretion modes and the dominate release of energy (radiative or mechanical; i.e., predominantly due to jets).

accretion rate (e.g., Nowak, 1995; Done et al., 2007). At high Eddington ratios ($\lambda \gtrsim 10^{-2}$) the X-ray emission is often dominated by a disc-like spectrum, assumed to be due to an optically thick accretion disc, with a weaker power-law continuum component. At low Eddington ratios ($\lambda \lesssim 10^{-2}$) the hard X-ray spectrum is dominated by the power-law continuum and has a weak disc-like spectrum; however, the conversion from the high-soft to the low-hard state is more complex than that briefly implied here and should not be taken as definitive (e.g., see Remillard & McClintock 2006 and Done et al. 2007 for a more in-depth discussion). In the high-soft state the accretion disc is optically thick, and therefore viscous, and emits a thermal spectrum, while in the low-hard state the accretion disc is optically thin and radiatively inefficient and the X-ray emission is dominated by the inverse Compton scattering of photons from the outer regions of the accretion disc (but can also have significant contributions from synchrotron emission and synchrotron self-Compton emission). Further X-ray states have also been identified, such as an intermediate very-high state (see Table 2 of Remillard & McClintock 2006), which likely correspond to differing contributions from the accretion disc, inverse Compton scattering, and an associated jet.

The radio emission from XRBs is found to be linked to the X-ray state (e.g., Fender et al., 2004). The radio emission is bright in the low-hard state and increases in luminosity in response to an increase in the Eddington ratio up until the low-hard-high-soft state transi-

tion at $\lambda \approx 10^{-2}$. The radio emission dramatically declines when the XRB traverses to the high-soft state (e.g., Gallo et al., 2003; Fender et al., 2004). The radio emission is consistent with that expected from a synchrotron emitting jet and the change in the radio power is possibly due to the scale height of the accretion disc (which is geometrically thick in the optically thin state) and provides the seed electrons to drive the jet.⁴ The jets in XRBs generate large amounts of mechanical energy which can have a significant effect on the surrounding interstellar medium.

The most luminous XRBs have X-ray luminosities $> 10^{39}$ erg s⁻¹ and are called ultra-luminous X-ray sources (ULXs). ULXs likely comprise a heterogeneous population (see King et al. 2001; Begelman 2002; Roberts 2007 and Gladstone et al. 2009 for a broader discussion of the nature of ULXs), of which a sizeable fraction are stellar-mass BHs accreting at super-Eddington rates. ULXs therefore provide direct insight into the properties of accretion discs at extreme mass accretion rates. The X-ray spectra of many ULXs can be fitted with an accretion-disc spectrum and an optically thick “corona” (e.g., Stobbart et al., 2006). However, the identification of the soft X-ray emission from the accretion disc in the presence of the large amounts of absorption inferred by the optically thick corona appears to be contradictory. A more physically plausible explanation is that the optically thick corona is an outflowing wind, launched in the vicinity of the accretion disc but more extended than the accretion disc and therefore not directly obscured. Hydrodynamical simulations of BHs accreting at super-Eddington rates indeed predict the presence of a radiatively driven high-column density wind (Ohsuga et al., 2005; Ohsuga, 2007), providing indirect support for this model. The potential impact of these winds can be seen from the production of “bubbles” or emission-line “nebulae” over ≈ 100 pc scales (e.g., Roberts et al., 2003; Pakull et al., 2010). These emission-line nebulae may be analogous to those seen in AGNs (i.e., the narrow-line region; e.g., Wilson et al. 1988; Schmitt & Kinney 1996).

2.3.2. Accretion onto massive black holes

The accretion-disc in AGNs peak at far-UV wavelengths, where we lack direct observational constraints due to absorption by interstellar gas in the Galaxy. However, the properties of the AGN accretion disc can be

⁴Strong radio-emitting XRBs have traditionally been called micro-quasars (e.g., Mirabel et al., 1992; Mirabel & Rodríguez, 1994, 1998) but it now appears likely that they are just the radio-bright subset of the XRB population.

indirectly inferred from the strength of the UV and optical emission lines. The UV continuum is efficient at photoionising the gas since the majority of the atomic transitions occur at energies corresponding to UV wavelengths. On the basis of this, the low-ionisation emission lines produced by Low-Ionised Nuclear Emission-line Regions (LINERs; e.g., Heckman 1980; Baldwin et al. 1981) would correspond to the low-hard power-law dominated state while the high-ionisation emission lines produced by Seyfert galaxies and quasars would correspond to the high-soft accretion-disc dominated state (e.g., Kewley et al., 2006; Sobolewska et al., 2011); see Fig. 3.

A major source of uncertainty in AGN studies is the mass-accretion rate, which requires an accurate estimate of the AGN bolometric luminosity. Since the majority of the accretion-disc emission in AGNs is produced at far-UV wavelengths, the AGN bolometric luminosity is typically determined using the continuum emission in a given wave band (L_λ ; typically at X-ray or optical wavelengths) with a wavelength dependent bolometric correction factor (BC_λ) applied to calculate the total radiative output (e.g., Elvis et al., 1994; Marconi et al., 2004; Hopkins et al., 2007); i.e.,

$$L_{\text{bol}} = L_\lambda BC_\lambda. \quad (7)$$

The majority of studies assume an optically thick accretion disc when determining BC. However, as shown for XRBs, an optically thick accretion disc is only likely to be valid at comparatively high Eddington ratios ($\lambda \gtrsim 10^{-2}$ – 10^{-3}) and therefore the mass-accretion rates estimated in studies of low-Eddington ratio AGNs will be wrong. Indeed by fitting the X-ray–optical SEDs of nearby AGNs, interpolating at UV wavelengths, Vasudevan & Fabian (2007, 2009) have shown that the AGN bolometric correction may be a strong function of the Eddington ratio: the X-ray–bolometric conversion factors change from ≈ 15 – 60 for Eddington ratios of $\lambda \approx 10^{-3}$ – 1 . The dominant factor in variations in the SEDs and emission-line properties of quasars may also be due to the Eddington ratio (e.g., Sulentic et al., 2000; Kuraszekiewicz et al., 2009).

Even greater insight into the bolometric output of AGNs can be made by carefully fitting the X-ray and optical spectra with physically motivated models. Recent work has focused on fitting the X-ray spectra of AGNs with an accretion disc, power law, and Compton component while taking account of the various stellar and AGN components in the optical spectra to search for connections between the underlying physical processes (e.g., Jin et al., 2009; Sobolewska et al., 2011). Hutton

et al. (in prep) have taken this approach for AGNs identified in the SDSS (e.g., York et al., 2000; Abazajian et al., 2009) with excellent-quality X-ray data obtained from the *XMM-Newton* serendipity survey (e.g., Watson et al., 2009). A wide diversity of X-ray–optical SEDs are found, which would otherwise not be apparent from the X-ray data alone. There is some evidence for correlations of the strength of the X-ray emitting components and the width of the $H\beta$ emission line. However, since AGNs vary significantly in the X-ray band, contemporaneous X-ray and UV-optical data are required to account for intrinsic variations (e.g., Vasudevan & Fabian, 2009).

2.3.3. *Sgr A* : the closest accreting massive black hole*

The closest massive BH to us is Sgr A*, which lies at a distance of ≈ 8.3 kpc in the centre of the Galaxy (e.g., Reid, 1993; Melia & Falcke, 2001; Gillessen et al., 2009). The BH mass of Sgr A* has been measured to unprecedented accuracy using ≈ 16 yrs of monitoring of the orbits of stars in the vicinity of Sgr A*: $M_{\text{BH}} = (4.3 \pm 0.2) \times 10^6 M_{\odot}$ (Gillessen et al. 2009; see also Ghez et al. 2008). Sgr A* produces emission over a broad waveband (radio–X-ray; e.g., Marrone et al. 2008; Dodds-Eden et al. 2011). However, with an estimated Eddington ratio of $\lambda \approx 10^{-8}$ – 10^{10} (e.g., Melia & Falcke, 2001; Eckart et al., 2006), Sgr A* is ≈ 5 – 8 orders of magnitude below the optically thick–optically thin accretion state and is only identifiable as “active” due to its proximity. For example, none of the AGNs and LINERs investigated in the nearby galaxy sample of (Ho et al., 1997a) have Eddington ratios of $\lambda < 10^{-8}$ (see Fig. 9 of Ho 2008), indicating that Sgr A* is in a quiescent state. Sgr A* therefore provides unique insight into low mass-accretion events onto a massive BH.

The broad-band emission from Sgr A* appears to have at least two components (e.g., Dodds-Eden et al., 2011) – a continuously emitting “quiescent” state and a flaring state. The flares are often quasi-periodic and can vary on short timescales (e.g., Baganoff et al., 2001; Genzel et al., 2003; Ghez et al., 2004; Marrone et al., 2008; Dodds-Eden et al., 2011); the radio–near-IR spectral energy distribution of the flares observed in Sgr A* are consistent with synchrotron emission from transiently heated electrons (e.g., Markoff et al., 2001; Gillessen et al., 2006; Trippe et al., 2007; Eckart et al., 2009; Dodds-Eden et al., 2010, 2011). The origin of the flaring emission is a topic of hot debate and may be due to an orbiting hot spot, magnetic heating/reconnection, stochastic acceleration processes, or accretion-rate enhancements (e.g., Markoff et al., 2001; Liu & Melia, 2002; Yuan et al., 2003; Dodds-Eden et al., 2011). The

modest BH accretion rates inferred by the emission from Sgr A* are consistent with that expected from the mass loss of stars in the Galactic centre (e.g., Cuadra et al., 2006, 2008).

On the basis of the current mass accretion rate onto Sgr A*, it would take ≈ 5 – 6 orders of magnitude longer than the Hubble time to grow the BH to its current mass, indicating that Sgr A* must have been orders of magnitude more active in the past. The identification of reflected X-ray emission off molecular clouds in the vicinity of Sgr A* provides a potential “X-ray echo” of past activity from Sgr A*. These data suggest that Sgr A* may have been up-to ≈ 3 orders of magnitude brighter ≈ 100 years ago (e.g., Munro et al., 2007; Ponti et al., 2010). However, these implied mass accretion rates are still extremely modest and Sgr A* must have been much more luminous in the past (Nayakshin et al., 2007); see Micic et al. (2011) for potential BH growth histories for Sgr A*.

3. What are the links between black-hole growth and their host galaxies and large-scale environments?

In the previous section we discussed the mechanics and processes of gas inflow from the host galaxy down to the central BH, across > 5 orders of magnitude in size scale. The BH–spheroid mass relationship implies that this, otherwise seemingly unlikely journey of gas inflow, has occurred in all spheroid-hosting galaxies at some point over the last ≈ 13 Gyrs. The tightness of the BH–spheroid mass relationship further suggests a connection between AGN activity and star formation over kpc scales. In this section we explore the triggering mechanisms and sites of AGN activity and investigate the connection between AGN activity, star formation, and large-scale environment. We also investigate the growth of BHs across cosmic time and explore how the properties and triggering of distant AGN activity differs from that found in the local Universe.

3.1. *The identification of AGN activity*

To accurately explore when, where, and how the growth of BHs has been triggered requires the identification of AGN activity across all environments and redshifts. The presence of dust and gas in the vicinity of the BH and star-forming regions along the line of sight means that penetrating observations are required to unambiguously reveal the signatures of AGN activity in all systems. The emission from star formation and starlight in the host galaxy can also dilute and mask the emission

from the AGN. These complications make the construction of a complete census of AGN activity a significant challenge.

The most extensive studies of AGN activity in the local Universe have utilised optical spectroscopy (e.g., Huchra & Burg, 1992; Maiolino & Rieke, 1995; Ho et al., 1997a,c,b; Kauffmann et al., 2003; Heckman et al., 2004; Ho, 2008). Since the AGN narrow-line region extends beyond the obscured central region (≈ 10 – 1000 pc versus ≈ 1 – 10 pc), optical spectroscopy is able to identify even heavily obscured AGNs, so long as the AGN narrow emission lines are not obscured by dust in the host galaxy. Sensitive radio, mid-IR spectroscopy, and X-ray observations (particularly at > 10 keV; e.g., Sazonov et al. 2007; Winter et al. 2009; Burlon et al. 2011) further extend our understanding and census of nearby AGN activity, providing the identification of AGNs even in the presence of significant host-galaxy dust and star formation (e.g., Ho et al., 2001; Ulvestad & Ho, 2002; Filho et al., 2006; Satyapal et al., 2008; Goulding & Alexander, 2009; Zhang et al., 2009; Winter et al., 2010; Nardini et al., 2010). From a combination of these multi-wavelength identification techniques, we are now close to a complete census of AGN activity in the local Universe down to a given sensitivity limit (i.e., lower-luminosity AGNs can still be unidentified). However, even intrinsically luminous AGNs can remain unidentified if the obscuration towards the BH is extremely high and the central region is heavily obscured by dust in the host galaxy (see the conflicting evidence for Arp 220; Clements et al. 2002; Spoon et al. 2004; Iwasawa et al. 2005; Downes & Eckart 2007). It is important to bear in mind these potential limitations.

Optical spectroscopy is also effective at identifying distant obscured AGNs (e.g., Steidel et al., 2002; Polletta et al., 2006; Alexander et al., 2008b; Juneau et al., 2011; Yan et al., 2011). However, since many of the key AGN emission-line diagnostics move into the near-IR band at $z \gtrsim 0.4$, optical spectroscopy alone can be quite limited in identifying large numbers of AGNs (but see Juneau et al. 2011; Yan et al. 2011; Trouille et al. 2011 for techniques that extend the utility of optical spectroscopy for AGN identification out to $z \approx 1$).⁵ Currently the most efficient and effective identification of distant AGNs is made with X-ray observations, which

⁵The optical signatures of distant AGNs are also more easily diluted from host-galaxy emission than nearby AGNs due to the larger angular-size distance for distant systems and the overall increase in star-formation activity at higher redshift (e.g., Noeske et al., 2007; Daddi et al., 2007b; Pannella et al., 2009; Rodighiero et al., 2010a; Elbaz et al., 2011).

can select AGNs almost irrespective of the presence of obscuration (e.g., Bauer et al., 2004; Tozzi et al., 2006; Gilli et al., 2007). X-ray observations are effective at identifying AGN activity because the X-ray emission from star formation is typically weak; the positive K correction at X-ray energies for distant obscured AGNs also means that < 10 keV observations are particularly effective at identifying heavily obscured AGNs at high redshift (e.g., Tozzi et al., 2006; Alexander et al., 2011; Comastri et al., 2011; Feruglio et al., 2011). Sensitive IR and radio observations can further extend the census of distant AGN activity by identifying AGNs where the absorbing column densities are so high that not even X-ray photons can escape (e.g., Lacy et al., 2004; Stern et al., 2005; Donley et al., 2005, 2008; Alonso-Herrero et al., 2006; Daddi et al., 2007a; Hickox et al., 2007; Fiore et al., 2008, 2009; Bauer et al., 2010; Luo et al., 2011). However, since star formation can also produce luminous IR and radio emission, it is often challenging to disentangle the AGN emission from that of the host galaxy (e.g., Polletta et al., 2007; Mullaney et al., 2011a).

Differences in the various approaches in AGN identification can also make it challenging to reconcile results from different studies. It is therefore important to always consider how obscuration or host-galaxy emission can effect the completeness of any AGN selection technique. In the following sub sections we explore the processes of AGN activity using observations at X-ray, optical, IR, and radio wavelengths. We investigate the ubiquity of AGN activity, the AGN triggering mechanisms, the connection between AGN activity and star formation, the evolution of AGN activity with redshift, and the role of environment in the triggering of AGN activity.

3.2. AGN activity in the local Universe

3.2.1. Where are the massive black holes growing?

AGN activity is common in the local Universe, with ≈ 5 – 10% of nearby galaxies found to clearly host optical AGN activity (i.e., identified as Seyfert galaxies from their optical emission-line properties; e.g., Veilleux & Osterbrock 1987; Kewley et al. 2001, 2006; Maiolino & Rieke 1995; Ho et al. 1997a; Hao et al. 2005). The optical AGN fraction can be significantly higher if galaxies with Low-Ionisation Nuclear Emission Regions (LINERs; Heckman 1980) are also taken into account (e.g., Ho et al., 1997a). However, LINERs comprise a heterogeneous mix of composite AGN–star-forming galaxies, optically obscured AGNs, low-luminosity AGNs, and early type galaxies without AGN

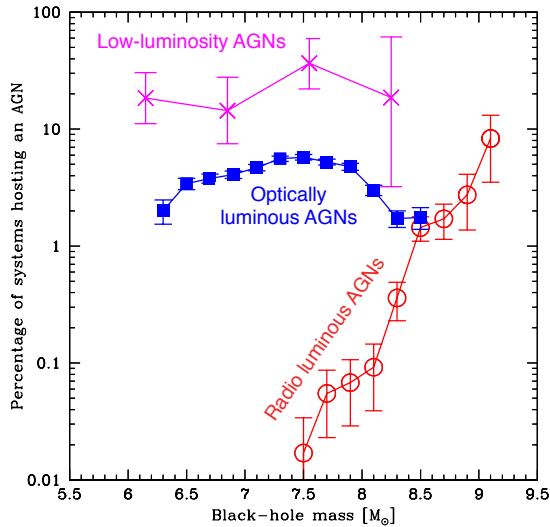


Figure 4: AGN fraction as a function of BH mass for different AGN selection approaches: optically identified luminous AGNs (filled squares; Best et al. 2005), lower-luminosity AGNs (crosses; Goulding et al. 2010), and radio-luminous AGNs (open circles; Best et al. 2005).

activity (e.g., Binette et al., 1994; Ho et al., 2001, 2003; Eracleous et al., 2002; Satyapal et al., 2004; Kewley et al., 2006; Shields et al., 2007; González-Martín et al., 2009; Goulding & Alexander, 2009; Sarzi et al., 2010; Capetti & Baldi, 2011), leaving some ambiguity over the true AGN fraction in the LINER population. Mid-IR spectroscopy can provide a more complete census of nearby AGN activity than that obtained from optical spectroscopy due to the identification of high-excitation emission lines (e.g., $[\text{Ne V}]\lambda 14.3 \mu\text{m}$) in systems where the narrow-line region is obscured by dust in the host galaxy (e.g., Satyapal et al., 2008; Goulding & Alexander, 2009; Tommasin et al., 2010; Petric et al., 2011a). However, at present, the number statistics obtained from high-resolution mid-IR spectroscopy are poor compared to those achieved from optical spectroscopy (samples of tens rather than thousands of objects).

The fraction of galaxies hosting AGN activity provides a measure of the duty cycle of BH growth. The fraction of local galaxies hosting AGN activity as a function of BH mass is shown in Fig. 4. The fraction of galaxies hosting optically luminous AGN activity ($L_{[\text{O III}]}$ $> 3 \times 10^7 L_{\odot}$, equivalent to a 2–10 keV luminosity of $L_X \gtrsim 10^{43} \text{ erg s}^{-1}$, assuming the conversion of Mulchaey et al. 1994) is approximately flat at $\approx 5\%$ over $M_{\text{BH}} \approx (0.3\text{--}10) \times 10^7 M_{\odot}$ and drops substantially to lower and higher BH masses (e.g., Best et al., 2005). The AGN fraction rises towards lower AGN luminosi-

ties, as expected since there will always be more low-accretion rate systems than high-accretion rate systems. For example, the fraction of galaxies hosting AGN activity ≈ 3 orders of magnitude fainter than the optically luminous AGNs is $\approx 20\text{--}30\%$ over $M_{\text{BH}} \approx (0.1\text{--}10) \times 10^7 M_{\odot}$ (e.g., Goulding et al., 2010). Note that Sgr A*, the active BH at the centre of the Galaxy is still ≈ 4 orders of magnitude fainter than these sensitivity limits! By contrast, the fraction of galaxies hosting luminous radio AGN activity ($L_{1.4\text{GHz}} > 10^{24} \text{ W Hz}^{-1}$) is strongly dependent on the BH mass, rising from $\lesssim 0.1\%$ at $M_{\text{BH}} < 10^8 M_{\odot}$ (where optical and mid-IR identified AGNs are common) to $\approx 10\%$ at $M_{\text{BH}} > 10^9 M_{\odot}$ (e.g., Best et al., 2005). Luminous radio AGNs represent the minority of the AGN population at all redshifts (radio-loud AGNs account for $\lesssim 10\%$ of the total AGN energy budget and cosmological BH growth) but they are likely to have played a crucial role in the evolution of the most massive galaxies and BHs (e.g., Bower et al. 2006; Croton et al. 2006; Merloni & Heinz 2008; see §5.1).⁶

These suite of results show that mass accretion onto the BH occurs relatively frequently in nearby galaxies. However, the AGN fraction does not reveal how quickly the BHs are growing, which requires a measurement of the mass accretion rate and Eddington ratio (see Eqn. 1 & 6 and Fig. 1). Using a broad range of methods to estimate BH masses and adopting the $[\text{O III}]\lambda 5007$ or $[\text{O IV}]\lambda 25.9 \mu\text{m}$ luminosity as a proxy for the mass accretion rate, the majority of AGNs in the local Universe have Eddington ratios of $\lambda \approx 10^{-6}\text{--}10^{-3}$, with a small tail towards higher Eddington ratios (see Fig. 9 of Ho 2008; Goulding et al. 2010; see also Fig. 1). Since the growth time (i.e., the time to double in mass) of a BH with an Eddington ratio of $\lambda \approx 10^{-3}$ is comparable to the age of the Universe (see Eqn. 10 in §4.3), these range of Eddington ratios are modest and suggest that the majority of the massive BHs in the local Universe must have grown more rapidly in the past. However, these results can also be a bit misleading since there is a small but very significant tail of AGNs with much higher Eddington ratios. Indeed, $\approx 50\%$ of the mass accretion onto BHs in the local Universe is found to occurred at high Eddington ratios of $\lambda > 0.1$, despite these systems only comprising $\approx 0.2\%$ of the optically identified AGN population (Heckman et al., 2004)! These results therefore

⁶Radio-loud AGNs are typically identified on the basis of luminous radio emission (e.g., $L_{1.4\text{GHz}} \gtrsim 10^{24} \text{ W Hz}^{-1}$) which is not due to star-formation activity. By comparison, the term “radio-quiet AGNs” refers to the majority of the X-ray, optical, and IR selected AGN populations, which are not luminous at radio wavelengths.

suggest that, while the vast majority of the massive BHs in the local Universe are growing slowly (potentially in the optically thin accretion mode), at least half of the mass accretion in the local Universe occurs in the optically thick accretion-disc mode (see §2.3 and Fig. 3).

AGN activity is transient and therefore the measured Eddington ratio of an individual object only provides a snapshot of its growth path. We clearly cannot watch an individual BH grow over Myrs of time to determine its time-average growth but we can measure the volume-average Eddington ratio of a group of systems, which will provide an *average* (and therefore typical) BH growth rate. On the basis of optical spectroscopy from the SDSS, Heckman et al. (2004) showed that the volume-average Eddington ratio for optically identified AGNs in the local Universe is inversely proportional to the BH mass; see Fig. 1 for a graphical representation of this result. The volume-average BH growth time for the lowest-mass BHs ($M_{\text{BH}} \approx 10^7 M_{\odot}$) is comparable to the age of the Universe, implying that their BHs have been growing steadily over cosmic time; Goulding et al. (2010) extended this work to lower BH masses and showed that the most rapidly growing BHs in the local Universe reside in late-type galaxies with low-mass BHs ($M_{\text{BH}} \approx 10^6\text{--}10^7 M_{\odot}$), many of which lack the clear optical signatures of AGN activity. By comparison, more massive BHs with $M_{\text{BH}} \gtrsim 10^8 M_{\odot}$ are typically growing $\approx 1\text{--}3$ orders of magnitude more slowly than the lower-mass BHs and must have undergone their dominant growth phases at higher redshifts. Kauffmann & Heckman (2009) extended these results by providing evidence for distinct regimes of BH fuelling in the local Universe. They showed that optically identified AGNs with significant star formation in the central kpc have a lognormal distribution of Eddington ratios (with the peak at an Eddington ratio of $\lambda \approx 10^{-2}$) while more quiescent AGNs were found to have a power-law distribution of Eddington ratios, where the BH accretion rate depends on the stellar spheroid mass and the ages of the stars in the bulge. The active and quiescent systems are broadly split on the basis of BH mass: the active systems have $M_{\text{BH}} \lesssim 10^8 M_{\odot}$ while the quiescent systems have $M_{\text{BH}} \gtrsim 10^8 M_{\odot}$. On the basis of these results, Kauffmann & Heckman (2009) argued that the BHs in the active systems are driven by a plentiful supply of cold gas while the BHs in the more massive quiescent systems are driven by stellar-mass loss in evolved stars, having presumably consumed their cold-gas supplies at higher redshift.

3.2.2. Is black hole and galaxy growth connected?

The BH–spheroid mass relationship in the local Universe suggests that AGN activity should be found in spheroid-hosting galaxies. Indeed, the majority of optically identified AGNs reside in comparatively early type galaxies (E–Sb galaxy morphologies; e.g., Ho 2008; Gadotti & Kauffmann 2009). However, a substantial fraction of the AGN population is also hosted in late-type galaxies (Sc–Sm). This was a somewhat unexpected result since late-type galaxies host pseudo bulges rather than classical spheroids (e.g., Kormendy & Kennicutt, 2004), and are therefore not expected to typically host massive BHs (since the BH–spheroid mass relationship is defined for galaxies with classical spheroids). Focused investigations have indeed shown that there are no significant correlations between BH mass and pseudo bulge luminosity (e.g., Greene et al., 2008; Jiang et al., 2011; Kormendy et al., 2011). The identification of growing BHs in late-type galaxies therefore suggests a different growth path to systems that host classical spheroids; for example, it is possible that these late-type systems have never undergone a galaxy major merger, and a non-negligible fraction of the BH mass may be from the massive BH seed formation (e.g., Kormendy & Kennicutt 2004; Volonteri & Natarajan 2009; see §4.3 for the discussion of the formation of massive BHs). AGNs hosted in late-type galaxies are often not revealed at optical wavelengths and mid-IR spectroscopy or hard X-ray observations are required to unambiguously identify them (e.g., Ho, 2008; Satyapal et al., 2008; Goulding & Alexander, 2009; Koss et al., 2011): the presence of dust and star formation in the host galaxy often dilute or extinguish the optical AGN signatures.

The host-galaxy properties of radio-loud AGNs are connected to their optical spectral properties. Radio-loud AGNs with low-excitation optical spectra (i.e., LINER classifications) are mostly found in massive red early type galaxies, while radio-loud AGNs with high-excitation optical spectra (i.e., Seyfert and quasar classifications) are typically hosted in less massive gas-rich galaxies (e.g., Willott et al., 2001; Chiaberge et al., 2005; Evans et al., 2006; Hardcastle et al., 2006, 2007; Baldi & Capetti, 2008; Kauffmann et al., 2008; Smolčić, 2009; Smolčić et al., 2009; Herbert et al., 2010; Smolčić & Riechers, 2011). To first order the high-excitation radio-loud AGNs are high-accretion rate systems and are believed to evolve strongly with redshift, a behaviour that would be similar to radio-quiet Seyfert galaxies and quasars; see §3.3.1. By contrast, low-excitation radio-loud AGNs are low-accretion rate systems, evolve slowly with redshift, and are the dominant radio-galaxy

population in the local Universe (e.g., Sadler et al., 2007; Smolčić et al., 2009). The low-excitation systems are the dominant radio-loud AGN population at modest radio luminosities ($L_{1.4\text{GHz}} \lesssim 3 \times 10^{25} \text{ W Hz}^{-1}$) and also dominate the global energetic output from radio galaxies (e.g., Hardcastle et al., 2007); these systems are typically classified as FR I radio galaxies (Fanaroff & Riley, 1974) and are important for the “radio-mode” AGN feedback (e.g., Merloni & Heinz 2008; see §5.1). The high-excitation systems are typically classified as FR II radio galaxies and typically have the highest radio luminosities but are comparatively rare at all redshifts.

The tightness of the BH–spheroid mass relationship suggests that galaxies hosting classical spheroids grew in concert with their BHs (i.e., for every ≈ 1000 units of star formation there is ≈ 1 – 2 units of BH accretion). As shown in §2.2, a direct link between star formation and AGN activity on ≈ 10 pc scales may be expected given that both processes are driven by the availability of cold gas on nuclear scales. However, a connection between AGN activity and star formation on the kpc scales of the galaxy spheroid is not expected *a priori* since the vast difference in size scale would preclude a direct causal link. Indeed, although the host galaxies of many AGNs are undergoing star-formation activity, there is large scatter in the observed AGN:star formation ratio (e.g., Netzer et al., 2007; Wild et al., 2007; Baum et al., 2010; Diamond-Stanic & Rieke, 2011). The scatter decreases when the star-formation rate is measured over < 1 kpc scales (e.g., Wild et al., 2007; Diamond-Stanic & Rieke, 2011), and is predicted to decrease yet further at smaller spatial scales, where a causal connection is expected between the gas that drives star formation and the gas that fuels the BH (e.g., Hopkins & Quataert, 2010). Despite this, using optical spectroscopy from the SDSS, Heckman et al. (2004) showed that the *volume-average* galaxy–BH growth rate is broadly consistent with that expected from the BH–spheroid mass relations (a factor of ≈ 1000) across kpc scales (i.e., the typical size scales corresponding to the SDSS fibres), for a wide range of BH masses (see Fig. 5 of Heckman et al. 2004).

The fraction of galaxies hosting AGN activity is correlated to the IR luminosity (8 – $1000 \mu\text{m}$) or star-formation rate, indicating a connection between the duty cycle of BH growth and the growth of the galaxy. On the basis of optical spectroscopy alone, the AGN fraction rises from $\approx 5\%$ for galaxies with $L_{\text{IR}} < 10^{11} L_{\odot}$ to $\approx 15\%$ for Luminous IR Galaxies (LIRGs; $L_{\text{IR}} \approx 10^{11}$ – $10^{12} L_{\odot}$) and $\approx 25\%$ for Ultraluminous IR Galaxies (ULIRGs; $L_{\text{IR}} > 10^{12} L_{\odot}$; e.g., Kim et al. 1998; Veilleux et al. 1999; Tran et al. 2001). However, optical spectroscopy does not identify all of the AGNs and

these AGN fractions increase to ≈ 50 – 80% in the LIRG and ULIRG populations when including mid-IR spectroscopy and X-ray data for the identification of AGNs (e.g., Alexander et al., 2008a; Lehmer et al., 2010; Nardini et al., 2010; Alonso-Herrero et al., 2011; Nardini & Risaliti, 2011). These results show that the BH grows almost continuously during periods of intense star formation.

3.2.3. How is AGN activity triggered?

Central to our understanding of the growth of BHs is the determination of the large-scale physical mechanisms that trigger the gas inflow towards the BH – either external (galaxy mergers or interactions) or internal (gas instabilities, galaxy bars, etc; see §2.1 and Fig. 2) processes. Internal processes and galaxy interactions are often referred to as “secular evolution” and can be further divided into internal secular evolution and external secular evolution, respectively (see Fig. 1 of Kormendy & Kennicutt 2004). An accurate determination of the fraction of AGN activity driven by these different processes is non trivial since it depends on the depth of the data, the spatial resolution of the data, the assumptions used on how the observed data relates to the triggering mechanism, and how the AGN activity is identified. Furthermore, given the gas-inflow times, there can be a significant delay between the initial triggering event and the onset of AGN activity (≈ 50 – 500 Myrs; e.g., Davies et al. 2007; Schawinski et al. 2009; Wild et al. 2010); see §2.1–2.2. These complications mean that it can be difficult reconciling the results from one study with the results from another study, let alone accurately measuring the true fraction of AGN activity that is triggered by external or internal processes.

For example, even in the local Universe there are large differences between published studies. Using morphological classifications of SDSS galaxies from the Galaxy Zoo project (Lintott et al., 2011), Darg et al. (2010) estimated that only $\approx 1\%$ of AGNs reside in systems clearly undergoing a major merger. By comparison, on the basis of a hard X-ray selected AGN sample (from the *Swift*-BAT survey; Tueller et al. 2008, 2010), Koss et al. (2010) estimated the rate of major mergers to be $\approx 20\%$; the fraction rises to $\approx 50\%$ if galaxy interactions are also included. Part of the discrepancy in the estimated rate of major mergers between these studies may be due to the AGN identification method, since the *Swift*-BAT AGN survey finds AGNs that lack unambiguous optical AGN signatures (e.g., Winter et al., 2009) and may probe higher intrinsic luminosities than the optical samples (Koss et al., 2011). Still, a factor ≈ 20 difference seems difficult to reconcile from

the AGN selection method alone. In another example, Liu et al. (2011) looked at the frequency of AGN pairs within $\approx 5\text{--}100$ kpc in the SDSS and found that $\approx 4\%$ of optically identified AGNs are found in pairs. However, only $\approx 30\%$ of these AGN pairs clearly showed the morphological features of a major merger, even though the host galaxies appear to be in the process of a galaxy merger or interaction. The depth of the imaging data used to identify the morphological signatures of major mergers can clearly have a large effect on the results. Using deep imaging data, Schawinski et al. (2010) identified the faint morphological signatures of galaxy major mergers in $> 50\%$ of blue early type galaxies (these weak features often referred to as “shells”; Malin & Carter 1983; Hernquist & Spergel 1992; Turnbull et al. 1999), which were not apparent in shallower data.

Spectroscopy can provide an alternative route to estimating the fraction of systems in major mergers by identifying systems with evidence for close-pair AGN activity. The identification of double peaked emission lines (broad or narrow) with significant velocity offset can indicate a binary system or a BH gravitational recoil (e.g., Volonteri, 2007; Komossa et al., 2008; Colpi & Dotti, 2009; Dotti et al., 2009; Civano et al., 2010; Robinson et al., 2010; Smith et al., 2010; Rosario et al., 2011; Barrows et al., 2011); however, see Dotti & Ruszkowski (2010) and Shen et al. (2011) for alternative interpretations of the presence of double-peaked emission lines. On the basis of the incidence of double-peaked emission lines, Comerford et al. (2009) estimated a $\approx 30\%$ merger fraction, similar to the upper end of merger fractions estimated from imaging data.

These suite of studies highlight the difficulties in accurately quantifying the triggering mechanism of AGN activity. Major mergers clearly occur and trigger AGN activity but there are significant uncertainties in the interpretation of the data; indeed, systems with classical spheroids may have undergone at least one major-merger event at some time during the past (e.g., Bournaud et al., 2005; Hopkins et al., 2010). Conversely, AGN activity is also clearly often triggered by galaxy interactions and internal processes (e.g., Malkan et al., 1998; Kuo et al., 2008; Ellison et al., 2011). An example of an AGN population where the majority of the BH growth may be *entirely* driven by secular processes are narrow-line Seyfert 1 galaxies (NLS1s), a subset of the Seyfert 1 population with comparatively narrow broad emission lines (permitted broad-line widths of $\approx 500\text{--}3000$ km s $^{-1}$; e.g., Osterbrock & Pogge 1985). The majority of NLS1s reside in galaxies with pseudo bulges, in contrast to the classical spheroids hosted by typical Seyfert galaxies (Mathur et al., 2011; Orban de Xivry

et al., 2011), and are therefore unlikely to have *ever* undergone a major merger (e.g., Kormendy & Kennicutt, 2004). Pseudo bulges have more angular momentum than classical spheroids, which inhibits the gas accretion on small scales. It is therefore significant that NLS1s are more likely to reside in barred spiral galaxies than typical Seyfert galaxies (Crenshaw et al., 2003) – without the galaxy bars, the host-galaxy gas is unlikely to be efficiently driven into the central kpc region of NLS1s (contrast with the lack of a strong correlation in the overall population; see §2.1).

3.3. The distant growth of massive black holes

3.3.1. Evolution of the AGN population

Extensive high-quality observations have provided valuable insight into the processes of BH growth in the local Universe. However, the vast majority of the mass accretion onto BHs occurred at higher redshift ($\approx 95\text{--}99\%$ of the integrated BH growth has occurred at $z > 0.1$; e.g., Marconi et al. 2004; Shankar et al. 2004, 2009; Hopkins et al. 2007; Merloni & Heinz 2008; Aird et al. 2010), and we must therefore look to the distant Universe to understand when, where, and how today’s massive BHs grew. Optical quasar surveys established more than four decades ago that luminous AGNs were orders of magnitude more common at $z \gtrsim 1\text{--}2$ than $z \approx 0$ (e.g., Schmidt, 1968; Schmidt & Green, 1983; Hartwick & Schade, 1990; Boyle et al., 2000; Richards et al., 2006). However, the optical photometric selection method used to identify quasars is only effective in selecting unobscured AGNs that are bright enough to outshine the host galaxy. Optical quasar surveys therefore provide limited constraints on the properties and evolution of the majority of the AGN population; i.e., either obscured AGNs or lower-luminosity AGNs.

Currently the most efficient and near-complete selection for distant AGNs is made using X-ray observations. X-ray observations provide an almost obscuration-independent selection of AGNs and, since star formation activity is comparatively weak at X-ray energies, can identify even low-luminosity systems. For example, the deepest X-ray surveys (the *Chandra* Deep Fields; CDFs; Brandt et al. 2001; Giacconi et al. 2002; Alexander et al. 2003b; Luo et al. 2008; Xue et al. 2011) can detect low-luminosity AGNs similar to NGC 4051 (see Fig. 1 and also Fig. 6 of Brandt & Hasinger 2005) out to $z \approx 1\text{--}2$, even in the presence of large amounts of absorption (up-to $N_{\text{H}} \approx 10^{23}\text{--}10^{24}$ cm $^{-2}$; e.g., Tozzi et al. 2006; Raimundo et al. 2010; Alexander et al. 2011; Comastri et al. 2011; Feruglio et al. 2011); AGNs $\approx 1\text{--}2$ orders of magnitude brighter can be identified to $z > 6$,

provided a sufficient number of objects exist in the comparatively small survey volumes. Often the significant challenge in the identification of distant X-ray selected AGNs is an accurate measurement of source redshifts (with spectroscopic or photometric data; e.g., Barger et al. 2003b; Szokoly et al. 2004; Zheng et al. 2004; Cardamone et al. 2010; Luo et al. 2010; Salvato et al. 2011), since the optical/near-IR counterparts for many of the AGNs are very faint (e.g., Alexander et al., 2001; Mainieri et al., 2005b; Rovilos et al., 2010). Furthermore, even the deepest X-ray surveys miss the most heavily obscured luminous AGNs where even hard X-ray photons are absorbed; selection techniques using optical spectroscopy, IR, and radio data are starting to identify large numbers of these systems (e.g., Donley et al., 2005; Daddi et al., 2007a; Alexander et al., 2008b; Fiore et al., 2008; Hickox et al., 2009; Yan et al., 2011; Juneau et al., 2011; Luo et al., 2011). However, despite these challenges, from a combination of X-ray observations across a broad range of the flux–solid angle plane (e.g., see Fig. 1 of Brandt & Hasinger 2005) we are starting to piece together a more complete picture of the evolution of AGN activity across cosmic time.

The evolution in the space density of high-luminosity AGNs broadly tracks that found from optical quasar surveys: the space density of luminous AGNs with $L_{2-10\text{keV}} > 10^{44}\text{--}10^{45} \text{ erg s}^{-1}$ peaks at $z_{\text{peak}} = 1\text{--}2$ and drops by $\approx 2\text{--}3$ orders of magnitude to $z \approx 0$ and $\approx 0\text{--}1$ order of magnitude to $z \approx 5$ (e.g., Fiore et al., 2003; Ueda et al., 2003; Shankar et al., 2004, 2009; Barger et al., 2005; Hasinger et al., 2005; Hopkins et al., 2007; Silverman et al., 2008a; Brusa et al., 2009a; Aird et al., 2010). The constraints are currently very uncertain for $z \gtrsim 5$ AGNs (e.g., Fan et al., 2001; Barger et al., 2003a; Willott et al., 2010); see §4.3. By contrast, lower luminosity AGNs evolve more slowly and their space density peaks at lower redshifts than high-luminosity AGNs: for example, the space density of moderate-luminosity AGNs with $L_{2-10\text{keV}} \approx 10^{43}\text{--}10^{44} \text{ erg s}^{-1}$ peaks at $z \approx 0.5\text{--}1.0$ and drops by $\approx 1\text{--}2$ orders of magnitude to $z \approx 0$ and $z \approx 5$, respectively. This differential redshift evolution of the AGN population is commonly modelled as luminosity dependent density evolution. The same behaviour is also found for optically selected and radio selected AGNs (e.g., Richards et al., 2005; Bongiorno et al., 2007; Hopkins et al., 2007; Rigby et al., 2008, 2011; Croom et al., 2009; Smolčić et al., 2009).⁷ Obscured AGNs are found to trace the same evolution as unobscured AGNs of the same lu-

minosity, although there is tentative evidence for an increase in the obscured AGN fraction with redshift (e.g., La Franca et al. 2005; Ballantyne et al. 2006; Treister & Urry 2006; Hasinger 2008; however, see also Akylas et al. 2006 and Dwelly & Page 2006), which would be expected if the nuclear regions of distant AGNs are more gas rich than lower-redshift AGNs.

The integrated growth of BHs is dominated by systems around the knee of the AGN luminosity function (e.g., Hopkins et al., 2007), which for X-ray detected AGNs is $L_{2-10\text{keV}} \approx 10^{44} \text{ erg s}^{-1}$: $\approx 75\%$ of the growth of BHs has occurred in luminous systems with $L_{2-10\text{keV}} \approx 10^{43}\text{--}10^{45} \text{ erg s}^{-1}$ (i.e., straddling the traditional Seyfert galaxy/quasar threshold; see footnote 1 of Alexander et al. 2008b). Approximately 30–50% of the integrated growth of BHs has occurred at comparatively low redshifts of $z < 1$, $\approx 35\text{--}45\%$ has occurred at $z \approx 1\text{--}2$, and $\approx 15\text{--}25\%$ at $z > 2$ (e.g., Marconi et al., 2004; Shankar et al., 2004, 2009; Hopkins et al., 2006a, 2007; Silverman et al., 2008a; Aird et al., 2010). Optically selected quasars account for $\approx 35\text{--}50\%$ of the integrated BH growth and radio-loud AGNs account for $\lesssim 10\%$ of the integrated BH growth. However, while comprising the minority of the overall AGN populations, both of these sub populations are important for the growth of BHs and galaxies: optically selected quasars appear to represent a rapid growth phase of massive BHs (see §4.2) and radio-selected AGNs appear to have played a significant role in the formation and evolution of galaxies (see §5.1).

The origin of the differential redshift evolution of the AGN population is presumably due to a decrease in the overall cold-gas fuel supply in the nuclear regions of galaxies, at least for the lower-redshift drop off in space density. The global drop off in space density at $z > 2$ may be limited by the maximum BH accretion rate for comparatively low-mass BHs (i.e., the AGN luminosity cannot be higher than the BH Eddington limit; e.g., Merloni & Heinz 2008; see Eqn. 6). However, it isn't immediately clear whether the decrease in the fuel supply is across all systems or only for systems in specific environments or BH mass ranges. Perhaps the strongest discriminator between these different scenarios comes from studies of nearby AGNs, where the long growth times of the most massive BHs at $z \approx 0.1$ ($M_{\text{BH}} > 10^8 M_{\odot}$) implies that they must have grown more rapidly

galaxies peaks at higher redshifts than lower-luminosity systems (e.g., Le Floch et al., 2005; Pérez-González et al., 2005). This behaviour is typically referred to as galaxy “downsizing” since there is clear evidence for a decrease in the mass of luminous star-forming galaxies with decreasing redshift (e.g., Cowie et al., 1996; Ballantyne et al., 2006; Bell et al., 2005; Juneau et al., 2005; Bundy et al., 2006).

⁷Analogous results are also found for the star-forming galaxy population, where the space density of high-luminosity star-forming

at higher redshifts (e.g., Heckman et al. 2004); see §3.2.1. Direct measurements of the Eddington ratios of the BHs in $z < 2$ quasars (BH masses estimated using the virial estimator; see §4.1) provide further support for this view by showing a decrease in both the characteristic active BH mass and Eddington ratio with decreasing redshift (e.g., McLure & Dunlop, 2004; Greene & Ho, 2007; Netzer & Trakhtenbrot, 2007). Lastly, on the basis of indirect BH mass estimates (based on the host-galaxy luminosities or velocity dispersions and the local BH–spheroid mass relationships; e.g., Magorrian et al. 1998; Gebhardt et al. 2000; Ferrarese & Merritt 2000; Tremaine et al. 2002; Marconi et al. 2004), the BHs of $z \approx 0.3$ – 1.5 X-ray AGNs appear to be massive and are growing more rapidly than similarly massive BH in the local Universe ($M_{\text{BH}} \approx 10^7$ – $10^9 M_{\odot}$ and typical Eddington ratios of $\lambda \approx 10^{-3}$ – 10^{-1} ; e.g., Babić et al. 2007; Ballo et al. 2007; Rovilos & Georgantopoulos 2007; Alonso-Herrero et al. 2008; Hickox et al. 2009; Raimundo et al. 2010; Simmons et al. 2011).

The current observational data therefore suggest “downsizing” in the active BH mass with decreasing redshift, in general agreement with that found for the galaxy population (see footnote 7). However, the current observations provide comparatively limited constraints in isolation since accurate determinations of the BH mass and Eddington ratio are only available for a small fraction of systems (i.e., AGNs with broad emission lines; see §4.1), and the constraints are very limited for $z > 1.5$ AGNs, where the most massive BHs are predicted to have been most active. To gain more detailed insight we can appeal to models and simulations, which provide solutions to the growth of the BH population from a broad suite of observational and physical constraints (e.g., BH mass density and distribution, evolving AGN luminosity functions, X-ray background spectrum; e.g., Marconi et al. 2004; Merloni 2004; Shankar et al. 2004, 2009; Hopkins et al. 2006a, 2008; Malbon et al. 2007; Di Matteo et al. 2008; Somerville et al. 2008; Fanidakis et al. 2011, 2012). Despite a broad range of different approaches, from simple analytical/synthetic models to more detailed semi-analytical models and N-body/hydrodynamical simulations some clear trends have emerged from these studies: (1) the average Eddington ratio for BHs decreases with redshift, from rapidly growing systems at $z \gtrsim 2$ – 3 to comparatively slow growing systems at $z < 1$, and (2) the characteristic “active” BH mass decreases with redshift. However, there are significant differences between the studies in terms of the build-up of the BH mass function with redshift. For example, in the semi-analytical model of Fanidakis et al. (2012), the lower-

mass end of the BH mass function ($M_{\odot} \lesssim 10^8 M_{\odot}$) is essentially in place by $z \approx 2$ while the high-mass end is predominantly built by BH mergers of lower-mass BHs and modest mass accretion rates through to the present day. By comparison, in the AGN synthesis models of Marconi et al. (2004) and Merloni & Heinz (2008) the lower-mass end of the BH mass function is only in place by $z \lesssim 0.1$ – 0.6 . Of course there are large differences in the complexities, scope, and assumptions made between these different models but they serve to illustrate some of the uncertainties that remain in modelling the evolution of the BH mass function.

Radio-loud AGNs are the minority AGN population at all redshifts and the majority of the growth of BHs has occurred in radio-quiet AGNs (e.g., Merloni & Heinz, 2008; Cattaneo et al., 2009). However, a large fraction of the radio emission associated with AGN activity is produced by jets and lobes, which are powered by synchrotron emission and shocks and therefore large amounts of kinetic/mechanical energy. If this kinetic energy is able to couple effectively to the gas in the host galaxy or larger-scale environment then it can prevent the gas from cooling and forming stars; see §5.1. The evolution of the radio luminosity density with redshift therefore provides direct constraints on the volume-average heating rate from AGN activity (e.g., Croton et al., 2006; Heinz et al., 2007; Lehmer et al., 2007; Merloni & Heinz, 2008; Cattaneo et al., 2009; Smolčić et al., 2009; La Franca et al., 2010). The conversion from radio luminosity to mechanical power is uncertain and relies on converting the synchrotron jet luminosity into a kinetic energy (e.g., Dunn & Fabian, 2004; Best et al., 2006; Rafferty et al., 2006; Heinz et al., 2007; Bîrzan et al., 2008; Cavagnolo et al., 2010). However, on the basis of the current conversion factors, the overall heating rate from AGN activity is predicted to be broadly flat over $z \approx 0$ – 4 , with low excitation AGNs dominating the overall heating, particularly at $z < 1$ when radio-loud high-excitation AGNs are rare (e.g., Merloni & Heinz, 2008; Cattaneo et al., 2009). There is evidence for a sharp drop in the heating rate at $z < 0.5$, which would indicate a weakening role of AGN activity towards the present day (e.g., Kõrding et al., 2008; La Franca et al., 2010). However, there are also significant differences between studies in the estimated evolution of the AGN heating rate, which are due in part to how the current radio luminosity functions are extrapolated down to low luminosities.

3.3.2. *The host galaxies of distant AGNs*

The strong evolution in the AGN population with redshift illustrates that conditions in the distant Universe

were different to that seen locally. How do the host galaxies of distant AGNs compare to the host galaxies of AGNs in the local Universe? Accurate measurements of the host-galaxy properties of distant AGNs can be determined from high-spatial resolution imaging, where the AGN component can be modelled as a point source, or from photometry for obscured and low-luminosity systems when the host-galaxy emission dominates at rest-frame optical–near-IR wavelengths.

The consensus view is that the majority of distant AGNs are hosted in massive galaxies. The host galaxies of X-ray AGNs with $L_X \gtrsim 10^{42}$ erg s⁻¹ at $z < 3$ are $M_* \approx (0.3\text{--}3) \times 10^{11} M_\odot$ (e.g., Akiyama, 2005; Babić et al., 2007; Ballo et al., 2007; Alonso-Herrero et al., 2008; Bundy et al., 2008; Brusa et al., 2009b; Hickox et al., 2009; Xue et al., 2010). Lower-mass systems ($M_* \approx (0.3\text{--}2) \times 10^{10} M_\odot$) are also identified but appear to comprise the minority population of X-ray AGNs (e.g., Shi et al., 2008; Xue et al., 2010); however, selection and sensitivity effects means that it is often challenging to identify distant AGNs in low-mass galaxies (i.e., for a given luminosity threshold, a low-mass BH needs to be growing at a higher Eddington ratio to be identified than a high-mass BH; see Fig. 1). Radio-loud AGNs are typically hosted in the most massive elliptical galaxies with $M_* \approx 10^{11}\text{--}10^{12} M_\odot$: systems with low-excitation optical spectra appear to be hosted in higher-mass galaxies than high-excitation radio-loud AGNs, as expected if the low-excitation systems reside in the most massive dark-matter halos and underwent their major growth phases at higher redshifts (e.g., Tasse et al., 2008; Herbert et al., 2010; Floyd et al., 2010); see §3.4. By comparison, optically selected quasars are predominantly hosted in less-massive elliptical galaxies, with a non-negligible fraction found in galaxies with a significant disc component (e.g., Dunlop et al., 2003; Floyd et al., 2004; Kotilainen et al., 2007; Bennert et al., 2008; Schramm et al., 2008; Tasse et al., 2008; Kotilainen et al., 2009; Veilleux et al., 2009; Floyd et al., 2010).

Various analyses show that the host-galaxy properties of distant AGNs are also similar to those of distant massive galaxies. In terms of the Colour-Magnitude Diagram (CMD; e.g., Strateva et al. 2001), distant X-ray AGNs predominantly lie in the “green valley” between the “red sequence” and “blue cloud” (e.g., Nandra et al., 2007; Rovilos & Georgantopoulos, 2007; Silverman et al., 2008b; Hickox et al., 2009; Xue et al., 2010; Cardamone et al., 2010), consistent with that of inactive galaxies over a similar mass range; however, we note that some AGN host galaxies will be red due to dust obscuration (e.g., Cardamone et al., 2010; Rovilos et al.,

2011). The host galaxy morphologies of X-ray detected AGNs are also comparable to those of similarly massive inactive galaxies (e.g., Sánchez et al., 2004; Grogan et al., 2005; Pierce et al., 2007; Gabor et al., 2009; Georgakakis et al., 2009; Kocevski et al., 2011; Schawinski et al., 2011), with a mix of bulge-dominated and disc-dominated systems. By comparison, the host galaxies of distant radio-loud AGNs typically lie in the “red sequence” of the CMD (e.g., Tasse et al., 2008; Hickox et al., 2009), as expected for massive elliptical galaxies. The morphologies and structural properties of distant radio-loud AGN are also typically consistent with those of distant elliptical galaxies (e.g., Dunlop et al., 2003; McLure et al., 2004; Floyd et al., 2010; Herbert et al., 2011).

The similarity in the host-galaxy properties of distant AGNs and coeval inactive galaxies suggests that the AGN fraction provides an estimate of the BH-growth duty cycle. The fraction of massive galaxies hosting X-ray AGN activity out to $z \approx 2\text{--}3$ is $\approx 10\text{--}20\%$ for systems with $L_X \gtrsim 10^{42}$ erg s⁻¹ (e.g., Bundy et al., 2008; Xue et al., 2010). The AGN fraction drops to $\approx 1\text{--}5\%$ for AGNs with $L_X \gtrsim 10^{43}$ erg s⁻¹, with some evidence for an increase with redshift (e.g., Xue et al., 2010; Georgakakis et al., 2011), comparable to that found in the local Universe but at higher BH and stellar masses (see Fig. 4). These results indicate that BH growth is recurrent and has a long duty cycle. The fraction of galaxies hosting radio-loud AGN activity out to $z \approx 1.3$ is also comparable to or slightly higher than that found for nearby galaxies, indicating that the duty cycle of radio-loud AGN activity has been relatively constant over at least the past ≈ 9 Gyrs (e.g., Tasse et al., 2008; Smolčić et al., 2009).

How is the distant AGN activity triggered? Contrary to initial expectations, only a comparatively small fraction of the X-ray AGNs out to $z \approx 3$ clearly reside in galaxy major mergers ($\approx 15\text{--}20\%$; e.g., Sánchez et al. 2004; Pierce et al. 2007; Georgakakis et al. 2009; Cisternas et al. 2011; Kocevski et al. 2011, comparable to that found for X-ray selected AGNs in the local Universe (e.g., Koss et al. 2010; see §3.2.3). However, the host galaxies of up-to $\approx 45\%$ of the X-ray AGNs show some evidence for disturbed morphologies, suggesting that a considerable fraction of the distant AGN activity could be driven by external processes (i.e., either galaxy major mergers or interactions; e.g., Kocevski et al. 2011; Silverman et al. 2011). As noted in §3.2.3, there are potential complications in the interpretation of the host-galaxy morphologies, making it difficult to determine the true fraction of distant AGN activity driven by external and internal processes. It is therefore important

to note that, irregardless of these complications, there are no clear differences in the morphological properties of AGNs and comparably massive inactive galaxies, suggesting that the mechanisms that trigger distant BH growth also trigger distant galaxy growth (e.g., Cisternas et al., 2011; Kocevski et al., 2011; Schawinski et al., 2011).

The fraction of optically selected quasars with evidence for morphological distortions varies from study to study but is always large (≈ 30 – 100%) and, importantly, is found to be higher than comparably massive distant galaxies (e.g., Bahcall et al., 1997; Canalizo & Stockton, 2001; Dunlop et al., 2003; Guyon et al., 2006; Bennert et al., 2008; Urrutia et al., 2008). The overall fraction of radio-loud AGNs with evidence for disturbed morphologies is also higher than that found for distant massive galaxies (e.g., de Koff et al., 1996; Dunlop et al., 2003; Ramos Almeida et al., 2011b,a). However, Ramos Almeida et al. (2011b,a) showed that the disturbed morphology fraction of radio-loud AGNs depends on the optical spectral properties: $> 90\%$ of the high-excitation systems have disturbed host-galaxy morphologies (i.e., similar to the optically selected quasars), as compared to only $\approx 30\%$ of the low-excitation systems. Overall these results therefore suggest that typical X-ray AGNs and low-excitation radio-loud AGNs evolve along with the coeval massive galaxy population, while quasars (either radio quiet or radio loud) are often triggered by external processes and evolve more rapidly (see §4.2 for further discussion of quasars), as predicted by some models (e.g., Hopkins et al., 2008; Hopkins & Hernquist, 2009).

3.3.3. The connection with star formation

There are a number of pieces of evidence that connects the global evolution of star formation with that seen for AGN activity: (1) the differential redshift evolution of the AGN population is also found for the star-forming galaxy population (see footnote 7), (2) the redshift distribution of the most strongly star-forming galaxies traces that seen in the optical quasar population (e.g., Chapman et al., 2005; Wardlow et al., 2011), and (3) the overall shapes of the volume-average mass accretion and star-formation histories are broadly similar (e.g., Boyle & Terlevich, 1998; Merloni et al., 2004; Silverman et al., 2008a; Aird et al., 2010). Such a connection is not unexpected given the tightness of the BH–spheroid mass relationship in the local Universe and the association between AGN activity and star formation in nearby galaxies; see §3.2.2. However, given the different conditions between the local and distant Universe, how does the connection between distant AGN activity

and star formation compare to that found in the local Universe?

The volume-average mass accretion and star-formation histories are similar up to $z \approx 1.0$ – 1.5 , when the mass accretion history is scaled up by a factor ≈ 5000 (e.g., Silverman et al., 2008a; Aird et al., 2010). However, there are significant differences at $z > 2$, where the slope of the mass accretion history is much steeper than that found the star-formation history; for example, there is potentially ≈ 1 – 2 orders of magnitude more star formation per unit volume than that found for the mass accretion at $z \approx 6$. At least part of the variation with redshift could be due to incompleteness in the AGN selection (e.g., there may be an increasing fraction of X-ray undetected heavily obscured AGNs with redshift; see §3.3.1) but it also possible that the connection between AGN activity and star formation was different at high redshift.

There is a general correlation between star-formation rate (SFR) and mass accretion rate for individual distant AGNs (e.g., Schweitzer et al., 2006; Lutz et al., 2008; Shi et al., 2009; Silverman et al., 2009b; Trichas et al., 2009; Rafferty et al., 2011). However, the correlation is broad, particularly for AGNs detected in X-ray surveys where the AGN selection is comparatively complete (i.e., up-to five orders of magnitude variation for individual X-ray AGNs; e.g., see Fig. 14 of Rafferty et al. 2011). Globally the star-formation rates of AGNs of all classes are found to increase with redshift, in general agreement with the broad trend found for the overall galaxy population (e.g., Archibald et al., 2001; Serjeant & Hatziminaoglou, 2009; Mullaney et al., 2010, 2011b; Lutz et al., 2010; Shao et al., 2010; Xue et al., 2010; Mainieri et al., 2011; Seymour et al., 2011). For example, the average star-formation rates of moderate-luminosity AGNs (i.e., systems with Seyfert galaxy luminosities of $L_{2-10\text{keV}} > 10^{43} \text{ erg s}^{-1}$) are ≈ 40 times higher at $z \approx 2$ – 3 than found for similarly luminous AGNs at < 0.1 (e.g., Mullaney et al., 2011b). This rate of increase is in good agreement with that found for comparably massive galaxies over the same redshift range (e.g., Daddi et al., 2007b; Pannella et al., 2009; Rodighiero et al., 2010a; Elbaz et al., 2011), suggesting that the presence of an AGN does not have a significant influence on the total amount of star formation in the host galaxy (e.g., Shao et al., 2010; Xue et al., 2010; Mullaney et al., 2011b); however, we note that the situation may be different for rapidly growing BHs in starburst galaxies, which may follow a different evolutionary path (see Fig. 6 in §4.2).

Taken at face value these results therefore indicate a *significant* increase in the amount of star-formation ac-

tivity for a fixed mass-accretion rate with redshift (i.e., there was ≈ 40 times more star formation per unit of AGN activity at $z \approx 2-3$ than found at $z < 0.1$; e.g., Mullaney et al. 2011b), which appears inconsistent with the concordant BH–galaxy growth ratio implied by the BH–spheroid mass relationship. These results can be reconciled with the relative growth implied by the BH–spheroid mass relationship if, for example, the AGN duty cycle increases significantly with redshift (see below for current constraints) or if the majority of the star formation in the distant Universe occurs in galaxy discs rather than galaxy spheroids.

The AGN fraction is found to be a strong function of star-formation rate in distant galaxies. For example, the fraction of moderate-luminosity AGNs with $L_X > 10^{43}$ erg s $^{-1}$ increases from $\approx 3-10\%$ for SFRs $\approx 30-200 M_\odot$ yr $^{-1}$ (i.e., equivalent to LIRGs) to $\approx 10-40\%$ for SFRs $\approx 100-500 M_\odot$ yr $^{-1}$ (i.e., equivalent to ULIRGs; e.g., Alexander et al. 2005; Laird et al. 2010; Symeonidis et al. 2010; Xue et al. 2010; Georgantopoulos et al. 2011; Rafferty et al. 2011). The AGN fraction increases further if lower-luminosity AGNs are considered (see Fig. 12 of Rafferty et al. 2011). The high AGN fraction at the highest SFRs indicates almost continuous BH growth during vigorous star-formation phases, as would be expected during rapid growth phases. However, the overall AGN fractions are broadly consistent with those found for intense star-forming galaxies in the local Universe (e.g., the fraction of nearby ULIRGs hosting AGNs with $L_X > 10^{43}$ erg s $^{-1}$ is $\approx 40\%$; Alexander et al. 2008b), suggesting that the duty cycle of BH growth in star-forming galaxies has remained relatively constant over the broad redshift range of $z \approx 0-3$. This result is found despite the large increase in SFR for AGNs over $z \approx 0-3$ and the global increase in the cold-gas mass fraction in massive galaxies with redshift (e.g., Daddi et al., 2010; Tacconi et al., 2010; Geach et al., 2011).

3.4. The role of environment

The BH-growth results discussed so far are predominantly for AGNs identified in field environments (i.e., the typical regions of the Universe). How does the growth of BHs differ as a function of large-scale structure and environment? Theories of large-scale structure formation predict that galaxy growth is accelerated in regions of high density (e.g., Kauffmann, 1996; De Lucia et al., 2006). The relationship between stellar age and local environment provides support for this hypothesis, showing that the most evolved and massive spheroids reside in the highest density regions (clusters) at the present day (e.g., Baldry et al., 2004; Smith et al.,

2009). Large-scale environment is therefore also likely to have a significant effect on the triggering of AGN activity.

In the nearby Universe, radio-quiet and radio-loud AGNs preferentially reside in different environments. On the basis of the two-point correlation function, which measures the clustering strength of selected populations, the dark matter halos of nearby radio-quiet and radio-loud AGNs are inferred to be $\approx 10^{12} M_\odot$ and $\approx 2 \times 10^{13} M_\odot$ (e.g., Mandelbaum et al., 2009; Donoso et al., 2010). The clustering strength of the optical AGNs is also consistent with that found for comparably massive galaxies. By comparison, radio-loud AGNs are preferentially found in galaxy groups and poor-to-moderate richness galaxy clusters (Best, 2004). For example, measuring environment as the local density of galaxies in a radius of 2 Mpc, the fraction of galaxies hosting radio-quiet AGN activity is ≈ 2 times higher in low-density regions than in high-density regions (Kauffmann et al., 2004), while the local galaxy density of radio-loud AGNs is ≈ 2 higher than that found for radio-quiet AGNs (Kauffmann et al., 2008).

Broadly similar results are found for distant AGNs. The clustering of radio-quiet AGNs is weaker than radio-loud AGNs out to $z \approx 1-2$, with implied dark-matter halo masses of $\approx 10^{12}-10^{13} M_\odot$ and $\approx (0.3-1.0) \times 10^{14} M_\odot$, respectively (e.g., Li et al. 2006; da Ângela et al. 2008; Coil et al. 2009; Gilli et al. 2009; Hickox et al. 2009, 2011; Mandelbaum et al. 2009; Krumpe et al. 2010; Fine et al. 2011; however, also see Bradshaw et al. 2011), with some evidence that the clustering strength is dependent on the adopted AGN luminosity thresholds (e.g., Krumpe et al., 2010); see Fig. 5. X-ray AGNs out to $z \approx 1$ are found to reside in a broad range of environments (from field galaxy environments to galaxy groups), consistent with those found for galaxies of the same mass, colour, and star-formation rate (e.g., Georgakakis et al., 2008; Silverman et al., 2009a; Tasse et al., 2011). The X-ray AGN fraction for galaxies found in the field and galaxy groups environments are also indistinguishable (e.g., Waskett et al., 2005; Silverman et al., 2009a). By comparison, distant radio-loud AGNs are found to typically reside in galaxy groups and clusters, where the radio source may be triggered by weak accretion of the hot group/cluster gas (e.g., Tasse et al., 2008; Bardelli et al., 2010; Smolčić et al., 2011); see Fig. 2.

Stark differences in the incidence of luminous AGN activity is found between distant galaxy clusters and distant field-galaxy regions. The moderate-luminosity AGN fraction ($L_{2-10\text{keV}} > 10^{43}$ erg s $^{-1}$) in cluster galaxies rises by an order of magnitude over the redshift range

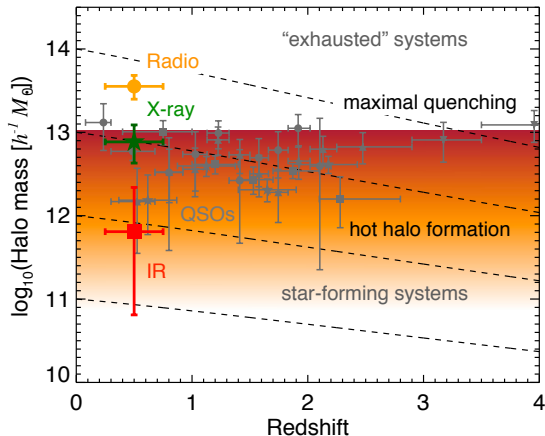


Figure 5: Illustration of the evolution of dark matter halo mass versus redshift for AGN populations. Lines show the evolution of halo mass with redshift for individual halos, based on the median growth rates from cosmological simulations (Fakhouri et al., 2010). Highlighted is the region of maximum “quenching”, in which halos transition from having large reservoirs of cold gas to being dominated by virialized hot atmospheres (e.g., Croton, 2009). The gray points show halo masses of optically-bright quasars derived from autocorrelation measurements (Croom et al. 2005, upright triangles; Myers et al. 2006, squares; Shen et al. 2007, inverted triangles; da Ángela et al. 2008, stars; Ross et al. 2009, circles). The colored points show the halo masses for radio, X-ray, and infrared-selected AGN at $z \sim 0.5$ (Hickox et al., 2009). This figure illustrates that massive rapidly growing BHs (optical quasars) are found in the most massive dark matter halos that have not yet reached the “exhausted” hot halo regime, while rapidly growing lower-mass BHs (as traced by mid-IR samples) are found in somewhat lower-mass halos typical of star-forming galaxies. All halo masses are calculated following Hickox et al. (2011) assuming a cosmology with $(\Omega_m, \Omega_\Lambda, \sigma_8) = (0.3, 0.7, 0.84)$.

$0.05 < z < 1.3$ from $\approx 0.1\text{--}1\%$ (e.g., Martini et al., 2006, 2009; Eastman et al., 2007). These luminous AGN fractions are approximately an order of magnitude *lower* than those found in field-galaxy regions over the same redshift. This decline in AGN activity with decreasing redshift broadly tracks that found for the star-forming population in galaxy clusters (e.g., Saintonge et al., 2008; Finn et al., 2010; Atlee et al., 2011), indicating a general shut-down of activity in the densest regions of the Universe over the last ≈ 9 Gyrs of cosmic time.

The results found for AGN activity in galaxy clusters suggest that growth of galaxies and BHs in overdense regions must have been significantly more rapid at higher redshift. Indeed, we find direct support for this view from deep X-ray observations of the densest regions in the distant Universe (protoclusters). For example, in the $z \approx 3.1$ SSA 22 protocluster, Lehmer et al. (2009b) found a factor of ≈ 6 increase in the fraction of galaxies hosting AGN activity compared to the field-

galaxy environment at $z \approx 3.1$, showing the opposite trend to that found for $z < 1.3$ galaxy clusters (see also Digby-North et al. 2010). Furthermore, there is tentative evidence that the largest incidence of AGN activity is in the densest regions of the protocluster (Lehmer et al., 2009a), suggesting that even the local environment has a large effect on the triggering of AGN activity, in contrast to AGNs identified in $z < 1$ overdense regions (e.g., Gilmour et al., 2007; Kocevski et al., 2009). The SSA 22 protocluster is predicted to become a large galaxy cluster by $z \approx 0$, with a similar mass to that of Coma ($\approx 10^{15} M_\odot$; Steidel et al. 1998). The stark difference in activity between this $z \approx 3$ protocluster and $z < 1.3$ galaxy clusters of similar mass therefore suggests a dramatic change in fuelling mode, from a large abundance of cold gas available at high redshift to the predominantly hot gas when the galaxy cluster virialises.

These studies show that environment has a major role in the growth of BHs. The optical and X-ray AGN activity is likely driven by the availability of a cold-gas supply. At high redshift this is most readily available in the densest environments but by lower redshifts the majority of the cold-gas in dense regions has been heated and cannot be accreted efficiently – at low redshifts AGN activity is more prevalent in typical regions of the Universe. This shut down of activity is most dramatically seen in galaxy clusters and it may be related to the dark-matter halo. For example, the lack of significant AGN activity with dark-matter haloes $\gg 10^{13} M_\odot$ may be due to the halo virialising and shock heating the gas and suppressing vigorous mass accretion (e.g., Cattaneo et al., 2006, 2008; Dekel & Birnboim, 2006; Kereš et al., 2009). Indeed, luminous AGNs and quasars appear to be universally hosted by dark-matter of $\approx 10^{12}\text{--}10^{13} M_\odot$; see Fig. 5. The dark-matter halo may therefore control the cold-gas accretion and may strongly influence the overall evolution of AGN activity with redshift.

4. What fuels the rapid growth of the most massive (and also the first) black holes?

In the previous section we discussed the host galaxies and evolution of AGNs, which provide the overall picture for the joint cosmological growth of galaxies and their BHs. However, the work from the majority of these studies focused on typical AGNs with luminosities near or below the break in the AGN luminosity function. While these objects represent the majority of AGN in the Universe and may play an important role in galaxy growth, they are unlikely to be responsible for the *bulk* of the accretion onto the most massive BHs.

Synthesis models of the BH population show that for systems with $M_{\text{BH}} > 10^8 M_{\odot}$, the major growth phase occurs in very powerful, high-Eddington ratio quasars at high redshift (see §3.3.1). The large-scale process that is likely to trigger this rapid BH growth phase is galaxy major mergers, which is also expected to initiate luminous star-formation activity. In this section we further discuss recent progress on the demographics of powerful quasars and the physical mechanisms that fuel their rapid growth. We also explore the formation and evolution of the initial BHs at high redshift that comprise the “seeds” which eventually grow into the BHs that power the quasars.

4.1. Masses and evolution of rapidly growing black holes

The foundations in understanding the rapid growth of massive BHs come from measurements of demographics (BH masses, Eddington ratios, and space densities). In recent years the most powerful observation tool has been spectroscopic studies of optically-selected quasars. Their high luminosity and characteristic colors mean that quasar luminosity functions can be traced out to high redshifts ($z \lesssim 7$; Fan et al., 2006; Mortlock et al., 2011), with the peak in the AGN space density of $z \approx 1-3$ (e.g., Richards et al., 2005; Croom et al., 2009); see §3.3.1. Compared to X-ray or IR observations, studies of optical quasars are strongly biased against selecting obscured sources, but they have the key advantage of enabling detailed studies of the mass accretion (e.g., Floyd et al., 2009; Down et al., 2010) and accurate BH masses (using virial mass estimators; e.g., Vestergaard 2002; Peterson et al. 2004; Vestergaard & Peterson 2006; Kollmeier et al. 2006; Shen et al. 2008; Merloni et al. 2010).

The virial BH mass estimators are based on the simple principle that the broad-line region (BLR) is in virial equilibrium, such that

$$M_{\text{BH}} = \frac{f v^2 R_{\text{BLR}}}{G}, \quad (8)$$

where f is a dimensionless quantity, of order unity, that depends on the geometry and kinematics of the BLR.⁸The velocity v can be measured from a single spectrum from the width of the broad lines, but the radius R_{BLR} is more challenging to estimate. All virial estimates are based on results from reverberation mapping of local AGN, in which the time lag between the light curves of the continuum luminosity and the broad lines allows an estimate of R_{BLR} (e.g., Kaspi et al., 2005; Bentz et al., 2009). These studies find a correlation of roughly $R_{\text{BLR}} \propto L_{\text{nuclear}}^{0.5}$, implying that $M_{\text{BH}} \propto v^2 L^{0.5}$,

with a normalization that needs to be calibrated against other BH mass estimators and which depends on the kinematics and structure of the BLR.

Repeated measurements of individual systems suggests that variation in the time lag and line widths result in constant M_{BH} estimates, supporting the validity of this technique (e.g., Peterson et al., 2004; Bentz et al., 2009). The local relation is generally calibrated on the width of $\text{H}\alpha$ or $\text{H}\beta$; however, at higher redshift we must use other lines (Mg II and C IV), which have also been validated from local measurements (e.g., McLure & Jarvis, 2002; Vestergaard, 2002; Vestergaard & Peterson, 2006) but for which the absolute calibrations are quite uncertain (as discussed below).

Despite these limitations, a number of authors have forged ahead to produce M_{BH} estimates for many thousands of quasars from large spectroscopic surveys, most prominently SDSS (e.g., Shen et al., 2008) but also with AGES (Kollmeier et al., 2006), zCOSMOS (Merloni et al., 2010) and other surveys. Typical quasars have relatively large BHs ($M_{\text{BH}} > 10^8 M_{\odot}$), with an effective upper limit around $M_{\text{BH}} \approx 10^{10} M_{\odot}$. Accurate BH mass estimates allow for a reasonable measurement of the Eddington ratio (see Eqn. 6 and Fig. 1). However, using optical spectra alone, these calculations require some estimate of the bolometric correction (BC) from the UV or optical continuum to obtain L_{bol} , which can depend on physical parameters (as discussed in § 2.3) such as luminosity, Eddington ratio, or BH mass (e.g., Marconi et al., 2004; Hopkins et al., 2007; Vasudevan & Fabian, 2007; Kelly et al., 2008; Davis & Laor, 2011; Raimundo et al., 2011). The Eddington ratio therefore becomes

$$\lambda \propto \text{BC} \frac{L^{0.5}}{v^2}, \quad (9)$$

meaning that the observed distribution in λ is primarily driven by the values of the broad emission line widths.

These estimates generally produce a distribution in λ which peaks around $\lambda = 0.1-0.3$, declining rapidly for $\lambda > 1$ and $\lambda < 0.01$ (e.g., Kollmeier et al., 2006; Shen et al., 2008); contrast with the Eddington ratios estimated for more typical X-ray AGNs (see §3.3.1). This confirms that optically-bright quasars do indeed represent rapid growth phases, and so are in the regime of

⁸For a spherical BLR geometry, $f = 3/4$ if the line width is expressed in terms of the full-width half maximum (FWHM), as is commonly adopted in virial BH mass estimates (e.g., Vestergaard, 2002; Kollmeier et al., 2006; Vestergaard & Peterson, 2006; Shen et al., 2008). Some studies have suggested, however, that FWHM is not a good way to characterize line widths, particularly for noisy data (e.g., Fromerth & Melia, 2000; Peterson et al., 2004; Peterson, 2011).

optically-thick, geometrically-thin disk accretion as discussed in §2.3. The fact that few quasars are detected at $\lambda \lesssim 0.01$ may result from the BH accretion flow switching to the optically-thin mode at low Eddington ratios, but may also be the result of selection effects that would prevent such a low-Eddington source from having the blue continuum and broad lines characteristic of quasars (Hopkins et al., 2009).

Comparison of measurements at $z \approx 6-7$ to $z \lesssim 3$ suggest that higher-redshift quasars are typically at lower M_{BH} but accreting at higher λ than their lower-redshift counterparts (e.g., Trakhtenbrot et al., 2011; De Rosa et al., 2011). However, interpretation of any observed Eddington ratios is complicated by selection effects that can strongly skew the λ distribution. Indeed, a full Bayesian treatment of the observed distributions suggests that the typical *intrinsic* Eddington ratio for massive BHs at high z is closer to $\lambda \approx 0.05$ or lower (Kelly et al., 2010).

When interpreting these results it is crucial to determine the random and systematic uncertainties in the estimates of M_{BH} . Comparing M_{BH} measurements for nearby objects using multiple techniques (including stellar and gas dynamics from spectroscopy, analysis of megamasers, and reverberation mapping), the error in virial M_{BH} estimators is found to be ≈ 0.4 dex (e.g., Onken et al., 2004; Woo et al., 2010). The latest measurements of the radius-luminosity relationship suggest that its intrinsic scatter is only ≈ 0.1 dex (Peterson, 2010). Thus in principle, radius-luminosity calibrators should be highly effective, but there are important systematic uncertainties. One of these is the overall normalization of the virial estimator, which is related to the structure and kinematics of the broad-line emitting gas and is calibrated by comparison to estimates from the $M_{\text{BH}} - \sigma$ relation (e.g., Onken et al., 2004; Woo et al., 2010). This calibration is performed using nearby low or moderate-luminosity AGN, but at higher Eddington ratios radiation pressure can significantly change the kinematics and geometry of the BLR (e.g., Marconi et al., 2008; Netzer & Marziani, 2010). Further issues are that low signal-to-noise measurements may introduce large asymmetric uncertainties in M_{BH} (Denney et al., 2009), and the value of luminosity included in the virial estimator may include a color term accounting for the slope of the continuum (Assef et al., 2011). These effects may account for claimed discrepancies in the M_{BH} estimates using the UV and Balmer lines.

Optically-bright spectroscopic quasars provide a wealth of information on demographics, but the samples are strongly biased against AGN that are obscured by dust and gas. Recent multiwavelength surveys have

shown that a significant fraction (likely a majority) of luminous AGN at $z \gtrsim 1$ are obscured (e.g., Tozzi et al., 2006; Hickox et al., 2007; Alexander et al., 2008b; Pozzi et al., 2010; Bauer et al., 2010; Treister et al., 2009, 2010b). A complete census requires a combination of selection techniques, including searching for X-ray sources with extremely low ratios of optical to X-ray flux (e.g., Pozzi et al., 2010; Bauer et al., 2010), X-ray spectroscopy of known quasars (e.g., Page et al., 2004; Comastri et al., 2011), detection of luminous, narrow emission lines (e.g., Zakamska et al., 2003; Alexander et al., 2008b; Reyes et al., 2008; Vignali et al., 2010; Gilli et al., 2010; Juneau et al., 2011), or through optical-to-mid-IR SEDs (e.g., Hickox et al., 2007; Bauer et al., 2010). Since most obscured quasars do not show bright optical continua or broad emission lines, estimates of the bolometric luminosity and M_{BH} are more difficult. However, given these limitations, in general it appears that the luminosity and Eddington ratio distributions are broadly similar to unobscured quasars detected using similar techniques (e.g., Hickox et al., 2007; Brusa et al., 2010; Mainieri et al., 2011). Even with the most powerful contemporary techniques that employ a combination of deep IR, optical, and X-ray data, the most heavily obscured quasars (Compton-thick sources with $N_{\text{H}} \gtrsim 10^{24} \text{ cm}^{-2}$) remain extremely difficult to identify (e.g., Alexander et al., 2008b; Treister et al., 2010b; Alexander et al., 2011). Therefore, estimates of the total obscured quasar population are either lower limits or depend on assumptions of the distribution of absorbing column densities (N_{H}); however, these studies robustly demonstrate that a large fraction of the rapid BH growth is obscured. The nature of this obscured population may shed light on the processes that fuel the growth of the most massive BHs, as discussed below.

4.2. Quasars, starbursts, mergers, and the evolutionary sequence

Given a cosmological census of rapidly growing BHs, the next challenge is to understand the physical processes responsible for driving the accretion. The accretion rates of up-to $\approx 10-100 M_{\odot} \text{ yr}^{-1}$ in quasars cannot easily be produced by secular processes that could trigger lower-luminosity AGNs (as discussed in §3.2.3 & §3.3.2). Powerful quasars require higher gas inflow rates and are more likely to be driven by gas-rich galaxy mergers (e.g., Kauffmann & Haehnelt, 2000; Springel et al., 2005b; Hopkins et al., 2006b); however, large-scale secular instabilities may also be effective in particularly gas-rich distant galaxies (e.g., Mo et al.,

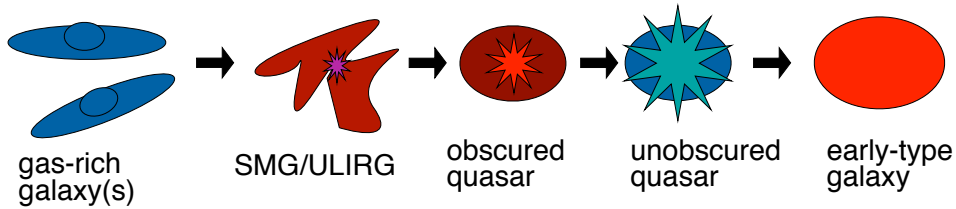


Figure 6: Schematic diagram to illustrate the main components in the major-merger evolutionary scenario first proposed by Sanders et al. (1988).

1998; Bower et al., 2006; Genzel et al., 2008; Bournaud et al., 2011). Support for major-merger driven quasar activity comes from (1) the large fraction of systems with disturbed morphologies (see §3.3.2), and (2) the good agreement between predictions for the merger rates from dark matter simulations (for adopted empirical prescriptions the quasar fueling) and the spatial clustering and space densities of distant quasars (e.g., Hopkins et al., 2008; Treister et al., 2010a).

While mergers are favoured by a number of models (e.g., Kauffmann & Haehnelt, 2000; Springel et al., 2005b; Hopkins et al., 2006b; Sijacki et al., 2007; Di Matteo et al., 2008), *any* quasar triggering mechanism requires relatively massive systems with large supplies of cold gas, which are generally found in dark matter halos with $M_{\text{halo}} \sim 10^{12}\text{--}10^{13} M_{\odot}$ (Croton Figure 4 2009; see also Fig. 5), just below the “maximal quenching” mass scales. Spatial clustering and environment measurements of quasars (e.g., Ross et al., 2009; Lietzen et al., 2009; Hickox et al., 2011; Carrera et al., 2011) suggest that quasars do indeed reside in halos of these masses at every redshift (as discussed in §3.4 and shown in Fig. 5). This implies that at high redshift, quasars are found in the largest collapsed system in the Universe (and are the progenitors of today’s most massive early-type galaxies) while in the local Universe quasars are found in much more typical galaxy environments. Thus the mass of the dark matter halo may itself be the key parameter in understanding the fuelling of quasars.

The rapid flow of cold gas that is necessary to fuel a quasar will inevitably be expected to also result in high rates of star formation (as discussed in § 2.1–2.2). Robust evidence for links between powerful starbursts and quasars come from studies of local powerful IR galaxies ($L_{\text{IR}} > 5 \times 10^{11} L_{\odot}$). The vast majority of such objects in the local Universe are major mergers of galaxies, with higher luminosities found during late stages when the galaxies are at small separations (e.g., Clements et al., 1996; Ishida, 2004). At higher L_{IR} the fraction of the luminosity from the AGN increases, and the large masses of nuclear gas and dust ensure that much of the BH

growth is observed to be heavily obscured (e.g., Tran et al., 2001; Yuan et al., 2010; Iwasawa et al., 2011; Petric et al., 2011b). The local results are broadly consistent with models in which mergers fuel a rapid starburst and a phase of obscured BH growth, followed by an unobscured phase after the gas is consumed or expelled from the galaxy by stellar or quasar feedback (e.g., Sanders et al., 1988; Di Matteo et al., 2005; Hopkins et al., 2008); see Fig. 6. However, powerful starbursts are rare in the local Universe, compared to higher redshift where they dominate the star formation density (e.g., Le Floch et al., 2005; Rodighiero et al., 2010b). A key question, then, is whether a similar starburst-quasar scenario is the dominant process at high redshift, during the peak epoch of quasar activity where the largest BHs accreted most of their mass. Testing this picture is the subject of a number of recent studies.

One approach is to select high-redshift starburst galaxies based on their IR or submillimeter emission, and study the growth of BHs in these systems. Useful observational tools are X-ray observations and mid-IR spectroscopy, which can distinguish between dust heated by star formation and the AGN. The most powerful starbursts at high redshift, submillimeter galaxies (SMGs), have gas kinematics and morphologies that are characteristic of mergers (e.g., Tacconi et al., 2008; Engel et al., 2010; Riechers et al., 2011). A high fraction of these objects also host AGN (e.g., Alexander et al., 2003a, 2005; Laird et al., 2010), but they generally have *Spitzer* IRS mid-IR spectra that are dominated by star formation as indicated by luminous PAH emission features (e.g., Valiante et al., 2007; Pope et al., 2008; Coppin et al., 2010). Only 15% of SMGs are dominated in the mid-IR by steep AGN continua, and even these powerful AGN generally do not produce the bulk of the bolometric output, which is dominated at longer wavelengths by the cool dust from star formation (as also found for star-forming galaxies detected at $70 \mu\text{m}$; Symeonidis et al. 2010). However, the presence of powerful AGN in some starbursts is consistent with a “transition” phase between powerful star formation

and rapid BH growth (e.g., Pope et al., 2008; Coppin et al., 2010) as predicted by major merger fueling models (e.g., Springel et al., 2005b; Di Matteo et al., 2005; Hopkins et al., 2008). In SMGs that host AGN activity, estimates of the galaxy luminosities and BH masses (as discussed in § 5.2; e.g., Alexander et al., 2008a; Carrera et al., 2011) indicate that the BH is undermassive relative to the host galaxy and may therefore be in an early stage of accretion that may precede the bright unobscured phase. These results give broad support to a picture in which a rapid starburst is associated with the triggering of accretion onto a BH which quickly grows in mass.

Further exploration of this “transition” population comes from studies of obscured quasars selected independently of any star-formation signatures (such as far-IR or submillimeter emission). In the unified AGN model, obscuration in quasars is purely due to orientation and so the host galaxies and large-scale structures of quasars would be independent of obscuration (e.g., Antonucci, 1993). In contrast, evolutionary scenarios would suggest significant differences in the host-galaxy properties (e.g., Sanders et al., 1988; Springel et al., 2005b; Di Matteo et al., 2005; Hopkins et al., 2008); see Fig. 6. Some studies have focused on the SEDs of X-ray selected obscured quasars, which can often be modeled with an extension of the simple “torus” geometry, but in many cases also require a contribution from the host galaxy at longer wavelengths indicating an energetically important starburst (e.g., Mainieri et al., 2005a; Vignali et al., 2009; Polletta et al., 2008; Pozzi et al., 2010).

Additional tests of this evolutionary scenario come from clustering analyses, as differences in host halo masses would be inconsistent with a simple “unified” picture in which obscuration is purely due to the orientation of an obscuring torus along the line of sight (e.g., Antonucci, 1993; Urry & Padovani, 1995). The first measurement of the spatial correlation of IR-selected obscured quasars (Hickox et al., 2011) indicates that they are clustered at least as strongly as their unobscured counterparts, with M_{halo} possibly above $10^{13} h^{-1} M_{\odot}$. This suggests the possibility that obscured quasars represent an earlier evolutionary phase in which the BH is undermassive relative to its host halo, such that obscured quasars are found in more massive halos compared to unobscured quasars with similar BH mass⁹.

⁹We note that lower-luminosity X-ray selected AGN appear to show the opposite trend, with stronger clustering for unobscured compared to obscured sources (Allevato et al., 2011). This suggests that this evolutionary scenario may not hold for lower-luminosity systems, and provides strong motivation for more precise future clustering measurements that probe a wide range of luminosity and redshift.

If obscured quasars represent an early phase of accretion then do we see the shutdown of star formation upon the emergence of an unobscured quasar? Evidence based on the submillimetre properties of quasars suggests that unobscured quasars do coincide with a significant decrease in star formation. Page et al. (2001, 2004) and Stevens et al. (2005) find a stark difference in the submillimetre emission between X-ray obscured optical quasars and X-ray unobscured optical quasars: the X-ray obscured optical quasars (which represent $\approx 15\%$ of the optical quasar population) have SFRs implied from the submillimetre data that are about an order of magnitude higher than the X-ray unobscured optical quasars. Tentative evidence for the catalyst of this decreased star formation is found from the spectra of these systems. The X-ray spectra of the X-ray obscured optical quasars indicate that the obscuration is due to an ionized wind, providing evidence for a quasar-driven outflow that may be associated with the short-lived transition from starburst to AGN-dominated systems (Page et al., 2011). Near-IR IFU spectroscopy of another X-ray obscured optical quasar shows evidence for an energetic outflow on scales of $\approx 4\text{--}8$ kpc, which may be starting to shut down the star formation across the whole galaxy (Alexander et al., 2010). At lower redshifts, massive and energetic molecular outflows have been observed in powerful AGN (Sturm et al., 2011) including the broad-absorption-line quasar Mrk 231 (Fischer et al., 2010), for which the outflow is extended on kpc scales (Ferguson et al., 2010). These results provide tentative evidence that AGN-driven winds may indeed influence gas on the scale of the host galaxy and help quench the formation of stars (as discussed in § 5).

Multiwavelength studies of optical quasars also indicate a small population ($\approx 10\%$) of objects that lack clear hot-dust signatures (e.g., Jiang et al., 2010; Hao et al., 2010, 2011). There are a number of interpretations for the lack of hot-dust emission in these objects,¹⁰ including the possibility that some hot dust-poor quasars represent the end stage of the quasar evolutionary sequence.

Taken together, the populations of the most-active systems at $z \approx 1\text{--}3$ may be tentatively placed into a broad evolutionary sequence (SMGs/ULIRGs–obscured quasars–unobscured quasars–“hot dust-poor” systems); see Fig. 6. However the precise relative number densities, duty cycles, and environments of these different objects remain poorly constrained, and it is

¹⁰In the highest-redshift ($z > 6$) systems, there may simply not be enough dust in the Universe to form a significant dusty torus (Jiang et al., 2010).

therefore not clear how well the different populations can be accounted for by a single evolutionary scenario. Future observations with larger samples and improved diagnostics will provide the tools to verify or falsify this general picture for the rapid growth of distant massive BHs.

4.3. Very high redshifts and the formation of “seed” black holes

Through the preceding sections we have discussed the significant progress made in understanding the processes that trigger the rapid growth of the most massive BHs. However, *any* scenario of quasar fuelling requires an initial BH onto which accretion-driven growth can occur, and the nature of how and when these initial seeds were formed remains an important open question. In many cosmological simulations that include BHs, these “seed” BHs are simply put in by hand with some arbitrary mass (e.g., Bower et al., 2006, 2008; Booth & Schaye, 2010; Fanidakis et al., 2011, 2012). The late-time properties of the BHs and galaxies are generally insensitive to the mass of the seeds, as later accretion “erases” any memory of the initial conditions. However, the precise nature of the seed BHs is still crucially important, as the early formation and growth of BHs may in fact represent a key component in the early formation of structure. Early BH accretion may also produce a significant fraction of the total radiation background responsible for reionization of the Universe at $z \gtrsim 7$ (e.g., Madau et al., 2004; Mirabel et al., 2011).

One primary challenge for any model of seed BH formation is posed by the existence of luminous quasars with $M_{\text{BH}} > 10^9 M_{\odot}$ at $z > 6$, when the Universe was $\lesssim 1$ Gyr old (e.g., Fan et al., 2006; Jiang et al., 2009; Willott et al., 2010; De Rosa et al., 2011; Mortlock et al., 2011). For a BH accreting with an Eddington ratio λ and assuming a radiative efficiency ϵ , the growth time of a BH from an initial mass M_{in} to a final mass M_{fin} is given by (e.g., Volonteri, 2010):

$$t_{\text{growth}} = 0.45 \text{ Gyr} \frac{\epsilon}{1 - \epsilon} \lambda^{-1} \ln \left(\frac{M_{\text{fin}}}{M_{\text{in}}} \right) \quad (10)$$

This formation time scale puts robust lower limits on the masses of the seed BHs, for there must be sufficient time in the history of the Universe for them to grow into the massive BHs seen in the high- z quasars. For an initial BH formed at a high redshift (say $z = 20$) to reach $10^9 M_{\odot} \approx 0.7$ Gyr later at $z = 6$, assuming standard $\epsilon = 0.1$ and continuous accretion at the Eddington limit, it must have started with $M_{\text{in}} \sim 100 M_{\odot}$ (with the caveat that some additional growth can occur through BH-BH mergers; e.g., Sesana et al. 2007;

Arun et al. 2009; Sereno et al. 2011). For a lower formation redshift or more stochastic accretion (and thus lower average λ) initial BH masses would necessarily have been higher. A successful model of seed formation must therefore produce sufficiently massive BHs to satisfy these constraints.

There are currently three main candidate mechanisms for seed formation: (1) remnants of massive population III stars (2) direct collapse of primordial gas clouds, and (3) runaway collisions in dense stellar clusters. Each model makes different predictions for the masses and number densities of the BH seeds (see Volonteri, 2010, for a detailed review).

The first candidate mechanism proposes that BH seeds are produced by the deaths of Population III stars. Stellar models suggest that this first generation of stars, which formed from very low-metallicity gas, can have large masses of $\approx 100\text{--}600 M_{\odot}$ (Abel et al., 2002; Bromm et al., 2009), and that the collapse of stars with masses $\gtrsim 260 M_{\odot}$ can produce $\sim 100 M_{\odot}$ BH remnants (e.g., Fryer & Kalogera, 2001; Madau & Rees, 2001). This model has the advantage of following the well-established mechanism for the formation of lower-mass BHs through stellar processes, but is limited by the small mass of the seeds. Radiative feedback limits the possible accretion rates onto seed stellar-mass BHs (e.g., Johnson & Bromm, 2007; Alvarez et al., 2009), making it difficult to construct mechanisms by which such BH seeds can achieve the high accretion rates required to produce the high-mass quasars observed at $z \gtrsim 6$ (e.g., Haiman & Loeb, 2001; Volonteri & Rees, 2005; Volonteri et al., 2006). Therefore, stellar processes may be responsible for a significant population of early BHs, but in the most biased regions (where we find the high- z quasars) another formation mechanism is required. However, recent studies have challenged the idea that the first stars are very massive, due to either fragmentation or feedback effects (e.g., Glover et al., 2008; McKee & Tan, 2008; Turk et al., 2009; Trenti & Stiavelli, 2009; Stacy et al., 2010; Greif et al., 2011), casting some doubt on the the role of Population III remnants as BH seeds.

The second candidate mechanism proposes that BHs form directly inside the densest peaks in the matter distribution. In certain circumstances, the BHs can be produced through the collapse of gas clouds. In regions with radiation fields that can dissociate H_2 molecules, star formation is suppressed and gas cooling proceeds through atomic processes. Detailed hydrodynamic simulations have explored this process (e.g., Wise et al., 2008; Regan & Haehnelt, 2009; Shang et al., 2010; Johnson et al., 2011) and indicate that supermassive

stars at the centers of halos can, in principle, accrete up to a few $\times 10^5 M_\odot$ over ~ 2 Myr (Johnson et al., 2011). A significant fraction of this mass may then go into a seed BH which can continue to grow, although less rapidly because of the effects of radiative feedback. A related possibility is that direct collapse does not occur in an isolated halo, but is triggered by the mergers of multiple halos, providing highly unstable conditions and large gas inflow rates $> 1 M_\odot \text{ yr}^{-1}$ (e.g., Volonteri & Begelman, 2010; Begelman, 2010). Such conditions can produce “quasistars”, massive optically-thick structures in which the radiation pressure from accretion is balanced by the ram pressure of infalling gas, in which gas accretion can significantly exceed the Eddington limit for the central BH (Begelman et al., 2006). This process can produce BH seeds with masses of up to $\sim 10^5 M_\odot$ in the most biased regions of the early Universe.

The third candidate mechanism proposes that the seed BH formation is preceded by the formation of dense stellar clusters, the centers of which then undergo runaway merging due to stellar-dynamical processes that produces a BH (e.g., Devecchi & Volonteri, 2009; Devecchi et al., 2010; Davies et al., 2011). This process can proceed in regions with significant molecular gas, and does not require extremely high inflow rates as in direct gas-dynamical collapse, but generally produces smaller BH seeds with masses $\sim 10^3 M_\odot$.

Given these possible mechanisms for the formation and growth of seed BHs, the challenge for observers is to distinguish between them. One possibility is to trace the high- z BH population through accurate measurements of the number density of AGN at $z \gtrsim 4$. The most progress has been made through studies of high- z optical quasars (e.g., Fan et al., 2006; Jiang et al., 2009; Willott et al., 2010; De Rosa et al., 2011; Mortlock et al., 2011). However, these samples comprise only the most massive end of the BH distribution, and these quasars appear to be growing more rapidly than their lower-redshift counterparts (De Rosa et al., 2011) indicating that they are also biased to higher Eddington ratios. In principle, X-ray observations allow us to explore further down the mass distribution, and some success has been achieved by searching for X-ray counterparts to high-redshift optical and IR sources (Fiore, 2010). In the future, a combination of sensitive, high angular resolution X-ray surveys (e.g., *eROSITA*, Predehl et al. 2007; *Wide-Field X-ray Telescope*, Murray et al. 2010; Brusa et al. 2011) over wide areas covered by IR and optical observations will be required to accurately measure the high- z AGN luminosity function to faint limits.

Measurements of the AGN space density are sensitive not only to the seed formation mechanisms, but

also the rate of BH growth and BH–BH mergers. In principle it may be possible to observe the seed BHs directly, by searching for the signatures of accretion onto $\lesssim 10^5 M_\odot$ BHs. Even for such BHs, the hard radiation field may produce characteristic nebular line emission (in particular, He II $\lambda 1640$) that could be detected with NIRSPEC on the *James Webb Space Telescope* (Johnson et al., 2011), while quasistars could produce a significant population of sources observable at mid-IR wavelengths with *JWST* (Volonteri & Begelman, 2010). In the more distant future, these BHs may also be detectable through gravitational wave signatures when they merge (e.g., Sesana et al., 2007; Arun et al., 2009; Sereno et al., 2011).

Finally, a complementary strategy for understanding seed BHs is to look for residual signatures at lower redshifts. For the most massive systems, the properties of the seeds have been “washed out” by subsequent mass accretion events. However, some of the lower-mass ($\lesssim 10^5 M_\odot$) BHs in the local Universe may represent relics of the initial epoch of seed formation (e.g., van Wassenhove et al., 2010). Therefore the formation process for seed BHs may be reflected in the distribution of low-mass BHs within dark matter halos at low redshift, which can be probed using accurate measurements of the relation between BH masses and galaxy properties (e.g., Volonteri et al., 2008). By studying seed BHs in concert with the subsequent fueling and evolution of powerful quasars, we can aim to produce a coherent picture of the growth of massive BHs from their early origins to the present epoch.

5. What is the detailed nature of AGN feedback and its effects on black-hole fuelling and star formation?

A recurring theme in any discussion of BH growth is the impact that energy released by accretion has on the surrounding gas in the system. In principle, a growing BH releases plenty of energy to impact its surroundings: the thermal energy of the hot gas atmosphere in a $10^{13} M_\odot$ dark-matter halo is $\approx 10^{61}$ erg, while the total accretion energy of a $10^9 M_\odot$ BH is $\approx 2 \times 10^{62}$ erg! Therefore, given a sufficiently strong coupling between the radiative or mechanical output of the BH and the surrounding gas, the AGN should be able to disrupt its environment and potentially regulate its own growth and star formation in the host galaxy (e.g. Silk & Rees, 1998; Bower et al., 2006). In this section we explore the various physical processes, such as winds and jets, by which energy from the BH can couple to the surrounding gas.

We also address the observed consequences of this feedback, with emphasis on the relations between BHs and their host stellar bulges, as well as the gas content of dark-matter halos.

5.1. Driving feedback through winds and jets

Any feedback process from a growing BH requires coupling between the energy released by the BH and the surrounding matter. In general these can take two forms: (1) “winds” (often referred to as superwind-mode), which comprise wide-angle, sub-relativistic outflows and tend to be driven by the radiative output of the AGN, and (2) “jets” (often referred to as radio-mode), which are relativistic outflows with narrow opening angles that are launched directly from the accretion flow itself; see Fig. 7. As described in §3.3.2, §3.3.2, & §4.2 the radiatively-dominated AGN that drive winds are expected to be relatively high-Eddington ratio systems, while jets are most commonly produced (except for the highest-power sources) by lower-Eddington ratio accretion flows.

5.1.1. Radiatively-driven winds

In recent years, a wide range of observational efforts have been aimed at searching for evidence for AGN winds, largely through the presence of highly blueshifted absorption and emission lines. Much work has focused on bright, nearby AGN, for which high signal-to-noise observations readily allow the detection of the relevant line features. As discussed in §2.1, IFU observations of local Seyferts show evidence for outflowing gas on scales of ~ 10 – 100 pc (e.g., Storchi-Bergmann et al., 2007; Davies et al., 2009; Storchi-Bergmann et al., 2010; Schnorr Müller et al., 2011), while spectropolarimetry of a low-redshift quasar shows a high-velocity ($\sim 4,000$ km s $^{-1}$) outflow within the nuclear torus itself, close to the accretion disk (Young et al., 2007). High-velocity winds are also commonly observed using X-ray spectroscopy, which can trace atomic transitions in ionized gas. The presence of highly blueshifted absorption and emission lines in a number of quasars and Seyferts (e.g., PDS 456, PG 1211+143, NGC 4051, 3C 455, MR2251-178) indicate outflows of $v \approx 0.1$ – $0.3c$ (Pounds et al., 2003; Reeves et al., 2003; Tombesi et al., 2010; Lobban et al., 2011; Gofford et al., 2011), as expected for models of momentum-driven winds, as discussed below. A lower velocity outflow (~ 500 km s $^{-1}$) is observed in the local Seyfert 2 galaxy NGC 1068 (although it is confined to the nuclear regions rather than extending on host galaxy scales). The high-resolution X-ray spectrum for NGC

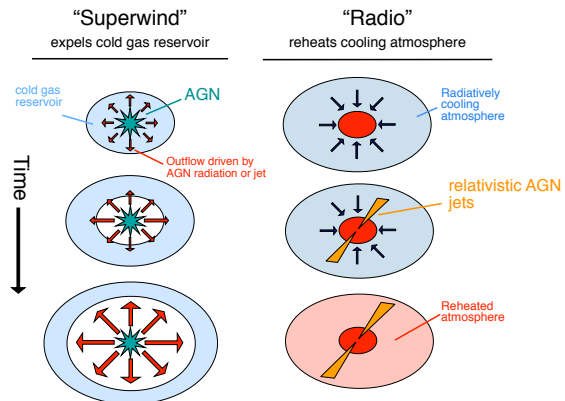


Figure 7: Schematic diagrams to illustrate the two main modes of AGN outflows: “superwind”-mode outflows such as those found in luminous AGNs and “radio”-mode outflows such as those found in low-excitation radio-loud AGNs.

1068 is characteristic of photoionization rather than collisional ionization, suggesting that the outflow is driven by a radiatively efficient wind rather than a jet (Evans et al., 2010).

Similar statistical analyses show evidence for powerful outflows in distant quasars. In the spectra of high- z quasars from SDSS, the peak of the broad C iv emission is typically blueshifted, indicating outflows with ~ 1000 km s $^{-1}$ (e.g., Richards et al., 2002, 2011). Quasars with larger blueshifts show lower equivalent widths of C iv as well as weaker observed X-ray emission. A similar trend with X-ray emission is found for broad absorption line (BAL) quasars, which are believed to represent the ≈ 20 – 40% of quasars (with evidence for a redshift dependence; e.g., Allen et al. 2011) for which the nuclear continuum is viewed through the outflow (there is evidence that maybe all quasars host energetic winds; Ganguly & Brotherton 2008). The maximum blueshift in BAL quasars (corresponding to the terminal velocity of the wind) is higher for sources with weaker X-ray emission (e.g., Gallagher et al., 2006; Gibson et al., 2009). Both these and the results on C iv blueshifts can be understood in terms of radiation driving of the quasar wind; with a weaker X-ray continuum (possibly associated with an absorber near the midplane), the gas close to the BH is less highly ionized and so more easily driven by the UV continuum radiation from the quasars.

Evidence for outflows also comes from statistical studies of large numbers of moderate-luminosity AGNs at $z \lesssim 0.4$. A number of narrow-line Seyfert galaxies show complex [O III] emission with a broad blue wing in addition to the main narrow component (e.g., Veilleux, 1991; Boroson, 2005), and statistical studies suggest

these may be ubiquitous (Mullaney et al., in prep). The width and luminosity of the broad component increase with $L_{[\text{O III}]}$ but are independent of radio-loudness, possibly indicating that the winds are driven by the radiative output of the AGN rather than by relativistic jets.

These studies demonstrate that energetic winds are common in the AGN population. However, they cannot establish on the basis of this data whether these winds generally have significant effects on the scale of the host galaxy since, in the majority of the cases the winds are observed only along the line of sight and there are no direct constraints on the spatial distribution of the outflowing gas (e.g., Tremonti et al., 2007; Arav et al., 2008; Dunn et al., 2010). To fully understand the mass distribution, velocity structure, and energetics of these winds requires improved constraints on the covering fraction and clumpiness the outflows, which are difficult or impossible to determine from spectroscopy along a single line of sight.

Recent observations have begun to overcome some of these challenges through spatially resolved spectroscopy (IFU observations). For example, a quasar hosted by a $z \sim 2$ SMG shows broad blue wings to [O III] lines extend out to several kpc (Alexander et al., 2010). The wind velocity in this case is $\approx 300 \text{ km s}^{-1}$, which suggests that it could possibly be driven by the powerful starburst instead of the AGN. In addition, the observed outflow is sufficient to strongly disturb gas in the galaxy, but is unlikely to completely unbind the material from the system (see §5.1.2 for IFU observations of several high- z radio-loud quasars). At lower redshifts, long-slit spectroscopy of luminous narrow-line quasars at $z < 0.5$ has revealed ubiquitous galaxy-scale ionized clouds with high velocity dispersions, which appear to be powered by the AGN and may be associated with outflows (Greene et al., 2011). An extreme example of an outflow has also been observed with CO line observations of the nearby quasar Mrk 231, in which broad wings to the observed lines indicate the presence of a high-velocity ($\sim 750 \text{ km s}^{-1}$) wind that is resolved on kpc scales and contains $\sim 700 M_{\odot} \text{ yr}^{-1}$ of molecular gas (Feruglio et al., 2010). This outflow may be expected to evacuate the cold gas content of the galaxy within $\sim 10 \text{ Myr}$. Observations are revealing more and more examples of powerful feedback from radiatively driven winds, but the overall prevalence of these outflows and their overall impact on the galaxy population remains to be determined.

5.1.2. Relativistic jets

In contrast to the picture for radiative winds, relativistic jets from AGN are commonly observed to influence

gas on the scales of the host galaxy or even its parent dark matter halo. Indeed, the brightest structures observed in radio AGN are often on $\gtrsim \text{kpc}$ scales and are produced by the coupling of the AGN outflow to its environment. The physical parameters that produce AGN jets (low accretion rates, fueling from hot atmospheres, BH spin) remain poorly understood; however, the impact of the jets on the hot gas in galaxies and dark-matter halos is relatively well established.

In massive systems with hot ionized atmospheres, AGN jets interact most strongly with the gas by inflating bubbles of relativistic plasma in the ambient medium. In the classical picture for radio lobe formation (Scheuer, 1974), the bubbles are strongly overpressured and so produce shocks that can directly heat the atmosphere. However, *Chandra* observations of hot gas around AGN jets yield only a few clear examples of large-scale shocks, and these are predominantly in low-luminosity AGN with FR I morphologies (e.g., Forman et al., 2007; Croston et al., 2009), as opposed to the powerful FR II sources that are expected to drive the strongest shocks. Therefore most of the mechanical energy from the jets is transferred in the form of PdV work by the inflating bubbles (e.g., Bîrzan et al., 2004; Bîrzan et al., 2008; Cavagnolo et al., 2010) rather than through strong shocks. The bubbles are observed to carve out cavities in the hot gas, so there is expected to be little mixing between the hot gas and the relativistic plasma. In this case the pressure is simply the external pressure P_{ext} (which can be measured from the X-ray images), so that $\Delta E = P_{\text{ext}} V_{\text{lobe}}$. Assuming a timescale for the lifetime of the radio source (for example from the buoyant rise time of the inflated bubble), we can then estimate the total mechanical power P_{mech} output by the AGN (e.g., Bîrzan et al., 2004; Dunn et al., 2005; Dunn & Fabian, 2008; Bîrzan et al., 2008; Cavagnolo et al., 2010).

Such estimates show that for most radio-loud AGN, the mechanical power in the relativistic outflows vastly exceeds (by as much as ~ 1000 times) the radiative output of the AGN (e.g., Bîrzan et al., 2008; Cavagnolo et al., 2010). These studies also find correlations between the radio luminosity and (much larger) mechanical power, which can be used to estimate overall distribution of mechanical energy input in the Universe (e.g., Heinz et al., 2007; Merloni & Heinz, 2008; La Franca et al., 2010); see §3.3.1. Analysis of the cavities can also be used to explore whether the mechanical output of the AGN is sufficient to balance the energy lost in the atmosphere through radiative cooling. While limited mainly to bright, massive clusters (where the cavities are most easily identified), the PdV work done by the

cavities can usually offset radiative losses (e.g., Birzan et al., 2004; Dunn & Fabian, 2008). Indeed, the heating from intermittent AGN activity and the radiative cooling are often in relatively close balance (Rafferty et al., 2008). These results suggest a limit cycle in which the cooling of hot gas onto the nucleus of the galaxy fuels intermittent AGN outbursts, which in turn provide sufficient heating to slow down or stop the accretion flow (e.g., Best et al., 2005; Pope, 2011). This scenario represents “feedback” in the true sense of the term, in that the energy output by the AGN has a direct impact on its own fuel supply.

While most systems are roughly consistent with obeying such a limit cycle, there are some examples in which the radio jets impart far more power than is necessary to simply reheat the gas, but instead may be sufficient to unbind much of the hot atmosphere. Such sources are common among galaxy groups (Giodini et al., 2010), but the most extreme case is in the massive cluster MS0735.6+7421 (e.g., McNamara et al., 2005, 2009); see also Siemiginowska et al. (2010). This object exhibits enormous cavities of ~ 200 kpc in diameter, for which the PdV work required is $\sim 10^{62}$ erg, or close to the entire accretion energy of a $10^9 M_{\odot}$ BH. The AGN in this source may be driven by the accretion of cold gas rather than fueling directly from the hot atmosphere, and may be an example of a radio-loud quasar (that is, a source with both powerful radiative *and* mechanical output), rather than lower-Eddington, optically faint AGN. In support of this picture, high-excitation (radiatively efficient) radio AGN are generally found in blue star-forming galaxies that are expected to be rich in cold gas, while low-excitation (radiatively inefficient) sources are found in red, passive galaxies with low cold gas content (e.g., Smolčić, 2009; Herbert et al., 2010; Smolčić & Riechers, 2011). In the case of MS0735.6+7421, the enormous mechanical power needed to produce the cavities has prompted a more extreme possibility, that the outflow must be powered not only by accretion energy but also by the extraction of BH spin energy by the relativistic jet (McNamara et al., 2009, 2011). Whatever the ultimate power source, these extremely powerful mechanical outflows may be responsible for expelling significant gas from the centers of halos, as discussed in § 5.2.3.

Finally, there are examples of relativistic jets interacting not only with hot, virialized plasma, but also with cooler gas in the host galaxy. IFU observations of powerful ($\gtrsim 10^{26}$ W Hz $^{-1}$ at 1.4 GHz) radio-loud quasars have revealed outflows in [O III] that are aligned with the radio jet axis over scales of ~ 10 kpc, with $v \sim 1000$ km s $^{-1}$ and FWHM ~ 1000 km s $^{-1}$ (e.g. Nesvadba et al.,

2006, 2007, 2008). These results suggest that relativistic jets can ionize and expel significant amounts of cool ($\sim 10^4$ K) gas, in addition to strong interactions with the virialized hot atmosphere.

5.2. Observational consequences of feedback

The discovery of the ubiquity of massive BHs in galactic centers and the apparently tight relationship between the mass of a central BH and the properties of its host stellar bulge has motivated a great deal of interest in the physical consequences of BH growth. These results provide compelling (although indirect) evidence for interplay between the growth of the BH and the formation of the host galaxy, despite enormous differences in mass (≈ 3 orders of magnitude) and linear scale (≈ 8 – 9 orders of magnitude). Given the energetic importance of BH accretion in the context of the galaxy, feedback from AGN was immediately recognized as a possible mechanism to produce these observed correlations (e.g., Silk & Rees, 1998; Fabian, 1999; King, 2003)

5.2.1. Correlations between BHs and galaxy spheroids

The first step in understanding BH-spheroid relationships is to measure accurately the nature and intrinsic scatter in the relations, as well as their evolution with redshift. A wide range of studies have explored correlations of M_{BH} with bulge mass, luminosity, velocity dispersion, and gravitational potential, and found a remarkably small intrinsic scatter for massive galaxies in the local Universe (e.g., Magorrian et al., 1998; Gebhardt et al., 2000; Ferrarese & Merritt, 2000; Gültekin et al., 2009). Recent studies of lower-mass galaxies suggest a change in relationship at the low end, with an increase in scatter (e.g., Greene et al., 2008, 2010), although some of this may be driven by the prevalence of pseudobulges in disk galaxies rather than classical bulges, where the correlations are much weaker or non-existent (e.g., Kormendy & Bender, 2011; Jiang et al., 2011).

To understand the physical origin of these correlations, important clues come from the *evolution* of the BH-spheroid mass relationship with cosmic time, which can now be explored observationally. The difficulty in measuring BH masses for distant galaxies restricts the current studies to systems hosting AGN activity. BH mass estimates are computed from either the virial method (for broad-line sources; e.g., Woo et al. 2008; Kim et al. 2008; Decarli et al. 2010b; Bennert et al. 2010; Merloni et al. 2010; see §4.1) or via some assumptions about the relationship between obscured and unobscured AGNs (as for SMGs; Alexander et al. 2008a), each of which have significant uncertainty. The

presence of an AGN also presents the additional challenge of separating the light from the host galaxy to that from the accreting BH, and difficulties in separating the mass or potential of the stellar bulge from the rest of the galaxy (e.g., Decarli et al., 2010a; Merloni et al., 2010).

Despite these challenges, a number of authors have explored the evolution in $M_{\text{BH}}-M_{\text{bulge}}$ for distant AGNs. Studies of broad-line quasars consistently find that the BH is *overmassive* relative to its host galaxy compared to the local relation (e.g., Walter et al., 2004; Woo et al., 2008; Decarli et al., 2010b; Bennert et al., 2010; Merloni et al., 2010). In most cases comparisons are made between M_{BH} and the total galaxy mass, rather than the spheroid properties, which are challenging to determine with current observations. These results have prompted speculation that BH growth precedes that of the host galaxy. However the observed evolution may be due in part to selection effects that cause more massive BHs to be more readily detected (e.g., Lauer et al., 2007; Shen & Kelly, 2010), and some observational results have shown little redshift evolution, at least in the relation between BH and total galaxy mass (e.g., Jahnke et al., 2009). In contrast, corresponding analyses of X-ray selected AGN in powerful starbursts (SMGs) indicate that the BHs lie up to an order of magnitude *below* the relationship for $z \approx 2$ quasars, suggesting that these BHs are in the processes of “catching up” to their final mass (Alexander et al., 2008a; Carrera et al., 2011); however, SMGs may represent an earlier stage in the evolution of quasars (see §4.2 and Fig. 6). At present, the significant uncertainties in the current approaches, as well as the biases inherent in limiting studies to galaxies hosting AGN, make it difficult to draw robust conclusions about the evolution of BH-spheroid mass relationships. Improved observations and larger, well-characterized galaxy and AGN samples should provide better constraints on this evolution in the future.

5.2.2. Physical drivers of BH-spheroid relationships

Redshift evolution notwithstanding, a great deal of theoretical effort has attempted to explain the observed BH-spheroid relationships in the local Universe, with a particular focus on the effects of outflows from AGN. As one example of the vast array of analytical models, King et al. (2011) consider roughly Eddington-limited accretion in which the optical depth to photon scattering is ~ 1 . In this case, the outflow momentum is comparable to the photon momentum, which yields a typical outflow velocity $v \simeq \epsilon/\lambda c \sim 0.1c$, as observed in the X-ray spectra of many AGN (discussed below). Compton cooling by the AGN radiation field allows this outflow to cool rapidly inside a radius of ~ 1 kpc, reducing

the thermal energy of the flow but conserving its momentum. Setting the thrust from such a “momentum-driven” flow to balance the gravitational force on the bulge gas naturally produces a BH-spheroid mass relationship with $M_{\text{BH}} \propto \sigma^4$, as observed (King, 2005). This model also predicts that BHs in AGN should in general be accreting near the Eddington limit, and growing up toward the $M_{\text{BH}}-\sigma$ relation that is observed for passive systems (King, 2010a).

Such analytical models provide a clear physical picture for simple generalized conditions (spherical symmetry, smooth matter distributions, and constant accretion rates). An alternative approach is to study the growth of BHs in the context of large cosmological hydrodynamic simulations, which provide more realistic physical conditions but have the limitation that they do not directly resolve the sphere of influence of the BH. Instead, a common approach is to assume that some fraction of the gas inflowing into the central \sim kpc (through mergers or other processes) accretes onto the BH, up to the Eddington limit (e.g., Springel et al., 2005b; Di Matteo et al., 2005, 2008; Booth & Schaye, 2010). This prescription is broadly valid if the transport of gas from \sim kpc scales down to the BH is indeed efficient, as discussed in §2.1–2.2. Feedback is modeled not as a full description of the outflow, but by transferring a fraction of the radiative output of the BH to the thermal energy of the surrounding gas. The feedback energy output is thus

$$\dot{E}_{\text{feed}} = \epsilon_f \epsilon_r \dot{m} c^2, \quad (11)$$

where $\epsilon_r \sim 0.1$ is the standard radiative efficiency, and ϵ_f is the fraction of the radiative output that couples to the gas. Such models naturally yield a relationship between M_{BH} and M_{sph} , and can reproduce the evolution with redshift as observed from broad-line quasar samples (e.g., Booth & Schaye, 2011). To reproduce the observed normalization for these relations requires $\epsilon_f \approx 0.05-0.15$ (depending on the specific subgrid prescriptions for feedback; Springel et al. 2005b; Di Matteo et al. 2008; Booth & Schaye 2009; Teyssier et al. 2011) suggesting relatively efficient coupling between the BH luminosity and the surrounding gas. A detailed study of the output of one model (Booth & Schaye, 2010) suggests that the most fundamental relationship is between M_{BH} and the binding energy of the host dark-matter halo. In this model, the BH grows until it is massive enough to unbind gas not only from its host galaxy but from the entire surrounding halo, and it is this feedback (along with correlations between the galaxy and M_{halo}) that give rise to the observed BH-spheroid correlations.

Recent observational results suggest that such a $M_{\text{BH}}-M_{\text{halo}}$ relation is not fundamental for lower-mass AGN (e.g., Greene et al., 2008, 2010; Kormendy & Bender, 2011) but it remains a valid possibility for higher-mass objects $M_{\text{BH}} \gtrsim 10^8 M_{\odot}$ for which BH, galaxy spheroid, and dark-matter halo correlations are more difficult to disentangle (Volonteri et al., 2011).

While feedback has naturally occupied a great deal of attention in understanding BH-spheroid relationships, recent work has also proposed that these relations do not imply a causal link between BHs and their host galaxies or halos, but are simply a consequence of the hierarchical growth of structure (e.g., Peng, 2007; Jahnke & Macciò, 2011). If mergers of galaxies are accompanied by the corresponding mergers of their central BHs, then a succession of mergers will tend to drive the resulting galaxies toward the “average” relationship between BH and spheroid mass, even if the initial galaxies show little or no correlation between BH and spheroid properties. These processes may also help explain the increased scatter at the low-mass end of the BH-spheroid relationship, for which the galaxies may have experienced fewer mergers. While in this picture mergers play the predominant role in producing the BH-spheroid relationships, AGN feedback may be important in setting the relative rates of BH and galaxy growth over the history of the Universe.

5.2.3. *The impact of feedback on gas in galaxies and halos*

The energy released by growing BHs can impact not only on the stellar content of their host galaxies (as suggested for feedback models of the BH-spheroid relationships) but also the diffuse gas in their host dark matter halos. In massive ($M_{\text{halo}} \gtrsim 10^{13} M_{\odot}$) halos with hot, ionized atmospheres, heating from relativistic jets (as discussed above) can regulate the temperature of the halos and prevent cooling to form new stars, as required in order to produce the observed stellar mass and luminosity functions of galaxies (e.g., Bower et al., 2006; Croton et al., 2006; Bower et al., 2008). Mechanically dominated AGN activity is observed to be most prevalent in passive systems in such massive halos (e.g., Best et al., 2005; Hickox et al., 2009; Wake et al., 2008; Mandelbaum et al., 2009; Smolčić, 2009); see §3.4 & Fig. 5. In contrast, moderate-luminosity radio-quiet AGN appear to have very little impact on the stellar populations or star formation rates of their host galaxies (e.g., Hickox et al., 2009; Cardamone et al., 2010; Xue et al., 2010; Lutz et al., 2010; Shao et al., 2010; Ammons et al., 2011; Mullaney et al., 2011b), although outflows in such systems may still play a significant role in moderating

the growth of the BH (e.g., King 2010b, Mullaney et al., in prep).

Some of the most compelling evidence for AGN feedback comes from observations of the hot gas itself, which represents the majority of the baryonic content of group- and cluster-scale systems. Of particular interest is the luminosity-temperature (L_X-T_X) relation, which is broadly related to the baryon fraction in a halo as a function of M_{halo} . Observations show that the L_X-T_X relation is remarkably steep at the low-temperature end, suggesting that small to moderate-mass groups have lower baryon fractions in the centers of their dark-matter halos than higher-mass systems (e.g., Sun et al., 2009; Giodini et al., 2009). Outflows must have removed some of the low-entropy gas from the centers of these halos, and simulations indicate that winds from stellar processes (stellar winds and supernovae) are insufficient to produce this deficit. However, models suggest that feedback from growing massive BHs (indeed, the same outflows that are invoked to produce the BH-spheroid relation) can naturally produce the L_X-T_X relations similar to those observed (e.g., Bower et al., 2008; Booth & Schaye, 2010; McCarthy et al., 2010, 2011). Unlike models for the galaxy luminosity function or BH-spheroid relationships, these predictions are independent of assumptions about the star formation processes within the host galaxy and depend only on the coupling of the AGN to the surrounding gas. As such, they represent one of the most promising avenues for quantifying the impact of growing BHs on their host galaxies and halos.

6. Concluding remarks

In this review we have discussed the processes and mechanics of BH growth and explored the connections between the growth of BHs and star formation, host-galaxy properties, signatures of interactions/mergers, and environment. We have explored these processes in a very broad range of systems, from the closest AGNs to AGNs at the highest redshifts, and also the formation of seed BHs. Our overarching aim has been to address the question: *What drives the growth of black holes?*

Surprisingly, there are often few external morphological and kinematical clues that reveal when significant BH growth has been triggered, with AGN host galaxies showing similar overall properties to inactive galaxies of comparable stellar mass. This appears to be true even down to small $\approx 10-100$ pc scales. However, the accurate identification of gas inflow on these scales is mostly restricted to low-luminosity AGNs in the local Universe,



Figure 8: The workshop participants before dinner at Durham Castle. Photograph taken by Sarah Noble.

and significant differences may be present in the central $\approx 10\text{--}100$ pc regions of luminous AGNs. Comparable linear spatial scales should be achievable for distant and high-luminosity AGNs over the coming years with the final configuration of ALMA at submm-mm wavelengths, which will provide direct insight into the properties and extent of the molecular gas and dust-continuum emission on ≈ 100 pc scales. A clear complication in identifying any large-scale catalysts that may have triggered AGN activity is the timescale required for the gas to flow from the host galaxy down to the BH, which can be $\gg 10^8$ yrs. Over such long timescales any clear morphological or kinematical signatures of the triggering event may be lost and therefore care needs to be taken when assessing the role of galaxy major mergers or interactions in the fueling of AGN activity.

A clear dependence between the SFR and luminous AGN fraction is found in both distant and local galaxies, implying a connection between BH and galaxy growth. This finding is perhaps not unsurprising since both star formation and AGN activity are predominantly driven by a cold-gas supply, either from the host galaxy and larger-scale environment, or from stellar winds and circumnuclear supernovae events. However, these results may also indicate a more direct and less coincidental connection between star formation and AGN activity in

at least some systems (such as in the common evolutionary scenario shown in Fig. 6). High-resolution observations with ALMA and *JWST* of well-selected galaxy samples could directly test this evolutionary scenario by simultaneously providing SFRs, gas-inflow rates, and BH mass accretion rates as a function of stellar age.

Recent results have shown that environment plays a major role in the triggering of AGN activity. The global peak in AGN activity in overdense regions occurred at higher redshifts than in the field, with a corresponding more rapid decline to the present day. The most rapid BH growth also appears to be found in dark-matter halos of $\approx 10^{12}\text{--}10^{13} M_{\odot}$ (see Fig. 5), with more massive dark-matter halos found to harbour low-accretion rate radio-loud AGNs hosted by relatively quiescent galaxies. This mass dependence on AGN activity may be due to “quenching” of the cold gas in massive dark-matter halos, which could be largely assisted by large-scale mechanically powerful (but often radiatively weak; see Fig. 7) outflows, such as those seen in nearby galaxy clusters. The strong dependence on the fraction of galaxies that host radio-loud AGN with galaxy mass provides further support for this picture.

However, on the basis of the current results it is not immediately apparent why there exists a tight correlation between the mass of the BH and the mass of the

spheroid in nearby galaxies. Many models argue that energetic radiatively driven outflows (such as those illustrated in Fig. 7) regulate star formation in the host galaxy and “forge” the BH–spheroid mass relationship. Energetic radiatively driven outflows are clearly seen in many luminous AGNs and may be a ubiquitous feature of the AGN population but it is not yet clear what impact these outflows have on star formation in the host galaxy. Spatially resolved spectroscopy of AGNs with IFU observations may provide important insight on this issue since they can reveal the presence of large-scale outflowing gas and address when and where energetic outflows are found. However, given the relatively modest BH mass accretion and SFRs for the majority of the AGN population (e.g., see Fig. 4 for the AGN fraction as a function of different AGN selection techniques), a “regulatory” mechanism may not be necessary every time the BH and galaxy grows. It is presumably only the rapidly evolving and gas-rich systems where the BH and galaxy growth can be so high that they can move substantially around the BH–spheroid mass plane on short timescales. These rapidly evolving systems are therefore the most promising sites to search for the evidence of large-scale energetic outflows. We should also bear in mind that the tight BH–spheroid mass relationship is only applicable for galaxies hosting classical bulges – there are no significant BH–galaxy correlations for systems hosted in pseudo bulges. Since galaxy major mergers are likely to be the catalyst for the formation of classical spheroids, this suggests that galaxy major mergers played a major role in forging the BH–spheroid mass relationship.

Although rare, luminous AGNs such as the quasars selected in optical surveys may play a much more important role in the evolution and growth of BHs and galaxies than would be apparent from their relatively low space density. An example of this is the finding that the most luminous AGNs in the local Universe are responsible for $\approx 50\%$ of the integrated BH growth, despite only comprising $\approx 0.2\%$ of the optical AGN population. However, since AGNs can be extremely variable, any measurement of the BH mass-accretion rate only provides a snapshot of its growth path (e.g., see Fig. 5 of Hopkins & Quataert 2010, which shows factors of ≈ 100 variation in the predicted gas inflow rate over Myr timescales). This adds significant complications to the interpretation of individual objects, which can be overcome to some extent from studying AGN populations as a function of a more stable property than mass accretion rate such as BH mass, stellar mass, and star-formation rate. This should be possible over the coming years with the advent of sensitive large facilities, particularly those

that combine depth with breadth and yield large source densities (e.g., BigBOSS, LSST, and *e-ROSITA*).

The current theoretical models focus on either small-scale processes at high resolution, with limited constraints on larger-scale processes, or explore the large-scale growth of BHs and galaxies in cosmological simulations using sub-grid models to account for the smaller-scale physics. Both approaches have clear strengths but evident weaknesses (i.e., either limited spatial and time resolution or limited cosmological volume). Since AGNs are gas-driven systems fed from gas inflow down to < 10 pc scales from typically > 1 kpc scales, high-resolution hydrodynamical simulations over a broad range of size scales would be particularly beneficial for a detailed understanding of AGN fueling and feedback processes. More detailed theoretical insight may also come from improvements in the sub-grid models using the physics learnt from yet higher-resolution small-scale models to produce more realistic fueling and feedback prescriptions for the cosmological simulations.

The next ≈ 5 –10 years therefore promise huge advances in our understanding of “What drives the growth of black holes?”. We look forward to hosting another exciting workshop and reviewing our progress on this issue over the next decade!

Acknowledgements:

The original date of the workshop was 19th–22nd April 2010 but the eruption of Icelandic volcano Eyjafjallajökull a few days before caused the majority of airspace in Europe to be shut down, and the workshop had to be rescheduled for 26th–29th July 2010. We would like to thank the workshop participants for being able to rapidly change their travel plans ($> 90\%$ of the original participants managed to attend the re-scheduled workshop) and for providing 3.5 days of excellent presentations and enthusiastic scientific discussions: **SOC:** P. Best, R. Davies, T. di Matteo, A. Fabian, J. Greene, M. Volonteri; **LOC:** L. Borrero, K. Coppin, A. Danielson, J. Geach, A. Goulding, J. Mullaney; **After-dinner speaker:** C. Macpherson; **Invited speakers:** R. Bower, N. Brandt, A. Coil, S. Gallagher, S. Gillessen, M. Hardcastle, P. Hopkins, J. Johnson, A. King, D. Lutz, P. Martini, B. McNamara, N. Nesvadba, D. Proga, D. Sanders, T. Storchi-Bergmann, M. Vestergaard, K. Wada; **Regular participants:** J. Aird, M. Akiyama, J. Allen, O. Almaini, M. Ammons, P. Barai, T. Bartakova, F. Bauer, J. Bellovary, C. Booth, E. Bradshaw, M. Bregman, M. Brusa, C. Cardamone, F. Carrera, M. Cisternas, F. Civano, A. Comastri, D. Cro-

ton, R. Decarli, G. DeRosa, D. del Moro C. Done, M. Dotti, E. Down, J. Dunlop, R. Dunn, A. Edge, M. Elvis, D. Evans, L. Fan, N. Fanidakis, C. Feruglio, F. Fiore, D. Floyd, C. Frenk, P. Gandhi, J. Gofford, H. Hao, C. Harrison, P. Herbert, A. Hobbs, S. Hutton, W. Ishibashi, K. Jahnke, B. Jungwiert, M. Kim, T. Kimm, J. Kuraszkiwicz, F. La Franca, C. Lacey, C. Lagos, A. Lawrence, H. Lietzen, N. Loiseau, R. McLure, A. Merloni, M. Micic, F. Mirabel, D. Murphy, E. Nardini, D. Nugroho, M. Page, F. Pedes, B. Peterson, E. Pope, C. Power, S. Raimundo, S. Raychaudhury, J. Reeves, T. Roberts, A. Robinson, Y. Rosas-Guevara, M. Schartmann, J. Scharwaechter, K. Schawinski, F. Shankar, A. Siemiginowska, J. Silverman, V. Smolcic, I. Stoklasova, M. Symeonidis, B. Trakhtenbrot, E. Treister, K. Tugwell, C. Vignali, M. Ward, P. Westoby, B. Wilkes, R. Yan, and J. Zuther.

We thank the New Astronomy Review editors and referees for their time and assistance in completing this review. We would also like to thank Sera Markoff and many workshop participants for providing feedback on earlier drafts of this review, and Sarah Noble for taking the workshop photograph. Special thanks to Darren Croton for the inspiration for the dark-matter halo figure and for sharing his original version with us, to Chris Done for giving us permission to use a revised version of the BH accretion mode figure originally published in Done, Gerlinkski, & Kubota (2007), to Philip Best, Andy Goulding, and Nic Ross for providing us with the data used in various figures, and to James Mulaney for producing an earlier version of the AGN outflow figure. We gratefully acknowledge the Science and Technology Facilities Council (STFC), Royal Society, and Leverhulme Trust for financial support.

References

Abazajian, K. N., et al. 2009, *ApJS*, 182, 543
 Abel, T., Bryan, G. L., & Norman, M. L. 2002, *Science*, 295, 93
 Agol, E. & Krolik, J. H. 2000, *ApJ*, 528, 161
 Aird, J., et al. 2010, *MNRAS*, 401, 2531
 Akiyama, M. 2005, *ApJ*, 629, 72
 Akylas, A., Georgantopoulos, I., Georgakakis, A., Kitsionas, S., & Hatziminaoglou, E. 2006, *A&A*, 459, 693
 Alexander, D. M., et al. 2011, *ApJ*, 738, 44
 Alexander, D. M., et al. 2003a, *AJ*, 125, 383
 Alexander, D. M., et al. 2003b, *AJ*, 126, 539
 Alexander, D. M., Bauer, F. E., Chapman, S. C., Smail, I., Blain, A. W., Brandt, W. N., & Ivison, R. J. 2005, *ApJ*, 632, 736
 Alexander, D. M., Brandt, W. N., Hornschemeier, A. E., Garmire, G. P., Schneider, D. P., Bauer, F. E., & Griffiths, R. E. 2001, *AJ*, 122, 2156
 Alexander, D. M., et al. 2008a, *AJ*, 135, 1968
 Alexander, D. M., et al. 2008b, *ApJ*, 687, 835
 Alexander, D. M., Swinbank, A. M., Smail, I., McDermid, R., & Nesvadba, N. P. H. 2010, *MNRAS*, 402, 2211

Allen, J. T., Hewett, P. C., Maddox, N., Richards, G. T., & Belokurov, V. 2011, *MNRAS*, 410, 860
 Allevato, V., et al. 2011, *ApJ*, 736, 99
 Alonso-Herrero, A., Pereira-Santaella, M., Rieke, G. H., & Rigopoulou, D. 2011, *ApJ* in press (arXiv:1109.1372)
 Alonso-Herrero, A., et al. 2006, *ApJ*, 640, 167
 Alonso-Herrero, A., et al. 2008, *ApJ*, 677, 127
 Alvarez, M. A., Wise, J. H., & Abel, T. 2009, *ApJ*, 701, L133
 Ammons, S. M., et al. 2011, *ApJ*, 740, 3
 Antonucci, R. 1993, *ARA&A*, 31, 473
 Arav, N., Moe, M., Costantini, E., Korista, K. T., Benn, C., & Ellison, S. 2008, *ApJ*, 681, 954
 Archibald, E. N., Dunlop, J. S., Hughes, D. H., Rawlings, S., Eales, S. A., & Ivison, R. J. 2001, *MNRAS*, 323, 417
 Arun, K. G., et al. 2009, *Classical and Quantum Gravity*, 26, 094027
 Assef, R. J., et al. 2011, *ApJ*, 742, 93
 Atlee, D. W., Martini, P., Assef, R. J., Kelson, D. D., & Mulchaey, J. S. 2011, *ApJ*, 729, 22
 Birzan, L., Rafferty, D. A., McNamara, B. R., Wise, M. W., & Nulsen, P. E. J. 2004, *ApJ*, 607, 800
 Babić, A., Miller, L., Jarvis, M. J., Turner, T. J., Alexander, D. M., & Croom, S. M. 2007, *A&A*, 474, 755
 Baganoff, F. K., et al. 2001, *Nature*, 413, 45
 Baganoff, F. K., et al. 2003, *ApJ*, 591, 891
 Bahcall, J. N., Kirhakos, S., Saxe, D. H., & Schneider, D. P. 1997, *ApJ*, 479, 642
 Balbus, S. A. 2003, *ARA&A*, 41, 555
 Balbus, S. A. & Hawley, J. F. 1991, *ApJ*, 376, 214
 —. 1998, *Reviews of Modern Physics*, 70, 1
 Baldi, R. D. & Capetti, A. 2008, *A&A*, 489, 989
 Baldry, I. K., Glazebrook, K., Brinkmann, J., Ivezić, Ž., Lupton, R. H., Nichol, R. C., & Szalay, A. S. 2004, *ApJ*, 600, 681
 Baldwin, J. A., Phillips, M. M., & Terlevich, R. 1981, *PASP*, 93, 5
 Ballantyne, D. R., Everett, J. E., & Murray, N. 2006, *ApJ*, 639, 740
 Ballo, L., et al. 2007, *ApJ*, 667, 97
 Bardelli, S., et al. 2010, *A&A*, 511, A1+
 Barger, A. J., et al. 2003a, *ApJ*, 584, L61
 Barger, A. J., et al. 2003b, *AJ*, 126, 632
 Barger, A. J., Cowie, L. L., Mushotzky, R. F., Yang, Y., Wang, W.-H., Steffen, A. T., & Capak, P. 2005, *AJ*, 129, 578
 Barnes, J. E. & Hernquist, L. 1992, *ARA&A*, 30, 705
 —. 1996, *ApJ*, 471, 115
 Barrows, R. S., et al. 2011, *ApJ* in press (arXiv:1109.3469)
 Bauer, F. E., Alexander, D. M., Brandt, W. N., Schneider, D. P., Treister, E., Hornschemeier, A. E., & Garmire, G. P. 2004, *AJ*, 128, 2048
 Bauer, F. E., Yan, L., Sajina, A., & Alexander, D. M. 2010, *ApJ*, 710, 212
 Baum, S. A., et al. 2010, *ApJ*, 710, 289
 Begelman, M. C. 2002, *ApJ*, 568, L97
 —. 2010, *MNRAS*, 402, 673
 Begelman, M. C., Volonteri, M., & Rees, M. J. 2006, *MNRAS*, 370, 289
 Bell, E. F., et al. 2005, *ApJ*, 625, 23
 Bender, R., et al. 2005, *ApJ*, 631, 280
 Bennert, N., Canalizo, G., Jungwiert, B., Stockton, A., Schweizer, F., Peng, C. Y., & Lacy, M. 2008, *ApJ*, 677, 846
 Bennert, V. N., Treu, T., Woo, J.-H., Malkan, M. A., Le Bris, A., Auger, M. W., Gallagher, S., & Blandford, R. D. 2010, *ApJ*, 708, 1507
 Bentz, M. C., Peterson, B. M., Netzer, H., Pogge, R. W., & Vestergaard, M. 2009, *ApJ*, 697, 160
 Best, P. N. 2004, *MNRAS*, 351, 70
 Best, P. N., Kaiser, C. R., Heckman, T. M., & Kauffmann, G. 2006, *MNRAS*, 368, L67

- Best, P. N., Kauffmann, G., Heckman, T. M., Brinchmann, J., Charlot, S., Ivezić, Ž., & White, S. D. M. 2005, *MNRAS*, 362, 25
- Binette, L., Magris, C. G., Stasińska, G., & Bruzual, A. G. 1994, *A&A*, 292, 13
- Birzan, L., McNamara, B. R., Nulsen, P. E. J., Carilli, C. L., & Wise, M. W. 2008, *ApJ*, 686, 859
- Blandford, R. D. & Begelman, M. C. 1999, *MNRAS*, 303, L1
- Bondi, H. 1952, *MNRAS*, 112, 195
- Bondi, H. & Hoyle, F. 1944, *MNRAS*, 104, 273
- Bongiorno, A., et al. 2007, *A&A*, 472, 443
- Booth, C. M. & Schaye, J. 2009, *MNRAS*, 398, 53
- . 2010, *MNRAS*, 405, L1
- . 2011, *MNRAS*, 413, 1158
- Boroson, T. 2005, *AJ*, 130, 381
- Bournaud, F. & Combes, F. 2002, *A&A*, 392, 83
- Bournaud, F., Dekel, A., Teyssier, R., Cacciato, M., Daddi, E., Juneau, S., & Shankar, F. 2011, *ApJ*, 741, L33
- Bournaud, F., Jog, C. J., & Combes, F. 2005, *A&A*, 437, 69
- Bower, R. G., Benson, A. J., Malbon, R., Helly, J. C., Frenk, C. S., Baugh, C. M., Cole, S., & Lacey, C. G. 2006, *MNRAS*, 370, 645
- Bower, R. G., McCarthy, I. G., & Benson, A. J. 2008, *MNRAS*, 390, 1399
- Boyle, B. J., Shanks, T., Croom, S. M., Smith, R. J., Miller, L., Loaring, N., & Heymans, C. 2000, *MNRAS*, 317, 1014
- Boyle, B. J. & Terlevich, R. J. 1998, *MNRAS*, 293, L49
- Bradshaw, E. J., et al. 2011, *MNRAS*, 415, 2626
- Braito, V., et al. 2004, *A&A*, 420, 79
- Brandt, W. N. & Alexander, D. M. 2010, *Proceedings of the National Academy of Science*, 107, 7184
- Brandt, W. N., et al. 2001, *AJ*, 122, 2810
- Brandt, W. N. & Hasinger, G. 2005, *ARA&A*, 43, 827
- Bregman, M. & Alexander, T. 2009, *ApJ*, 700, L192
- Bromm, V., Yoshida, N., Hernquist, L., & McKee, C. F. 2009, *Nature*, 459, 49
- Brusa, M., et al. 2010, *ApJ*, 716, 348
- Brusa, M., et al. 2009a, *ApJ*, 693, 8
- Brusa, M., et al. 2009b, *A&A*, 507, 1277
- Brusa, M., Gilli, R., Civano, F., Comastri, A., Fiore, R., & Vignali, C. 2011, *Memorie della Societa Astronomica Italiana Supplementi*, 17, 106
- Bundy, K., et al. 2006, *ApJ*, 651, 120
- Bundy, K., et al. 2008, *ApJ*, 681, 931
- Burlon, D., Ajello, M., Greiner, J., Comastri, A., Merloni, A., & Gehrels, N. 2011, *ApJ*, 728, 58
- Canalizo, G. & Stockton, A. 2001, *ApJ*, 555, 719
- Capetti, A. & Baldi, R. D. 2011, *A&A*, 529, A126+
- Cappi, M., et al. 2006, *A&A*, 446, 459
- Cardamone, C. N., Urry, C. M., Schawinski, K., Treister, E., Brammer, G., & Gawiser, E. 2010, *ApJ*, 721, L38
- Carrera, F. J., Page, M. J., Stevens, J. A., Ivison, R. J., Dwelly, T., Ebrero, J., & Falocco, S. 2011, *MNRAS*, 413, 2791
- Cattaneo, A., Dekel, A., Devriendt, J., Guiderdoni, B., & Blaizot, J. 2006, *MNRAS*, 370, 1651
- Cattaneo, A., Dekel, A., Faber, S. M., & Guiderdoni, B. 2008, *MNRAS*, 389, 567
- Cattaneo, A., et al. 2009, *Nature*, 460, 213
- Cavagnolo, K. W., McNamara, B. R., Nulsen, P. E. J., Carilli, C. L., Jones, C., & Birzan, L. 2010, *ApJ*, 720, 1066
- Chapman, S. C., Blain, A. W., Smail, I., & Ivison, R. J. 2005, *ApJ*, 622, 772
- Chiaberge, M., Capetti, A., & Macchetto, F. D. 2005, *ApJ*, 625, 716
- Cid Fernandes, R., et al. 2004, *ApJ*, 605, 105
- Cisternas, M., et al. 2011, *ApJ*, 726, 57
- Civano, F., et al. 2010, *ApJ*, 717, 209
- Clements, D. L., McDowell, J. C., Shaked, S., Baker, A. C., Borne, K., Colina, L., Lamb, S. A., & Mundell, C. 2002, *ApJ*, 581, 974
- Clements, D. L., Sutherland, W. J., McMahon, R. G., & Saunders, W. 1996, *MNRAS*, 279, 477
- Coil, A. L., et al. 2009, *ApJ*, 701, 1484
- Colpi, M. & Dotti, M. 2009, *Review in Advanced Science Letters* (arXiv:0906.4339)
- Comastri, A., et al. 2011, *A&A*, 526, L9+
- Comerford, J. M., et al. 2009, *ApJ*, 698, 956
- Coppin, K., et al. 2010, *ApJ*, 713, 503
- Cowie, L. L., Songaila, A., Hu, E. M., & Cohen, J. G. 1996, *AJ*, 112, 839
- Crenshaw, D. M., Kraemer, S. B., & Gabel, J. R. 2003, *AJ*, 126, 1690
- Croom, S. M., et al. 2005, *MNRAS*, 356, 415
- Croom, S. M., et al. 2009, *MNRAS*, 399, 1755
- Croston, J. H., et al. 2009, *MNRAS*, 395, 1999
- Croton, D. J. 2009, *MNRAS*, 394, 1109
- Croton, D. J., et al. 2006, *MNRAS*, 365, 11
- Cuadra, J., Nayakshin, S., & Martins, F. 2008, *MNRAS*, 383, 458
- Cuadra, J., Nayakshin, S., Springel, V., & Di Matteo, T. 2006, *MNRAS*, 366, 358
- da Ângela, J., et al. 2008, *MNRAS*, 383, 565
- Daddi, E., et al. 2007a, *ApJ*, 670, 173
- Daddi, E., et al. 2010, *ApJ*, 713, 686
- Daddi, E., et al. 2007b, *ApJ*, 670, 156
- Darg, D. W., et al. 2010, *MNRAS*, 401, 1552
- Davies, M. B., Miller, M. C., & Bellovary, J. M. 2011, *ApJ*, 740, L42
- Davies, R. I., Maciejewski, W., Hicks, E. K. S., Tacconi, L. J., Genzel, R., & Engel, H. 2009, *ApJ*, 702, 114
- Davies, R. I., Müller Sánchez, F., Genzel, R., Tacconi, L. J., Hicks, E. K. S., Friedrich, S., & Sternberg, A. 2007, *ApJ*, 671, 1388
- Davis, S. W. & Laor, A. 2011, *ApJ*, 728, 98
- de Koff, S., Baum, S. A., Sparks, W. B., Biretta, J., Golombek, D., Macchetto, F., McCarthy, P., & Miley, G. K. 1996, *ApJS*, 107, 621
- De Lucia, G., Springel, V., White, S. D. M., Croton, D., & Kauffmann, G. 2006, *MNRAS*, 366, 499
- De Rosa, G., Decarli, R., Walter, F., Fan, X., Jiang, L., Kurk, J., Pasquali, A., & Rix, H. W. 2011, *ApJ*, 739, 56
- Decarli, R., Falomo, R., Treves, A., Kotilainen, J. K., Labita, M., & Scarpa, R. 2010a, *MNRAS*, 402, 2441
- Decarli, R., Falomo, R., Treves, A., Labita, M., Kotilainen, J. K., & Scarpa, R. 2010b, *MNRAS*, 402, 2453
- Dekel, A. & Birnboim, Y. 2006, *MNRAS*, 368, 2
- Denney, K. D., Peterson, B. M., Dietrich, M., Vestergaard, M., & Bentz, M. C. 2009, *ApJ*, 692, 246
- Devecchi, B. & Volonteri, M. 2009, *ApJ*, 694, 302
- Devecchi, B., Volonteri, M., Colpi, M., & Haardt, F. 2010, *MNRAS*, 409, 1057
- Di Matteo, T., Allen, S. W., Fabian, A. C., Wilson, A. S., & Young, A. J. 2003, *ApJ*, 582, 133
- Di Matteo, T., Colberg, J., Springel, V., Hernquist, L., & Sijacki, D. 2008, *ApJ*, 676, 33
- Di Matteo, T., Springel, V., & Hernquist, L. 2005, *Nature*, 433, 604
- Diamond-Stanic, A. M. & Rieke, G. H. 2011, *ApJ* submitted (arXiv:1106.3565)
- Digby-North, J. A., et al. 2010, *MNRAS*, 407, 846
- Dodds-Eden, K., et al. 2011, *ApJ*, 728, 37
- Dodds-Eden, K., Sharma, P., Quataert, E., Genzel, R., Gillessen, S., Eisenhauer, F., & Porquet, D. 2010, *ApJ*, 725, 450
- Done, C., Gierliński, M., & Kubota, A. 2007, *A&A Rev.*, 15, 1
- Donley, J. L., Rieke, G. H., Pérez-González, P. G., & Barro, G. 2008, *ApJ*, 687, 111
- Donley, J. L., Rieke, G. H., Rigby, J. R., & Pérez-González, P. G. 2005, *ApJ*, 634, 169
- Donoso, E., Li, C., Kauffmann, G., Best, P. N., & Heckman, T. M. 2010, *MNRAS*, 407, 1078

- Dotti, M., Montuori, C., Decarli, R., Volonteri, M., Colpi, M., & Haardt, F. 2009, *MNRAS*, 398, L73
- Dotti, M. & Ruszkowski, M. 2010, *ApJ*, 713, L37
- Down, E. J., Rawlings, S., Sivia, D. S., & Baker, J. C. 2010, *MNRAS*, 401, 633
- Downes, D. & Eckart, A. 2007, *A&A*, 468, L57
- Dumas, G., Mundell, C. G., Emsellem, E., & Nagar, N. M. 2007, *MNRAS*, 379, 1249
- Dunlop, J. S., McLure, R. J., Kukula, M. J., Baum, S. A., O’Dea, C. P., & Hughes, D. H. 2003, *MNRAS*, 340, 1095
- Dunn, J. P., et al. 2010, *ApJ*, 709, 611
- Dunn, R. J. H. & Fabian, A. C. 2004, *MNRAS*, 355, 862
- . 2008, *MNRAS*, 385, 757
- Dunn, R. J. H., Fabian, A. C., & Taylor, G. B. 2005, *MNRAS*, 364, 1343
- Dwelly, T. & Page, M. J. 2006, *MNRAS*, 372, 1755
- Eastman, J., Martini, P., Sivakoff, G., Kelson, D. D., Mulchaey, J. S., & Tran, K.-V. 2007, *ApJ*, 664, L9
- Eckart, A., et al. 2009, *A&A*, 500, 935
- Eckart, A., et al. 2006, *A&A*, 450, 535
- Efstathiou, A., Hough, J. H., & Young, S. 1995, *MNRAS*, 277, 1134
- Efstathiou, A. & Rowan-Robinson, M. 1995, *MNRAS*, 273, 649
- Elbaz, D., et al. 2011, *A&A*, 533, A119
- Elitzur, M. & Shlosman, I. 2006, *ApJ*, 648, L101
- Ellison, S. L., Patton, D. R., Mendel, J. T., & Scudder, J. M. 2011, *MNRAS*, 1541
- Elvis, M., et al. 1994, *ApJS*, 95, 1
- Engel, H., et al. 2010, *ApJ*, 724, 233
- Englmaier, P. & Shlosman, I. 2004, *ApJ*, 617, L115
- Eracleous, M., Shields, J. C., Chartas, G., & Moran, E. C. 2002, *ApJ*, 565, 108
- Esin, A. A., McClintock, J. E., & Narayan, R. 1997, *ApJ*, 489, 865
- Evans, D. A., et al. 2010, in *Astronomical Society of the Pacific Conference Series*, Vol. 427, *Accretion and Ejection in AGN: a Global View*, ed. L. Maraschi, G. Ghisellini, R. Della Ceca, & F. Tavecchio, 97–+
- Evans, D. A., Worrall, D. M., Hardcastle, M. J., Kraft, R. P., & Birkinshaw, M. 2006, *ApJ*, 642, 96
- Fabian, A. C. 1999, *MNRAS*, 308, L39
- Fakhouri, O., Ma, C.-P., & Boylan-Kolchin, M. 2010, *MNRAS*, 406, 2267
- Falcke, H., Kording, E., & Markoff, S. 2004, *A&A*, 414, 895
- Fan, X., et al. 2001, *AJ*, 122, 2833
- Fan, X., et al. 2006, *AJ*, 131, 1203
- Fanaroff, B. L. & Riley, J. M. 1974, *MNRAS*, 167, 31P
- Fanidakis, N., Baugh, C. M., Benson, A. J., Bower, R. G., Cole, S., Done, C., & Frenk, C. S. 2011, *MNRAS*, 410, 53
- Fanidakis, N., et al. 2012, *MNRAS* in press
- Fathi, K., Storchi-Bergmann, T., Riffel, R. A., Winge, C., Axon, D. J., Robinson, A., Capetti, A., & Marconi, A. 2006, *ApJ*, 641, L25
- Fender, R. P., Belloni, T. M., & Gallo, E. 2004, *MNRAS*, 355, 1105
- Ferrarese, L. & Merritt, D. 2000, *ApJ*, 539, L9
- Feruglio, C., Daddi, E., Fiore, F., Alexander, D. M., Piconcelli, E., & Malacaria, C. 2011, *ApJ*, 729, L4+
- Feruglio, C., Maiolino, R., Piconcelli, E., Menci, N., Aussel, H., Lamastra, A., & Fiore, F. 2010, *A&A*, 518, L155+
- Filho, M. E., Barthel, P. D., & Ho, L. C. 2006, *A&A*, 451, 71
- Fine, S., Shanks, T., Nikoloudakis, N., & Sawangwit, U. 2011, *MNRAS* in press (arXiv:1107.5666)
- Finn, R. A., et al. 2010, *ApJ*, 720, 87
- Fiore, F. 2010, in *American Institute of Physics Conference Series*, Vol. 1248, *American Institute of Physics Conference Series*, ed. A. Comastri, L. Angelini, & M. Cappi, 373–380
- Fiore, F., et al. 2003, *A&A*, 409, 79
- Fiore, F., et al. 2008, *ApJ*, 672, 94
- Fiore, F., et al. 2009, *ApJ*, 693, 447
- Fischer, J., et al. 2010, *A&A*, 518, L41
- Floyd, D. J. E., et al. 2010, *ApJ*, 713, 66
- Floyd, D. J. E., Bate, N. F., & Webster, R. L. 2009, *MNRAS*, 398, 233
- Floyd, D. J. E., Kukula, M. J., Dunlop, J. S., McLure, R. J., Miller, L., Percival, W. J., Baum, S. A., & O’Dea, C. P. 2004, *MNRAS*, 355, 196
- Forman, W., et al. 2007, *ApJ*, 665, 1057
- Fromerth, M. J. & Melia, F. 2000, *ApJ*, 533, 172
- Fryer, C. L. & Kalogera, V. 2001, *ApJ*, 554, 548
- Gabor, J. M., et al. 2009, *ApJ*, 691, 705
- Gadotti, D. A. & Kauffmann, G. 2009, *MNRAS*, 399, 621
- Gallagher, S. C., Brandt, W. N., Chartas, G., Priddey, R., Garnire, G. P., & Sambruna, R. M. 2006, *ApJ*, 644, 709
- Gallo, E., Fender, R. P., & Pooley, G. G. 2003, *MNRAS*, 344, 60
- Gandhi, P., Horst, H., Smette, A., Hönig, S., Comastri, A., Gilli, R., Vignali, C., & Duschl, W. 2009, *A&A*, 502, 457
- Ganguly, R. & Brotherton, M. S. 2008, *ApJ*, 672, 102
- García-Burillo, S., Combes, F., Schinnerer, E., Boone, F., & Hunt, L. K. 2005, *A&A*, 441, 1011
- Geach, J. E., Smail, I., Moran, S. M., MacArthur, L. A., Lagos, C. d. P., & Edge, A. C. 2011, *ApJ*, 730, L19+
- Gebhardt, K., et al. 2000, *ApJ*, 539, L13
- Genzel, R., et al. 2008, *ApJ*, 687, 59
- Genzel, R., Schödel, R., Ott, T., Eckart, A., Alexander, T., Lacombe, F., Rouan, D., & Aschenbach, B. 2003, *Nature*, 425, 934
- Georgakakis, A., et al. 2009, *MNRAS*, 397, 623
- Georgakakis, A., et al. 2011, *MNRAS*, 1658
- Georgakakis, A., et al. 2008, *MNRAS*, 385, 2049
- Georgantopoulos, I., Rovilos, E., & Comastri, A. 2011, *A&A*, 526, A46+
- Ghez, A. M., et al. 2008, *ApJ*, 689, 1044
- Ghez, A. M., et al. 2004, *ApJ*, 601, L159
- Giacconi, R., et al. 2002, *ApJS*, 139, 369
- Gibson, R. R., Brandt, W. N., Gallagher, S. C., & Schneider, D. P. 2009, *ApJ*, 696, 924
- Gillessen, S., et al. 2006, *ApJ*, 640, L163
- Gillessen, S., Eisenhauer, F., Trippe, S., Alexander, T., Genzel, R., Martins, F., & Ott, T. 2009, *ApJ*, 692, 1075
- Gilli, R., Comastri, A., & Hasinger, G. 2007, *A&A*, 463, 79
- Gilli, R., Vignali, C., Mignoli, M., Iwasawa, K., Comastri, A., & Zamorani, G. 2010, *A&A*, 519, A92+
- Gilli, R., et al. 2009, *A&A*, 494, 33
- Gilmour, R., Gray, M. E., Almaini, O., Best, P., Wolf, C., Meisenheimer, K., Papovich, C., & Bell, E. 2007, *MNRAS*, 380, 1467
- Giodini, S., et al. 2009, *ApJ*, 703, 982
- Giodini, S., et al. 2010, *ApJ*, 714, 218
- Gladstone, J. C., Roberts, T. P., & Done, C. 2009, *MNRAS*, 397, 1836
- Glover, S. C. O., Clark, P. C., Greif, T. H., Johnson, J. L., Bromm, V., Klessen, R. S., & Stacy, A. 2008, in *IAU Symposium*, Vol. 255, *IAU Symposium*, ed. L. K. Hunt, S. Madden, & R. Schneider, 3–17
- Gofford, J., et al. 2011, *MNRAS*, 414, 3307
- González Delgado, R. M., Heckman, T., & Leitherer, C. 2001, *ApJ*, 546, 845
- González-Martín, O., Masegosa, J., Márquez, I., Guainazzi, M., & Jiménez-Bailón, E. 2009, *A&A*, 506, 1107
- Goodman, J. 2003, *MNRAS*, 339, 937
- Goulding, A. D. & Alexander, D. M. 2009, *MNRAS*, 398, 1165
- Goulding, A. D., Alexander, D. M., Lehmer, B. D., & Mullaney, J. R. 2010, *MNRAS*, 406, 597
- Granato, G. L. & Danese, L. 1994, *MNRAS*, 268, 235
- Greene, J. E. & Ho, L. C. 2007, *ApJ*, 667, 131
- Greene, J. E., Ho, L. C., & Barth, A. J. 2008, *ApJ*, 688, 159
- Greene, J. E., et al. 2010, *ApJ*, 721, 26

- Greene, J. E., Zakamska, N. L., Ho, L. C., & Barth, A. J. 2011, *ApJ*, 732, 9
- Greenhill, L. J. & Gwinn, C. R. 1997, *Ap&SS*, 248, 261
- Greif, T. H., Springel, V., White, S. D. M., Glover, S. C. O., Clark, P. C., Smith, R. J., Klessen, R. S., & Bromm, V. 2011, *ApJ*, 737, 75
- Grogin, N. A., et al. 2005, *ApJ*, 627, L97
- Guainazzi, M., Matt, G., & Perola, G. C. 2005, *A&A*, 444, 119
- Gültekin, K., et al. 2009, *ApJ*, 698, 198
- Guyon, O., Sanders, D. B., & Stockton, A. 2006, *ApJS*, 166, 89
- Haiman, Z. & Loeb, A. 2001, *ApJ*, 552, 459
- Hao, H., et al. 2010, *ApJ*, 724, L59
- Hao, H., Elvis, M., Civano, F., & Lawrence, A. 2011, *ApJ*, 733, 108
- Hao, L., et al. 2005, *AJ*, 129, 1783
- Hardcastle, M. J., Evans, D. A., & Croston, J. H. 2006, *MNRAS*, 370, 1893
- . 2007, *MNRAS*, 376, 1849
- Hartwick, F. D. A. & Schade, D. 1990, *ARA&A*, 28, 437
- Hasinger, G. 2008, *A&A*, 490, 905
- Hasinger, G., Miyaji, T., & Schmidt, M. 2005, *A&A*, 441, 417
- Heckman, T. M. 1980, *A&A*, 87, 152
- Heckman, T. M., Kauffmann, G., Brinchmann, J., Charlot, S., Tremonti, C., & White, S. D. M. 2004, *ApJ*, 613, 109
- Heinz, S., Merloni, A., & Schwab, J. 2007, *ApJ*, 658, L9
- Herbert, P. D., Jarvis, M. J., Willott, C. J., McLure, R. J., Mitchell, E., Rawlings, S., Hill, G. J., & Dunlop, J. S. 2010, *MNRAS*, 406, 1841
- . 2011, *MNRAS*, 410, 1360
- Hernquist, L. & Spiegel, D. N. 1992, *ApJ*, 399, L117
- Hickox, R. C., et al. 2007, *ApJ*, 671, 1365
- Hickox, R. C., et al. 2009, *ApJ*, 696, 891
- Hickox, R. C., et al. 2011, *ApJ*, 731, 117
- Hicks, E. K. S., Davies, R. I., Malkan, M. A., Genzel, R., Tacconi, L. J., Müller Sánchez, F., & Sternberg, A. 2009, *ApJ*, 696, 448
- Ho, L. C. 2008, *ARA&A*, 46, 475
- Ho, L. C., et al. 2001, *ApJ*, 549, L51
- Ho, L. C., Filippenko, A. V., & Sargent, W. L. W. 1997a, *ApJS*, 112, 315
- . 1997b, *ApJ*, 487, 568
- . 2003, *ApJ*, 583, 159
- Ho, L. C., Filippenko, A. V., Sargent, W. L. W., & Peng, C. Y. 1997c, *ApJS*, 112, 391
- Hobbs, A., Nayakshin, S., Power, C., & King, A. 2011, *MNRAS*, 413, 2633
- Hönig, S. F., Beckert, T., Ohnaka, K., & Weigelt, G. 2006, *A&A*, 452, 459
- Hönig, S. F. & Kishimoto, M. 2010, *A&A*, 523, A27
- Hopkins, P. F. 2011, *MNRAS* in press (arXiv:1101.4230)
- Hopkins, P. F., et al. 2010, *ApJ*, 715, 202
- Hopkins, P. F. & Hernquist, L. 2009, *ApJ*, 694, 599
- Hopkins, P. F., Hernquist, L., Cox, T. J., Di Matteo, T., Robertson, B., & Springel, V. 2006a, *ApJS*, 163, 1
- Hopkins, P. F., Hernquist, L., Cox, T. J., & Kereš, D. 2008, *ApJS*, 175, 356
- Hopkins, P. F., Hickox, R., Quataert, E., & Hernquist, L. 2009, *MNRAS*, 398, 333
- Hopkins, P. F. & Quataert, E. 2010, *MNRAS*, 407, 1529
- Hopkins, P. F., Richards, G. T., & Hernquist, L. 2007, *ApJ*, 654, 731
- Hopkins, P. F., Somerville, R. S., Hernquist, L., Cox, T. J., Robertson, B., & Li, Y. 2006b, *ApJ*, 652, 864
- Horst, H., Duschl, W. J., Gandhi, P., & Smette, A. 2009, *A&A*, 495, 137
- Horst, H., Gandhi, P., Smette, A., & Duschl, W. J. 2008, *A&A*, 479, 389
- Huchra, J. & Burg, R. 1992, *ApJ*, 393, 90
- Hunt, L. K. & Malkan, M. A. 2004, *ApJ*, 616, 707
- Ishida, C. M. 2004, PhD thesis, University of Hawai'i
- Iwasawa, K., Sanders, D. B., Evans, A. S., Trentham, N., Miniutti, G., & Spoon, H. W. W. 2005, *MNRAS*, 357, 565
- Iwasawa, K., et al. 2011, *A&A*, 529, A106+
- Jahnke, K., et al. 2009, *ApJ*, 706, L215
- Jahnke, K. & Macciò, A. V. 2011, *ApJ*, 734, 92
- Jiang, L., et al. 2009, *AJ*, 138, 305
- Jiang, L., et al. 2010, *Nature*, 464, 380
- Jiang, Y.-F., Greene, J. E., Ho, L. C., Xiao, T., & Barth, A. J. 2011, *ApJ*, 742, 68
- Jin, C., Done, C., Ward, M., Gierliński, M., & Mullaney, J. 2009, *MNRAS*, 398, L16
- Jogee, S. 2006, in *Lecture Notes in Physics*, Berlin Springer Verlag, Vol. 693, *Physics of Active Galactic Nuclei at all Scales*, ed. D. Alloin, 143–+
- Johnson, J. L. & Bromm, V. 2007, *MNRAS*, 374, 1557
- Johnson, J. L., Khochfar, S., Greif, T. H., & Durier, F. 2011, *MNRAS*, 410, 919
- Juneau, S., Dickinson, M., Alexander, D. M., & Salim, S. 2011, *ApJ*, 736, 104
- Juneau, S., et al. 2005, *ApJ*, 619, L135
- Jungwiert, B., Combes, F., & Palouš, J. 2001, *A&A*, 376, 85
- Kaspi, S., Maoz, D., Netzer, H., Peterson, B. M., Vestergaard, M., & Jannuzi, B. T. 2005, *ApJ*, 629, 61
- Kauffmann, G. 1996, *MNRAS*, 281, 487
- Kauffmann, G. & Haehnelt, M. 2000, *MNRAS*, 311, 576
- Kauffmann, G. & Heckman, T. M. 2009, *MNRAS*, 397, 135
- Kauffmann, G., Heckman, T. M., & Best, P. N. 2008, *MNRAS*, 384, 953
- Kauffmann, G., et al. 2003, *MNRAS*, 346, 1055
- Kauffmann, G., White, S. D. M., Heckman, T. M., Ménard, B., Brinchmann, J., Charlot, S., Tremonti, C., & Brinkmann, J. 2004, *MNRAS*, 353, 713
- Kawakatu, N., Imanishi, M., & Nagao, T. 2007, *ApJ*, 661, 660
- Kawakatu, N. & Wada, K. 2008, *ApJ*, 681, 73
- Kelly, B. C., Bechtold, J., Trump, J. R., Vestergaard, M., & Siemiginowska, A. 2008, *ApJS*, 176, 355
- Kelly, B. C., Vestergaard, M., Fan, X., Hopkins, P., Hernquist, L., & Siemiginowska, A. 2010, *ApJ*, 719, 1315
- Kennicutt, Jr., R. C. 1989, *ApJ*, 344, 685
- Kereš, D., Katz, N., Fardal, M., Davé, R., & Weinberg, D. H. 2009, *MNRAS*, 395, 160
- Kerr, R. P. 1963, *Physical Review Letters*, 11, 237
- Kewley, L. J., Dopita, M. A., Sutherland, R. S., Heisler, C. A., & Trevena, J. 2001, *ApJ*, 556, 121
- Kewley, L. J., Groves, B., Kauffmann, G., & Heckman, T. 2006, *MNRAS*, 372, 961
- Kim, D.-C., Veilleux, S., & Sanders, D. B. 1998, *ApJ*, 508, 627
- Kim, M., Ho, L. C., Peng, C. Y., Barth, A. J., Im, M., Martini, P., & Nelson, C. H. 2008, *ApJ*, 687, 767
- King, A. 2003, *ApJ*, 596, L27
- . 2005, *ApJ*, 635, L121
- King, A. R. 2010a, *MNRAS*, 408, L95
- . 2010b, *MNRAS*, 402, 1516
- King, A. R., Davies, M. B., Ward, M. J., Fabbiano, G., & Elvis, M. 2001, *ApJ*, 552, L109
- King, A. R. & Pringle, J. E. 2007, *MNRAS*, 377, L25
- King, A. R., Zubovas, K., & Power, C. 2011, *MNRAS*, L263+
- Kishimoto, M., Hönig, S. F., Antonucci, R., Barvainis, R., Kotani, T., Tristram, K. R. W., Weigelt, G., & Levin, K. 2011, *A&A*, 527, A121+
- Knapen, J. H., Shlosman, I., & Peletier, R. F. 2000, *ApJ*, 529, 93
- Kocevski, D. D., et al. 2011, *ApJ* submitted (arXiv:1109.2588)
- Kocevski, D. D., Lubin, L. M., Gal, R., Lemaux, B. C., Fassnacht,

- C. D., & Squires, G. K. 2009, *ApJ*, 690, 295
- Kollmeier, J. A., et al. 2006, *ApJ*, 648, 128
- Komossa, S., Zhou, H., & Lu, H. 2008, *ApJ*, 678, L81
- Körding, E. G., Jester, S., & Fender, R. 2008, *MNRAS*, 383, 277
- Kormendy, J. & Bender, R. 2011, *Nature*, 469, 377
- Kormendy, J., Bender, R., & Cornell, M. E. 2011, *Nature*, 469, 374
- Kormendy, J. & Kennicutt, Jr., R. C. 2004, *ARA&A*, 42, 603
- Kormendy, J. & Richstone, D. 1995, *ARA&A*, 33, 581
- Koss, M., Mushotzky, R., Veilleux, S., & Winter, L. 2010, *ApJ*, 716, L125
- Koss, M., Mushotzky, R., Veilleux, S., Winter, L. M., Baumgartner, W., Tueller, J., Gehrels, N., & Valencic, L. 2011, *ApJ*, 739, 57
- Kotilainen, J. K., Falomo, R., Decarli, R., Treves, A., Uslenghi, M., & Scarpa, R. 2009, *ApJ*, 703, 1663
- Kotilainen, J. K., Falomo, R., Labita, M., Treves, A., & Uslenghi, M. 2007, *ApJ*, 660, 1039
- Krumpe, M., Miyaji, T., & Coil, A. L. 2010, *ApJ*, 713, 558
- Kuo, C.-Y., Lim, J., Tang, Y.-W., & Ho, P. T. P. 2008, *ApJ*, 679, 1047
- Kuraszkiewicz, J., Wilkes, B. J., Schmidt, G., Smith, P. S., Cutri, R., & Czerny, B. 2009, *ApJ*, 692, 1180
- La Franca, F., et al. 2005, *ApJ*, 635, 864
- La Franca, F., Melini, G., & Fiore, F. 2010, *ApJ*, 718, 368
- Lacy, M., et al. 2004, *ApJS*, 154, 166
- Laine, S., Shlosman, I., Knapen, J. H., & Peletier, R. F. 2002, *ApJ*, 567, 97
- Laird, E. S., Nandra, K., Pope, A., & Scott, D. 2010, *MNRAS*, 401, 2763
- Lauer, T. R., Tremaine, S., Richstone, D., & Faber, S. M. 2007, *ApJ*, 670, 249
- Lawrence, A. 1991, *MNRAS*, 252, 586
- Lawrence, A. & Elvis, M. 2010, *ApJ*, 714, 561
- Le Floch, E., et al. 2005, *ApJ*, 632, 169
- Lehmer, B. D., Alexander, D. M., Bauer, F. E., Brandt, W. N., Goulding, A. D., Jenkins, L. P., Ptak, A., & Roberts, T. P. 2010, *ApJ*, 724, 559
- Lehmer, B. D., et al. 2009a, *MNRAS*, 400, 299
- Lehmer, B. D., et al. 2009b, *ApJ*, 691, 687
- Lehmer, B. D., et al. 2007, *ApJ*, 657, 681
- Li, C., Kauffmann, G., Wang, L., White, S. D. M., Heckman, T. M., & Jing, Y. P. 2006, *MNRAS*, 373, 457
- Lietzen, H., et al. 2009, *A&A*, 501, 145
- Lintott, C., et al. 2011, *MNRAS*, 410, 166
- Liu, S. & Melia, F. 2002, *ApJ*, 566, L77
- Liu, X., Shen, Y., Strauss, M. A., & Hao, L. 2011, *ApJ*, 737, 101
- Lobban, A. P., Reeves, J. N., Miller, L., Turner, T. J., Braito, V., Kraemer, S. B., & Crenshaw, D. M. 2011, *MNRAS*, 544
- Luo, B., et al. 2008, *ApJS*, 179, 19
- Luo, B., et al. 2011, *ApJ*, 740, 37
- Luo, B., et al. 2010, *ApJS*, 187, 560
- Lutz, D., et al. 2010, *ApJ*, 712, 1287
- Lutz, D., Maiolino, R., Spoon, H. W. W., & Moorwood, A. F. M. 2004, *A&A*, 418, 465
- Lutz, D., et al. 2008, *ApJ*, 684, 853
- Lynden-Bell, D. 1969, *Nature*, 223, 690
- Maccarone, T. J. 2003, *A&A*, 409, 697
- Maciejewski, W. 2004, *MNRAS*, 354, 892
- Madau, P. & Rees, M. J. 2001, *ApJ*, 551, L27
- Madau, P., Rees, M. J., Volonteri, M., Haardt, F., & Oh, S. P. 2004, *ApJ*, 604, 484
- Magorrian, J., et al. 1998, *AJ*, 115, 2285
- Mainieri, V., et al. 2011, *A&A*, 535, A80
- Mainieri, V., et al. 2005a, *MNRAS*, 356, 1571
- Mainieri, V., et al. 2005b, *A&A*, 437, 805
- Maiolino, R. & Rieke, G. H. 1995, *ApJ*, 454, 95
- Malbon, R. K., Baugh, C. M., Frenk, C. S., & Lacey, C. G. 2007, *MNRAS*, 382, 1394
- Malin, D. F. & Carter, D. 1983, *ApJ*, 274, 534
- Malkan, M. A., Gorjian, V., & Tam, R. 1998, *ApJS*, 117, 25
- Mandelbaum, R., Li, C., Kauffmann, G., & White, S. D. M. 2009, *MNRAS*, 393, 377
- Marconi, A., Axon, D. J., Maiolino, R., Nagao, T., Pastorini, G., Pietrini, P., Robinson, A., & Torricelli, G. 2008, *ApJ*, 678, 693
- Marconi, A. & Hunt, L. K. 2003, *ApJ*, 589, L21
- Marconi, A., Risaliti, G., Gilli, R., Hunt, L. K., Maiolino, R., & Salvati, M. 2004, *MNRAS*, 351, 169
- Markoff, S., Falcke, H., Yuan, F., & Biermann, P. L. 2001, *A&A*, 379, L13
- Marrone, D. P., et al. 2008, *ApJ*, 682, 373
- Martini, P., Kelson, D. D., Kim, E., Mulchaey, J. S., & Athey, A. A. 2006, *ApJ*, 644, 116
- Martini, P., Regan, M. W., Mulchaey, J. S., & Pogge, R. W. 2003, *ApJ*, 589, 774
- Martini, P., Sivakoff, G. R., & Mulchaey, J. S. 2009, *ApJ*, 701, 66
- Mathur, S., Fields, D., Peterson, B. M., & Grupe, D. 2011, *ApJ* submitted (1102.0537)
- McCarthy, I. G., Schaye, J., Bower, R. G., Ponman, T. J., Booth, C. M., Dalla Vecchia, C., & Springel, V. 2011, *MNRAS*, 412, 1965
- McCarthy, I. G., et al. 2010, *MNRAS*, 406, 822
- McHardy, I. M., Koending, E., Knigge, C., Uttley, P., & Fender, R. P. 2006, *Nature*, 444, 730
- McKee, C. F. & Ostriker, E. C. 2007, *ARA&A*, 45, 565
- McKee, C. F. & Tan, J. C. 2008, *ApJ*, 681, 771
- McLure, R. J. & Dunlop, J. S. 2004, *MNRAS*, 352, 1390
- McLure, R. J. & Jarvis, M. J. 2002, *MNRAS*, 337, 109
- McLure, R. J., Willott, C. J., Jarvis, M. J., Rawlings, S., Hill, G. J., Mitchell, E., Dunlop, J. S., & Wold, M. 2004, *MNRAS*, 351, 347
- McNamara, B. R., Kazemzadeh, F., Rafferty, D. A., Birzan, L., Nulsen, P. E. J., Kirkpatrick, C. C., & Wise, M. W. 2009, *ApJ*, 698, 594
- McNamara, B. R. & Nulsen, P. E. J. 2007, *ARA&A*, 45, 117
- McNamara, B. R., Nulsen, P. E. J., Wise, M. W., Rafferty, D. A., Carilli, C., Sarazin, C. L., & Blanton, E. L. 2005, *Nature*, 433, 45
- McNamara, B. R., Rohanizadegan, M., & Nulsen, P. E. J. 2011, *ApJ*, 727, 39
- Melia, F. & Falcke, H. 2001, *ARA&A*, 39, 309
- Merloni, A. 2004, *MNRAS*, 353, 1035
- Merloni, A., et al. 2010, *ApJ*, 708, 137
- Merloni, A. & Heinz, S. 2008, *MNRAS*, 388, 1011
- Merloni, A., Heinz, S., & di Matteo, T. 2003, *MNRAS*, 345, 1057
- Merloni, A., Rudnick, G., & Di Matteo, T. 2004, *MNRAS*, 354, L37
- Micic, M., Holley-Bockelmann, K., & Sigurdsson, S. 2011, *MNRAS*, 414, 1127
- Mihos, J. C. & Hernquist, L. 1996, *ApJ*, 464, 641
- Mirabel, I. F., Dijkstra, M., Laurent, P., Loeb, A., & Pritchard, J. R. 2011, *A&A*, 528, A149+
- Mirabel, I. F. & Rodríguez, L. F. 1994, *Nature*, 371, 46
- , 1998, *Nature*, 392, 673
- Mirabel, I. F., Rodríguez, L. F., Cordier, B., Paul, J., & Lebrun, F. 1992, *Nature*, 358, 215
- Mo, H. J., Mao, S., & White, S. D. M. 1998, *MNRAS*, 295, 319
- Mortlock, D. J., et al. 2011, *Nature*, 474, 616
- Mulchaey, J. S., Koratkar, A., Ward, M. J., Wilson, A. S., Whittle, M., Antonucci, R. R. J., Kinney, A. L., & Hurt, T. 1994, *ApJ*, 436, 586
- Mulchaey, J. S. & Regan, M. W. 1997, *ApJ*, 482, L135+
- Mullaney, J. R., Alexander, D. M., Goulding, A. D., & Hickox, R. C. 2011a, *MNRAS*, 414, 1082
- Mullaney, J. R., Alexander, D. M., Huynh, M., Goulding, A. D., & Frayer, D. 2010, *MNRAS*, 401, 995
- Mullaney, J. R., et al. 2011b, *MNRAS*, 1756
- Müller Sánchez, F., et al. 2009, *ApJ*, 691, 749

- Muno, M. P., Baganoff, F. K., Brandt, W. N., Park, S., & Morris, M. R. 2007, *ApJ*, 656, L69
- Murray, S., et al. 2010, in American Institute of Physics Conference Series, Vol. 1248, American Institute of Physics Conference Series, ed. A. Comastri, L. Angelini, & M. Cappi, 549–554
- Myers, A. D., et al. 2006, *ApJ*, 638, 622
- Nandra, K., et al. 2007, *ApJ*, 660, L11
- Narayan, R. & Yi, I. 1994, *ApJ*, 428, L13
- Nardini, E. & Risaliti, G. 2011, *MNRAS*, 415, 619
- Nardini, E., Risaliti, G., Watabe, Y., Salvati, M., & Sani, E. 2010, *MNRAS*, 405, 2505
- Nayakshin, S., Cuadra, J., & Springel, V. 2007, *MNRAS*, 379, 21
- Nayakshin, S. & Sunyaev, R. 2005, *MNRAS*, 364, L23
- Nayakshin, S., Wilkinson, M. I., & King, A. 2009, *MNRAS*, 398, L54
- Nenkova, M., Ivezić, Ž., & Elitzur, M. 2002, *ApJ*, 570, L9
- Nenkova, M., Sirocky, M. M., Nikutta, R., Ivezić, Ž., & Elitzur, M. 2008, *ApJ*, 685, 160
- Nesvadba, N. P. H., Lehnert, M. D., De Breuck, C., Gilbert, A., & van Breugel, W. 2007, *A&A*, 475, 145
- Nesvadba, N. P. H., Lehnert, M. D., De Breuck, C., Gilbert, A. M., & van Breugel, W. 2008, *A&A*, 491, 407
- Nesvadba, N. P. H., Lehnert, M. D., Eisenhauer, F., Gilbert, A., Tecza, M., & Abuter, R. 2006, *ApJ*, 650, 693
- Netzer, H., et al. 2007, *ApJ*, 666, 806
- Netzer, H. & Marziani, P. 2010, *ApJ*, 724, 318
- Netzer, H. & Trakhtenbrot, B. 2007, *ApJ*, 654, 754
- Noeske, K. G., et al. 2007, *ApJ*, 660, L43
- Nowak, M. A. 1995, *PASP*, 107, 1207
- Ohsuga, K. 2007, *ApJ*, 659, 205
- Ohsuga, K., Mori, M., Nakamoto, T., & Mineshige, S. 2005, *ApJ*, 628, 368
- Onken, C. A., Ferrarese, L., Merritt, D., Peterson, B. M., Pogge, R. W., Vestergaard, M., & Wandel, A. 2004, *ApJ*, 615, 645
- Orban de Xivry, G., Davies, R., Schartmann, M., Komossa, S., Marconi, A., Hicks, E., Engel, H., & Tacconi, L. 2011, *MNRAS*, 1359
- Osterbrock, D. E. & Pogge, R. W. 1985, *ApJ*, 297, 166
- Page, M. J., Carrera, F. J., Stevens, J. A., Ebrero, J., & Blustin, A. J. 2011, *MNRAS*, 416, 2792
- Page, M. J., Stevens, J. A., Ivison, R. J., & Carrera, F. J. 2004, *ApJ*, 611, L85
- Page, M. J., Stevens, J. A., Mittaz, J. P. D., & Carrera, F. J. 2001, *Science*, 294, 2516
- Pakull, M. W., Soria, R., & Motch, C. 2010, *Nature*, 466, 209
- Pannella, M., et al. 2009, *ApJ*, 698, L116
- Paumard, T., et al. 2006, *ApJ*, 643, 1011
- Peng, C. Y. 2007, *ApJ*, 671, 1098
- Pérez-González, P. G., et al. 2005, *ApJ*, 630, 82
- Peterson, B. M. 2010, in IAU Symposium, Vol. 267, IAU Symposium, 151–160
- Peterson, B. M. 2011, arXiv:1109.4181
- Peterson, B. M., et al. 2004, *ApJ*, 613, 682
- Petric, A. O., et al. 2011a, *ApJ*, 730, 28
- . 2011b, *ApJ*, 730, 28
- Pier, E. A. & Krolik, J. H. 1992, *ApJ*, 401, 99
- Pierce, C. M., et al. 2007, *ApJ*, 660, L19
- Pogge, R. W. & Martini, P. 2002, *ApJ*, 569, 624
- Polletta, M., et al. 2007, *ApJ*, 663, 81
- Polletta, M., Weedman, D., Hönig, S., Lonsdale, C. J., Smith, H. E., & Houck, J. 2008, *ApJ*, 675, 960
- Polletta, M. D. C., et al. 2006, *ApJ*, 642, 673
- Ponti, G., Terrier, R., Goldwurm, A., Belanger, G., & Trap, G. 2010, *ApJ*, 714, 732
- Pooley, D., Blackburne, J. A., Rappaport, S., & Schechter, P. L. 2007, *ApJ*, 661, 19
- Pope, A., et al. 2008, *ApJ*, 675, 1171
- Pope, E. C. D. 2011, *MNRAS*, 755
- Pounds, K. A., Reeves, J. N., Page, K. L., Edelson, R., Matt, G., & Perola, G. C. 2003, *MNRAS*, 341, 953
- Power, C., Nayakshin, S., & King, A. 2011, *MNRAS*, 412, 269
- Pozzi, F., et al. 2010, *A&A*, 517, A11+
- Predehl, P., et al. 2007, in Proceedings of the SPIE, Volume 6686, pp. 668617–668617-9, Vol. 6686
- Prieto, M. A., Maciejewski, W., & Reunanen, J. 2005, *AJ*, 130, 1472
- Pringle, J. E. 1981, *ARA&A*, 19, 137
- Raban, D., Jaffe, W., Röttgering, H., Meisenheimer, K., & Tristram, K. R. W. 2009, *MNRAS*, 394, 1325
- Rafferty, D. A., Brandt, W. N., Alexander, D. M., Xue, Y. Q., Bauer, F. E., Lehmer, B. D., Luo, B., & Papovich, C. 2011, *ApJ*, 742, 3
- Rafferty, D. A., McNamara, B. R., & Nulsen, P. E. J. 2008, *ApJ*, 687, 899
- Rafferty, D. A., McNamara, B. R., Nulsen, P. E. J., & Wise, M. W. 2006, *ApJ*, 652, 216
- Raimundo, S. I., Fabian, A. C., Bauer, F. E., Alexander, D. M., Brandt, W. N., Luo, B., Vasudevan, R. V., & Xue, Y. Q. 2010, *MNRAS*, 408, 1714
- Raimundo, S. I., Fabian, A. C., Vasudevan, R. V., Gandhi, P., & Wu, J. 2011, *MNRAS* in press (arXiv:1109.6225)
- Ramos Almeida, C., et al. 2011a, *MNRAS*, 1702
- Ramos Almeida, C., Tadhunter, C. N., Inskip, K. J., Morganti, R., Holt, J., & Dicken, D. 2011b, *MNRAS*, 410, 1550
- Rees, M. J. 1984, *ARA&A*, 22, 471
- Reeves, J. N., O’Brien, P. T., & Ward, M. J. 2003, *ApJ*, 593, L65
- Regan, J. A. & Haehnelt, M. G. 2009, *MNRAS*, 396, 343
- Reid, M. J. 1993, *ARA&A*, 31, 345
- Remillard, R. A. & McClintock, J. E. 2006, *ARA&A*, 44, 49
- Reyes, R., et al. 2008, *AJ*, 136, 2373
- Richards, G. T., et al. 2005, *MNRAS*, 360, 839
- Richards, G. T., et al. 2011, *AJ*, 141, 167
- Richards, G. T., et al. 2006, *AJ*, 131, 2766
- Richards, G. T., Vanden Berk, D. E., Reichard, T. A., Hall, P. B., Schneider, D. P., SubbaRao, M., Thakar, A. R., & York, D. G. 2002, *AJ*, 124, 1
- Riechers, D. A., et al. 2011, *ApJ*, 733, L11+
- Riffel, R. A., Storchi-Bergmann, T., Winge, C., McGregor, P. J., Beck, T., & Schmitt, H. 2008, *MNRAS*, 385, 1129
- Rigby, E. E., Best, P. N., Brookes, M. H., Peacock, J. A., Dunlop, J. S., Röttgering, H. J. A., Wall, J. V., & Ker, L. 2011, *MNRAS*, 416, 1900
- Rigby, E. E., Best, P. N., & Snellen, I. A. G. 2008, *MNRAS*, 385, 310
- Risaliti, G., Elvis, M., & Nicastro, F. 2002, *ApJ*, 571, 234
- Risaliti, G., Maiolino, R., & Salvati, M. 1999, *ApJ*, 522, 157
- Roberts, T. P. 2007, *Ap&SS*, 311, 203
- Roberts, T. P., Goad, M. R., Ward, M. J., & Warwick, R. S. 2003, *MNRAS*, 342, 709
- Robinson, A., Young, S., Axon, D. J., Kharb, P., & Smith, J. E. 2010, *ApJ*, 717, L122
- Rodighiero, G., et al. 2010a, *A&A*, 518, L25+
- Rodighiero, G., et al. 2010b, *A&A*, 515, A8+
- Rodríguez-Zaurín, J., Arribas, S., Monreal-Ibero, A., Colina, L., Alonso-Herrero, A., & Alfonso-Garzón, J. 2011, *A&A*, 527, A60+
- Rosario, D. J., McGurk, R. C., Max, C. E., Shields, G. A., Smith, K. L., & Ammons, S. M. 2011, *ApJ*, 739, 44
- Ross, N. P., et al. 2009, *ApJ*, 697, 1634
- Rovilos, E., Fotopoulou, S., Salvato, M., Burwitz, V., Egami, E., Hasinger, G., & Szokoly, G. 2011, *A&A*, 529, A135+
- Rovilos, E. & Georgantopoulos, I. 2007, *A&A*, 475, 115
- Rovilos, E., Georgantopoulos, I., Akylas, A., & Fotopoulou, S. 2010, *A&A*, 522, A11+
- Sadler, E. M., et al. 2007, *MNRAS*, 381, 211
- Saintonge, A., Tran, K.-V. H., & Holden, B. P. 2008, *ApJ*, 685, L113

- Salpeter, E. E. 1964, *ApJ*, 140, 796
- Salvato, M., et al. 2011, *ApJ*, 742, 61
- Sánchez, S. F., et al. 2004, *ApJ*, 614, 586
- Sanders, D. B., Soifer, B. T., Elias, J. H., Madore, B. F., Matthews, K., Neugebauer, G., & Scoville, N. Z. 1988, *ApJ*, 325, 74
- Sarzi, M., et al. 2010, *MNRAS*, 402, 2187
- Satyapal, S., Sambruna, R. M., & Dudik, R. P. 2004, *A&A*, 414, 825
- Satyapal, S., Vega, D., Dudik, R. P., Abel, N. P., & Heckman, T. 2008, *ApJ*, 677, 926
- Sazonov, S., Revnivtsev, M., Krivonos, R., Churazov, E., & Sunyaev, R. 2007, *A&A*, 462, 57
- Schartmann, M., Burkert, A., Krause, M., Camenzind, M., Meisenheimer, K., & Davies, R. I. 2010, *MNRAS*, 403, 1801
- Schartmann, M., Meisenheimer, K., Camenzind, M., Wolf, S., Tristram, K. R. W., & Henning, T. 2008, *A&A*, 482, 67
- Schartmann, M., Meisenheimer, K., Klahr, H., Camenzind, M., Wolf, S., & Henning, T. 2009, *MNRAS*, 393, 759
- Schawinski, K., Dowlin, N., Thomas, D., Urry, C. M., & Edmondson, E. 2010, *ApJ*, 714, L108
- Schawinski, K., Treister, E., Urry, C. M., Cardamone, C. N., Simmons, B., & Yi, S. K. 2011, *ApJ*, 727, L31+
- Schawinski, K., Virani, S., Simmons, B., Urry, C. M., Treister, E., Kaviraj, S., & Kushkuley, B. 2009, *ApJ*, 692, L19
- Scheuer, P. A. G. 1974, *MNRAS*, 166, 513
- Schmidt, M. 1968, *ApJ*, 151, 393
- Schmidt, M. & Green, R. F. 1983, *ApJ*, 269, 352
- Schmitt, H. R. & Kinney, A. L. 1996, *ApJ*, 463, 498
- Schnorr Müller, A., Storchi-Bergmann, T., Riffel, R. A., Ferrari, F., Steiner, J. E., Axon, D. J., & Robinson, A. 2011, *MNRAS*, 413, 149
- Schödel, R., et al. 2007, *A&A*, 469, 125
- Schramm, M., Wisotzki, L., & Jahnke, K. 2008, *A&A*, 478, 311
- Schweitzer, M., et al. 2008, *ApJ*, 679, 101
- Schweitzer, M., et al. 2006, *ApJ*, 649, 79
- Sereno, M., Jetzer, P., Sesana, A., & Volonteri, M. 2011, *MNRAS*, 415, 2773
- Serjeant, S. & Hatziminaoglou, E. 2009, *MNRAS*, 397, 265
- Sesana, A., Volonteri, M., & Haardt, F. 2007, *MNRAS*, 377, 1711
- Seymour, N., et al. 2011, *MNRAS*, 413, 1777
- Shakura, N. I. & Sunyaev, R. A. 1973, *A&A*, 24, 337
- Shang, C., Bryan, G. L., & Haiman, Z. 2010, *MNRAS*, 402, 1249
- Shankar, F. 2009, *New Astronomy Reviews*, 53, 57
- Shankar, F., Salucci, P., Granato, G. L., De Zotti, G., & Danese, L. 2004, *MNRAS*, 354, 1020
- Shankar, F., Weinberg, D. H., & Miralda-Escudé, J. 2009, *ApJ*, 690, 20
- Shao, L., et al. 2010, *A&A*, 518, L26+
- Shapiro, S. L. & Teukolsky, S. A. 1983, *Black holes, white dwarfs, and neutron stars: The physics of compact objects* (New York: Wiley-Interscience)
- Shen, Y., Greene, J. E., Strauss, M. A., Richards, G. T., & Schneider, D. P. 2008, *ApJ*, 680, 169
- Shen, Y. & Kelly, B. C. 2010, *ApJ*, 713, 41
- Shen, Y., Liu, X., Greene, J. E., & Strauss, M. A. 2011, *ApJ*, 735, 48
- Shen, Y., et al. 2007, *AJ*, 133, 2222
- Shi, Y., Rieke, G., Donley, J., Cooper, M., Willmer, C., & Kirby, E. 2008, *ApJ*, 688, 794
- Shi, Y., Rieke, G. H., Ogle, P., Jiang, L., & Diamond-Stanic, A. M. 2009, *ApJ*, 703, 1107
- Shields, J. C., et al. 2007, *ApJ*, 654, 125
- Shlosman, I., Begelman, M. C., & Frank, J. 1990, *Nature*, 345, 679
- Shlosman, I., Frank, J., & Begelman, M. C. 1989, *Nature*, 338, 45
- Siemiginowska, A., Burke, D. J., Aldcroft, T. L., Worrall, D. M., Allen, S., Bechtold, J., Clarke, T., & Cheung, C. C. 2010, *ApJ*, 722, 102
- Sijacki, D., Springel, V., Di Matteo, T., & Hernquist, L. 2007, *MNRAS*, 380, 877
- Silk, J. & Rees, M. J. 1998, *A&A*, 331, L1
- Silverman, J. D., et al. 2008a, *ApJ*, 679, 118
- Silverman, J. D., et al. 2011, *ApJ* in press (arXiv:1109.1292)
- Silverman, J. D., et al. 2009a, *ApJ*, 695, 171
- Silverman, J. D., et al. 2009b, *ApJ*, 696, 396
- Silverman, J. D., et al. 2008b, *ApJ*, 675, 1025
- Simões Lopes, R. D., Storchi-Bergmann, T., de Fátima Saraiva, M., & Martini, P. 2007, *ApJ*, 655, 718
- Simmons, B. D., Van Duyne, J., Urry, C. M., Treister, E., Koekemoer, A. M., Grogan, N. A., & The GOODS Team. 2011, *ApJ*, 734, 121
- Simpson, C. 2005, *MNRAS*, 360, 565
- Smith, J. E., Robinson, A., Alexander, D. M., Young, S., Axon, D. J., & Corbett, E. A. 2004, *MNRAS*, 350, 140
- Smith, K. L., Shields, G. A., Bonning, E. W., McMullen, C. C., Rosario, D. J., & Salviander, S. 2010, *ApJ*, 716, 866
- Smith, R. J., Lucey, J. R., & Hudson, M. J. 2009, *MNRAS*, 400, 1690
- Smolčić, V. 2009, *ApJ*, 699, L43
- Smolčić, V., Finoguenov, A., Zamorani, G., Schinnerer, E., Tanaka, M., Giodini, S., & Scoville, N. 2011, *MNRAS*, 416, L31
- Smolčić, V. & Riechers, D. A. 2011, *ApJ*, 730, 64
- Smolčić, V., et al. 2009, *ApJ*, 696, 24
- Sobolewska, M. A., Siemiginowska, A., & Gierliński, M. 2011, *MNRAS*, 413, 2259
- Soltan, A. 1982, *MNRAS*, 200, 115
- Somerville, R. S., Hopkins, P. F., Cox, T. J., Robertson, B. E., & Hernquist, L. 2008, *MNRAS*, 391, 481
- Spoon, H. W. W., Moorwood, A. F. M., Lutz, D., Tielens, A. G. G. M., Siebenmorgen, R., & Keane, J. V. 2004, *A&A*, 414, 873
- Springel, V., Di Matteo, T., & Hernquist, L. 2005a, *ApJ*, 620, L79
- . 2005b, *MNRAS*, 361, 776
- Stacy, A., Greif, T. H., & Bromm, V. 2010, *MNRAS*, 403, 45
- Steidel, C. C., Adelberger, K. L., Dickinson, M., Giavalisco, M., Pettini, M., & Kellogg, M. 1998, *ApJ*, 492, 428
- Steidel, C. C., Hunt, M. P., Shapley, A. E., Adelberger, K. L., Pettini, M., Dickinson, M., & Giavalisco, M. 2002, *ApJ*, 576, 653
- Stern, D., et al. 2005, *ApJ*, 631, 163
- Stevens, J. A., Page, M. J., Ivison, R. J., Carrera, F. J., Mittaz, J. P. D., Smail, I., & McHardy, I. M. 2005, *MNRAS*, 360, 610
- Stobbart, A.-M., Roberts, T. P., & Wilms, J. 2006, *MNRAS*, 368, 397
- Stoklasová, I., Ferruit, P., Emsellem, E., Jungwiert, B., Pécontal, E., & Sánchez, S. F. 2009, *A&A*, 500, 1287
- Storchi-Bergmann, T., Dors, Jr., O. L., Riffel, R. A., Fathi, K., Axon, D. J., Robinson, A., Marconi, A., & Östlin, G. 2007, *ApJ*, 670, 959
- Storchi-Bergmann, T., González Delgado, R. M., Schmitt, H. R., Cid Fernandes, R., & Heckman, T. 2001, *ApJ*, 559, 147
- Storchi-Bergmann, T., Lopes, R. D. S., McGregor, P. J., Riffel, R. A., Beck, T., & Martini, P. 2010, *MNRAS*, 402, 819
- Storchi-Bergmann, T., Nemmen, R. S., Spinelli, P. F., Eracleous, M., Wilson, A. S., Filippenko, A. V., & Livio, M. 2005, *ApJ*, 624, L13
- Strateva, I., et al. 2001, *AJ*, 122, 1861
- Sturm, E., et al. 2011, *ApJ*, 733, L16
- Sulentic, J. W., Zwitter, T., Marziani, P., & Dultzin-Hacyan, D. 2000, *ApJ*, 536, L5
- Sun, M., Voit, G. M., Donahue, M., Jones, C., Forman, W., & Vikhlinin, A. 2009, *ApJ*, 693, 1142
- Symeonidis, M., Rosario, D., Georgakakis, A., Harker, J., Laird, E. S., Page, M. J., & Willmer, C. N. A. 2010, *MNRAS*, 403, 1474
- Szokoly, G. P., et al. 2004, *ApJS*, 155, 271
- Tacconi, L. J., et al. 2010, *Nature*, 463, 781
- Tacconi, L. J., et al. 2008, *ApJ*, 680, 246
- Tasse, C., Best, P. N., Röttgering, H., & Le Borgne, D. 2008, *A&A*, 490, 893
- Tasse, C., Röttgering, H., & Best, P. N. 2011, *A&A*, 525, A127+

- Teysseier, R., Moore, B., Martizzi, D., Dubois, Y., & Mayer, L. 2011, *MNRAS*, 414, 195
 Thompson, T. A., Quataert, E., & Murray, N. 2005, *ApJ*, 630, 167
 Tombesi, F., Cappi, M., Reeves, J. N., Palumbo, G. G. C., Yaqoob, T., Braitto, V., & Dadina, M. 2010, *A&A*, 521, A57+
 Tommasin, S., Spinoglio, L., Malkan, M. A., & Fazio, G. 2010, *ApJ*, 709, 1257
 Toomre, A. 1964, *ApJ*, 139, 1217
 Tozzi, P., et al. 2006, *A&A*, 451, 457
 Trakhtenbrot, B., Netzer, H., Lira, P., & Shemmer, O. 2011, *ApJ*, 730, 7
 Tran, Q. D., et al. 2001, *ApJ*, 552, 527
 Treister, E., et al. 2009, *ApJ*, 706, 535
 Treister, E., Natarajan, P., Sanders, D. B., Urry, C. M., Schawinski, K., & Kartaltepe, J. 2010a, *Science*, 328, 600
 Treister, E. & Urry, C. M. 2006, *ApJ*, 652, L79
 Treister, E., Urry, C. M., Schawinski, K., Cardamone, C. N., & Sanders, D. B. 2010b, *ApJ*, 722, L238
 Tremaine, S., et al. 2002, *ApJ*, 574, 740
 Tremonti, C. A., Moustakas, J., & Diamond-Stanic, A. M. 2007, *ApJ*, 663, L77
 Trenti, M. & Stiavelli, M. 2009, *ApJ*, 694, 879
 Trichas, M., Georgakakis, A., Rowan-Robinson, M., Nandra, K., Clements, D., & Vaccari, M. 2009, *MNRAS*, 399, 663
 Trippe, S., Paumard, T., Ott, T., Gillessen, S., Eisenhauer, F., Martins, F., & Genzel, R. 2007, *MNRAS*, 375, 764
 Tristram, K. R. W., et al. 2007, *A&A*, 474, 837
 Tristram, K. R. W., et al. 2009, *A&A*, 502, 67
 Trouille, L., Barger, A. J., & Tremonti, C. 2011, *ApJ*, 742, 46
 Tueller, J., et al. 2010, *ApJS*, 186, 378
 Tueller, J., Mushotzky, R. F., Barthelmy, S., Cannizzo, J. K., Gehrels, N., Markwardt, C. B., Skinner, G. K., & Winter, L. M. 2008, *ApJ*, 681, 113
 Turk, M. J., Abel, T., & O'Shea, B. 2009, *Science*, 325, 601
 Turnbull, A. J., Bridges, T. J., & Carter, D. 1999, *MNRAS*, 307, 967
 Ueda, Y., Akiyama, M., Ohta, K., & Miyaji, T. 2003, *ApJ*, 598, 886
 Ulrich, M.-H., Maraschi, L., & Urry, C. M. 1997, *ARA&A*, 35, 445
 Ulvestad, J. S. & Ho, L. C. 2002, *ApJ*, 581, 925
 Urrutia, T., Lacy, M., & Becker, R. H. 2008, *ApJ*, 674, 80
 Urry, C. M. & Padovani, P. 1995, *PASP*, 107, 803
 Uttley, P., McHardy, I. M., & Vaughan, S. 2005, *MNRAS*, 359, 345
 Valiante, E., Lutz, D., Sturm, E., Genzel, R., Tacconi, L. J., Lehnert, M. D., & Baker, A. J. 2007, *ApJ*, 660, 1060
 van Wassenhove, S., Volonteri, M., Walker, M. G., & Gair, J. R. 2010, *MNRAS*, 408, 1139
 Vasudevan, R. V. & Fabian, A. C. 2007, *MNRAS*, 381, 1235
 —. 2009, *MNRAS*, 392, 1124
 Vaughan, S., Edelson, R., Warwick, R. S., & Uttley, P. 2003, *MNRAS*, 345, 1271
 Veilleux, S. 1991, *ApJS*, 75, 383
 Veilleux, S., Cecil, G., & Bland-Hawthorn, J. 2005, *ARA&A*, 43, 769
 Veilleux, S., et al. 2009, *ApJ*, 701, 587
 Veilleux, S., Kim, D.-C., & Sanders, D. B. 1999, *ApJ*, 522, 113
 Veilleux, S. & Osterbrock, D. E. 1987, *ApJS*, 63, 295
 Vestergaard, M. 2002, *ApJ*, 571, 733
 Vestergaard, M. & Peterson, B. M. 2006, *ApJ*, 641, 689
 Vignali, C., Alexander, D. M., Gilli, R., & Pozzi, F. 2010, *MNRAS*, 404, 48
 Vignali, C., et al. 2009, *MNRAS*, 395, 2189
 Vollmer, B., Beckert, T., & Davies, R. I. 2008, *A&A*, 491, 441
 Volonteri, M. 2007, *ApJ*, 663, L5
 —. 2010, *A&A Rev.*, 18, 279
 Volonteri, M. & Begelman, M. C. 2010, *MNRAS*, 409, 1022
 Volonteri, M., Lodato, G., & Natarajan, P. 2008, *MNRAS*, 383, 1079
 Volonteri, M. & Natarajan, P. 2009, *MNRAS*, 400, 1911
 Volonteri, M., Natarajan, P., & Gültekin, K. 2011, *ApJ*, 737, 50
 Volonteri, M. & Rees, M. J. 2005, *ApJ*, 633, 624
 Volonteri, M., Salvaterra, R., & Haardt, F. 2006, *MNRAS*, 373, 121
 Wada, K. & Norman, C. A. 2002, *ApJ*, 566, L21
 Wada, K., Papadopoulos, P. P., & Spaans, M. 2009, *ApJ*, 702, 63
 Wake, D. A., Croom, S. M., Sadler, E. M., & Johnston, H. M. 2008, *MNRAS*, 391, 1674
 Walter, F., Carilli, C., Bertoldi, F., Menten, K., Cox, P., Lo, K. Y., Fan, X., & Strauss, M. A. 2004, *ApJ*, 615, L17
 Wardlow, J. L., et al. 2011, *MNRAS*, 415, 1479
 Waskett, T. J., Eales, S. A., Gear, W. K., McCracken, H. J., Lilly, S., & Brodwin, M. 2005, *MNRAS*, 363, 801
 Watson, M. G., et al. 2009, *A&A*, 493, 339
 Wild, V., Heckman, T., & Charlot, S. 2010, *MNRAS*, 405, 933
 Wild, V., Kauffmann, G., Heckman, T., Charlot, S., Lemson, G., Brinchmann, J., Reichard, T., & Pasquali, A. 2007, *MNRAS*, 381, 543
 Willott, C. J., et al. 2010, *AJ*, 139, 906
 Willott, C. J., Rawlings, S., & Blundell, K. M. 2001, *MNRAS*, 324, 1
 Wilson, A. S., Ward, M. J., & Haniff, C. A. 1988, *ApJ*, 334, 121
 Winter, L. M., Lewis, K. T., Koss, M., Veilleux, S., Keeney, B., & Mushotzky, R. F. 2010, *ApJ*, 710, 503
 Winter, L. M., Mushotzky, R. F., Reynolds, C. S., & Tueller, J. 2009, *ApJ*, 690, 1322
 Wise, J. H., Turk, M. J., & Abel, T. 2008, *ApJ*, 682, 745
 Woo, J., Treu, T., Malkan, M. A., & Blandford, R. D. 2008, *ApJ*, 681, 925
 Woo, J.-H., et al. 2010, *ApJ*, 716, 269
 Xue, Y. Q., et al. 2010, *ApJ*, 720, 368
 Xue, Y. Q., et al. 2011, *ApJS*, 195, 10
 Yamada, S., Itoh, T., Makishima, K., & Nakazawa, K. 2009, *PASJ*, 61, 309
 Yan, R., et al. 2011, *ApJ*, 728, 38
 York, D. G., et al. 2000, *AJ*, 120, 1579
 Young, A. J., Wilson, A. S., Terashima, Y., Arnaud, K. A., & Smith, D. A. 2002, *ApJ*, 564, 176
 Young, S. 2000, *MNRAS*, 312, 567
 Young, S., Axon, D. J., Robinson, A., Hough, J. H., & Smith, J. E. 2007, *Nature*, 450, 74
 Yuan, F., Quataert, E., & Narayan, R. 2003, *ApJ*, 598, 301
 Yuan, T.-T., Kewley, L. J., & Sanders, D. B. 2010, *ApJ*, 709, 884
 Zakamska, N. L., et al. 2003, *AJ*, 126, 2125
 Zhang, W. M., Soria, R., Zhang, S. N., Swartz, D. A., & Liu, J. F. 2009, *ApJ*, 699, 281
 Zheng, W., et al. 2004, *ApJS*, 155, 73